Alkenes and Allyl Complexes of the Group 3 Metals and Lanthanides in

Maxime Beauvois, Yohan Champouret, Fanny Bonnet, Marc Visseaux

Chapter **30010. Alkenes and allyl complexes of the group 3 metals and lanthanides**

Maxime Beauvois, Yohan Champouret, Fanny Bonnet* and Marc Visseaux*

Maxime Beauvois
Unité de Catalyse et Chimie du Solide (UCCS) - UCCS 8181
Ecole Nationale Supérieure de Chimie de Lille
Cité Scientifique, Bâtiment C7 - BP 90108
59652 Villeneuve d'Ascq Cedex
France
Maxime.Beauvois@univ-lille.fr

Dr Yohan Champouret
Unité de Catalyse et Chimie du Solide (UCCS) - UCCS 8181
Ecole Nationale Supérieure de Chimie de Lille
Cité Scientifique, Bâtiment C7 - BP 90108
59652 Villeneuve d'Ascq Cedex
France
yohan.champouret@univ-lille.fr
0033 374951331

Dr Fanny Bonnet
Unité Matériaux Et Transformation (UMET) - UMR 8207
Bâtiment Chevreul
Université de Lille
59655 Villeneuve d'Ascq Cedex
France
fanny.bonnet@univ-lille.fr
0033 320434711

Pr Marc Visseaux
Unité de Catalyse et Chimie du Solide (UCCS) - UCCS 8181
Ecole Nationale Supérieure de Chimie de Lille
Cité Scientifique, Bâtiment C7 - BP 90108
59652 Villeneuve d'Ascq Cedex
France
marc.visseaux@univ-lille.fr
0033 74951400

Keywords: alkene lanthanides; alkenyl lanthanides; alkynyl lanthanides; allyl lanthanides; organolanthanides; coordination complexes; organometallic complexes; rare earths; group 3 metals; lanthanide catalysts; polymerization; hydrogenolysis; insertion reaction; catalysis

Abstract: This chapter focuses on recent advances on the synthesis, structure, characterization and chemical reactivity of alkenes, alken(yn)yl and allyl-based group 3 and lanthanide organometallic complexes. The synthetic methods to access to such compounds are presented in detail, followed

when particularly relevant by some typical structural data issued from usual characterization methods in solution and in the solid state, such as NMR spectroscopy and X-ray diffraction studies. The chemical properties of the complexes are briefly described, including stoichiometric as well as catalytic reactions. Theoretical studies in support of experimental results are also presented in this chapter.

Abbreviations:
Bd = 1,3-butadiene
CCG = catalyzed chain growth
CGC = constrained geometry catalyst
Cp = cyclopentadienyl
Cp* = pentamethylcyclopentadienyl
diox = dioxane
DFT = density functional theory
Dipp = 2,6-$^{i}Pr_2C_6H_3$
DME = dimethoxyethane
Fc = ferrocene
Flu = fluorenyl
Ip = isoprene
Ind = indenyl
MAO = methyl aluminoxane
NMR = nuclear magnetic resonance
PB = polybutadiene
PI = polyisoprene
PS = polystyrene
ROP = Ring Opening Polymerization
THF = tetrahydrofuran
TMEDA = *N*,*N*,*N'*,*N'*-tetramethylethylenediamine
TOF = turn-over frequency
TON = turn-over-number
St = styrene
XRD = X-ray diffraction

1 Introduction

This chapter reviews the chemistry of lanthanide and group 3 metals (which corresponds to rare earth metals and herein designed as Ln or *lanthanides*) alkene and allyl organometallic complexes over the period 2006-2020. It follows previous developments on the chemistry of these complexes in preceding editions of COMC in 1982, 1995 and 2007.[1]

Alkene and alkyne complexes are compounds in which the hydrocarbon molecule behaves as L-type ligand towards the metal center. In this chapter, we will also present literature works regarding alkenyl and alkynyl (X-type ligand).

As far as allyl organolanthanides are concerned, we wish to bring to the reader's attention that this field has been addressed by Carpentier and collaborators in their well-documented review published in 2010 in *C.R. Chimie*. [2] However, with the aim to be as exhaustive as possible, we included herein all information that seemed essential to us and was already cited earlier. All complexes comprising the "simple" [Ln](C_3H_5) and "substituted" [Ln]($C_3H_nR_{5-n}$) (R = alkyl, n = 1-4) allyl motive will be the subject of this chapter. The complexes bearing an heteroallyl (*i.e*. allyl comprising a heteroatom in the carbon framework) group will be also addressed.

Allyl complexes are a valuable alternative to their alkyl counterparts, which are often less stable and coordinated by an external base, for reactivity or catalysis purposes, while having appropriate activities. Regarding synthetic approaches, a convenient method to prepare [Ln]-allyl compounds is to use ionic metathesis, by reacting a lanthanide precursor ([Ln]-X, X = halide, borohydride, etc.) with an anionic allyl reagent, typically a Grignard (allyl)MgX (X = Cl, Br) or $(allyl)_nM$ (n = 1, 2; M = alkaline, alkaline-earth metal) reagent. Alternatively, the homoleptic tris(allyl)Ln(solvent)$_x$[3,4,5,6] may be used as

starting material, which is reacted with a given proligand (*i.e.* the conjugate acid of an anionic ligand). In some rare cases, the strategy of the insertion reaction of an allene into a lanthanide hydride bond has been reported too to create the lanthanide-allyl motive[7] (or the insertion of a ketenimine to produce an (azallyl)-Ln moiety).

In terms of molecular structure, the allyl group is generally bonded in a trihapto η^3- mode to a lanthanide metal. However, the ligand can occasionally be found under an η^1- coordination arrangement. The allyl group may be fluxional in solution, which results in a typical 1H/4H or 1H/2H/2H pattern of allyl resonances by ^{1}H NMR spectroscopy.

Concerning chemical reactivity, the lanthanide allyl moiety has been the subject of numerous reactions, including insertions of small molecules, hydrogenolysis, protonation by acid reagents, hydrosilylation, substitution, photolytic activation, and reduction. All these kinds of reactivity will be addressed in this chapter. In addition, polymerization catalysis represents a whole and very specific part of the applications of lanthanide allyl complexes. In particular, it is well-established that Ln-allyl species are involved in polymerization processes of conjugated dienes when lanthanide catalysts are implemented.[8,9,10,11,12,13]Advances in this field have been reviewed recently[14] and they will be included here when relevant for the period covered in this chapter.

Finally, complexes in which an unusual coordination mode of allyl-type is found are also reviewed. In turn, fluorenyl rare earth complexes where the ligand is in some cases coordinated in an η^3- trihapto mode to the metal are not included herein. Such complexes, which have been reviewed in 2005,[15] are covered in another chapter of the present edition of COMC.

For ease of reading and for all practical purposes, a table containing the main structural information on the complexes described is provided at the end of each section.

2 Alkene, Alkyne, alkenyl, alkynyl complexes of the lanthanides

2.1 Alkene and alkyne complexes

Isolated lanthanide-alkene species are extremely rare in the literature, even though there are some evidence of their existence via NMR studies. As a matter of facts, they are most of the time found as intermediates in various catalytic reactions such as olefin[16,17] and 1,3-diene[18,19] polymerization, hydrogenation,[20] hydroamination,[21,22] hydrophosphination[23] and hydrosilylation.[24] Nearly all structurally characterized lanthanide-alkene complexes involve an alkene that is tethered to another coordinating group due to the weakness and lability of the lanthanide-alkene bond. Ethylene coordination to [$(C_5Me_5)_2$Eu] was highlighted via NMR paramagnetic shifts[25] and dynamic NMR behavior of the yttrium alkyl-tethered alkene complex $(C_5Me_5)_2Y(\eta^1{:}\eta^5\text{-}CH_2CH_2CR_2CR'{=}CH_2)$ [**1$_Y$**] (R = H, Me and R' = H, Me) was extensively studied.[26,27,28,29,30,31,32,33,34]

In 1987, Andersen and Burns reported the first lanthanide-alkene structure of a divalent ytterbium-platinum (μ-bridged) alkene complex, $(C_5Me_5)_2Yb(\mu\text{-}\eta^2{:}\eta^2\text{-}C_2H_4)Pt(PPh_3)_2$ [**2$_{Yb}$**].[35] In 1999, the synthesis and X-ray structure of the interesting alkene ytterbium complex [Yb{$\eta^1{:}\eta^2$-$C(SiMe_3)_2SiMe_2CH{=}CH_2$}{$OEt_2$}]$_2$($\mu$-I)$_2$ [**3$_{Yb}$**] (Fig. 1, left) was reported by the group of Smith and co-workers.[36] Some years later, Evans[37] and Schumann[38,39] and coworkers detailed the structures of several alkene-tethered cyclopentadienyl complexes of divalent lanthanides (**4$_{Yb}$**, **5$_{Sm}$**, **5$_{Eu}$**, **5$_{Yb}$**, Fig. 1, middle and right) and the closely related alkaline earths that display alkene coordination.

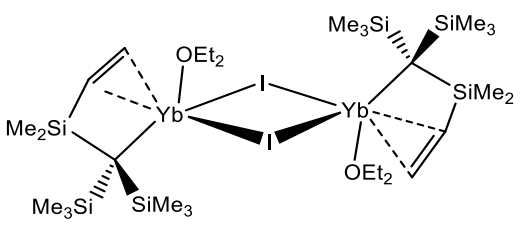

3$_{Yb}$

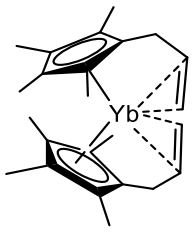

4$_{Yb}$

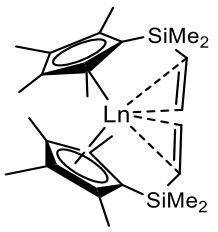

5$_{Ln}$, Ln = Sm, Eu, Yb

Fig. 1. Molecular structures of some alkene complexes of the lanthanides

Regarding more recent work, Berg *et al.* reported in 2010 the synthesis, solid state structure and the solution behavior of dimeric lanthanide aryloxides bearing one or two allyl groups in the *o*-aryl positions: $\{Ln[DALP]_2\}_2[\mu\text{-}DALP]_2$ [$\mathbf{6}_{Ln}$] (with H-DALP = 2,6-diallyl-4-methylphenol and Ln = La, Ce, Nd, Er, Yb, Y) and $\{Ln[MALP]_2\}_2[\mu\text{-}MALP]_2$ [$\mathbf{7}_{Ln}$] (with H-MALP = 2-allyl-4,6-dimethylphenol and Ln = La, Sm, Y) complexes.[40] The coordination of the alkenes from the allyl groups to the Ln^{3+} center was observed crystallographically across the lanthanide series (Fig. 2). Variable temperature NMR studies revealed that the dimeric structures remain intact in non-coordinating solvents with rapid bridge-terminal aryloxide exchange taking place above about 275-295 K for all DALP complexes, except erbium. These complexes were the first neutral trivalent lanthanide-alkene complexes that have been structurally characterized.

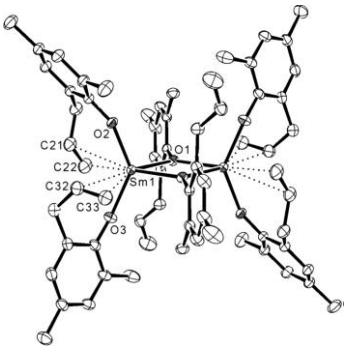

Fig. 2 Molecular structure of $\mathbf{7}_{Sm}$ (thermal ellipsoids are drawn at the 30% probability level). Reprinted with the authorization of Elsevier.[40]

More recently, the group of Trifonov described the synthesis of divalent $(Cp^{Bn5})_2Ln$ [$\mathbf{8}_{Ln}$] (Cp^{Bn5} = $C_5(CH_2Ph)_5$, Ln = Yb, Sm and Eu) by combining the potassium salt KCp^{Bn5} with 0.5 equiv. of $LnI_2(THF)_n$ (Scheme 1).[41]

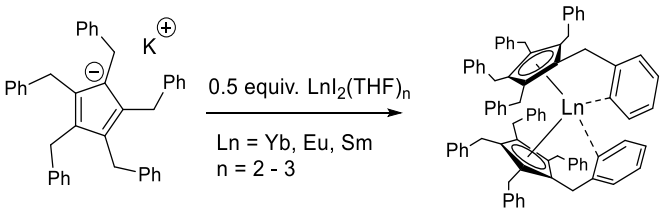

$\mathbf{8}_{Ln}$

Scheme 1 Synthesis of $\mathbf{8}_{Ln}$ complexes

The X-ray diffraction studies revealed that the three complexes are isostructural with the Ln(II) metal being coordinated by two η^5-Cp^{Bn5} rings with an additional interaction of one C-sp^2 carbon in ortho position of the two pendant phenyl moiety (Fig. 3).

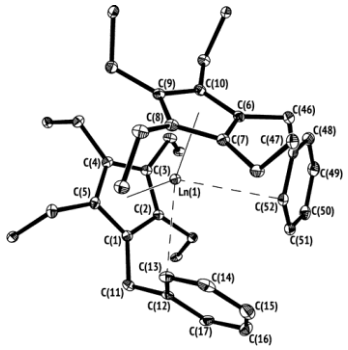

Fig. 3 Molecular structure of **8$_{Ln}$** complexes (Ln = Yb, Sm and Eu) (thermal ellipsoids are drawn at the 30% probability level). Carbon atoms of Ph groups and hydrogen atoms are omitted for clarity. Reprinted with the authorization of the American Chemical Society.[41]

Reaction of **8$_{Sm}$** with 1 equiv. of phenazine afforded the $[(Cp^{Bn5})_2Sm]_2[\mu\text{–}\eta^3\text{:}\eta^3\text{-}(C_{12}H_8N_2)]$ [**8'$_{Sm}$**] adduct that was isolated as single crystals (Scheme 2).

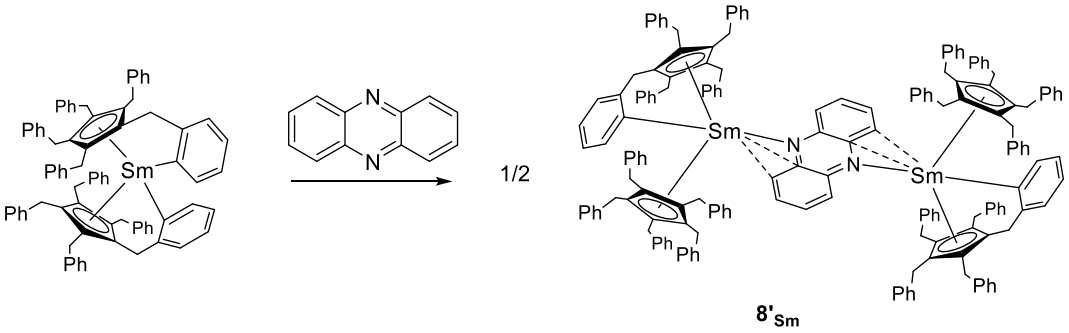

Scheme 2 Synthesis of **8'$_{Sm}$** adduct

X-ray diffraction analysis of **8'$_{Sm}$** showed that the μ-bridged phenazine ligand is coordinated to both samarium centers through one nitrogen atom and two neighboring carbon atoms of the phenazine (Fig. 4). Furthermore, it was found that the Sm-C(Cp) bond distances fall in the range typical for Sm(III) compounds, indicating that oxidation of Sm(II) occurs during the reaction.

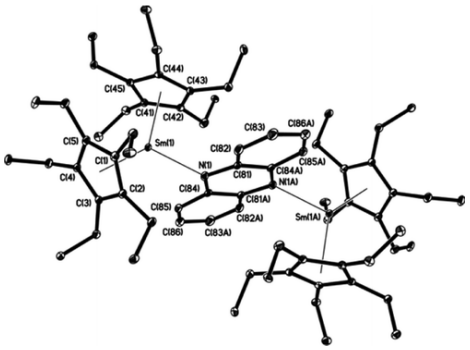

Fig. 4 Molecular structure of **8$_{Sm}$'** (thermal ellipsoids with a 30% probability level). Carbon atoms of Ph groups and hydrogen atoms are omitted for clarity. Reprinted with the authorization of the American Chemical Society.[41]

The preparation of lanthanide complexes supported with a functionalized indolyl ligand was carried out by the group of Wang using $[Ln(CH_2SiMe_3)_3(THF)_2]$ (Ln = Yb, Er and Y) precursors in presence of 1 equiv. of 3-(CyN=CH)C_8H_5NH proligand in toluene, which yields the dinuclear lanthanide alkyl complexes [**9$_{Ln}$**] (Scheme 3).[42]

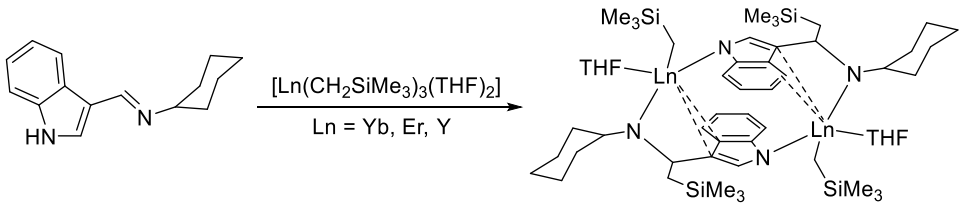

9_{Ln}

Scheme 3 Synthesis of complexes **9_{Ln}**

The molecular structure of the three complexes was determined by X-ray diffraction studies and revealed, in particular, that the two metal centers are bridged by the indolyl ligand through the two carbons of the five membered ring in η^2-fashion and through the nitrogen atom in an η^1-mode (Fig. 5). Interestingly, the η^2-coordination mode of the two carbons of the five-membered ring was not observed when the reaction was conducted in THF, due to the presence of an additional THF ligand in the coordination sphere of the metal center.

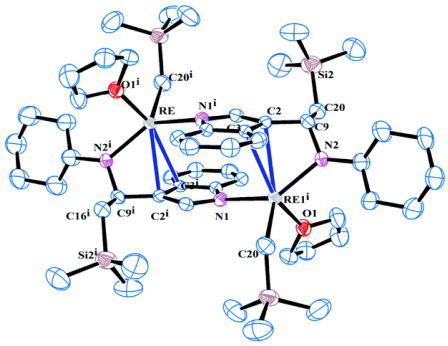

Fig. 5 Representative molecular structure of complexes **9_{Ln}** showing the bridging mode as {[η^2:η^1–μ–η^1-3-[(CyNCH(CH_2SiMe_3))Ind]RE(THF)(CH_2SiMe_3)}$_2$ (Cy = cyclohexyl, Ind = indolyl, RE = Ln = Yb, Er, Y) lanthanide complexes (thermal ellipsoids are drawn at the 30% probability level). Hydrogen atoms are omitted for clarity. Reprinted with the authorization of the Royal Society of Chemistry.[42]

In the same study, upon treatment of 3-(^{t}BuNH-CH_2)C_8H_5NH proligand with Ln(CH_2SiMe_3)$_3$(THF)$_2$ (Ln = Y, Er and Dy) in THF, trinuclear complexes **10_{Ln}** were formed (Scheme 4, up). On the other hand, a dinuclear species **11_{Yb}** could be isolated just one year earlier from the reaction of the same 3-(^{t}BuNH-CH_2)C_8H_5NH proligand with Yb(CH_2SiMe_3)$_3$(THF)$_2$, which includes a metal with a smaller ionic radius.(Scheme 4, down).[43]

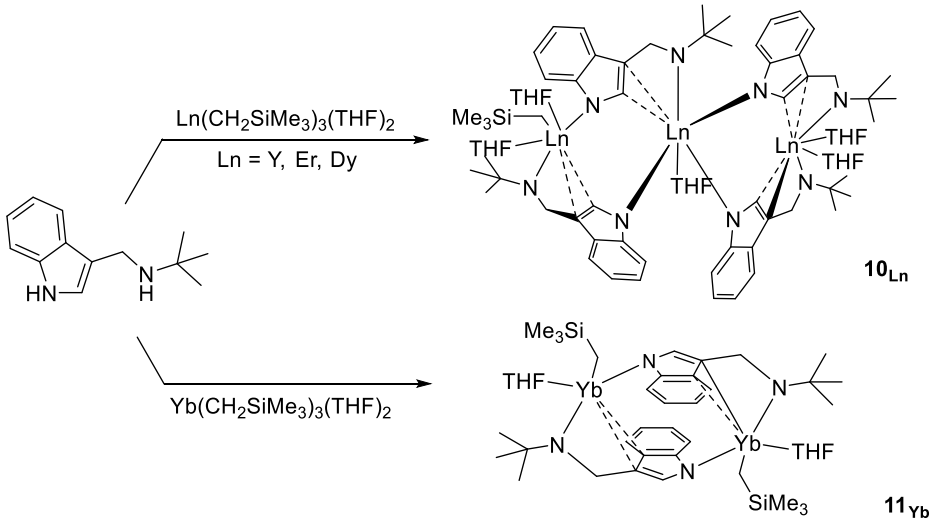

Scheme 4 Synthesis of indenyl alkyl complexes $\mathbf{10_{Ln}}$ and $\mathbf{11_{Yb}}$ showing a different result depending on the nature of the lanthanide precursor

In the case of the trinuclear complexes $\mathbf{10_{Ln}}$, the X-ray diffraction analysis indicates a distorted octahedral geometry around the metal center that comprises an η^2-coordination mode of the carbon atoms and η^1-fashion of the nitrogen atom from the indolyl moiety, one nitrogen atom from the amido group and two additional THF molecules (Fig. 6, left). Similar η^2-coordination binding mode of the carbon atom of the indolyl ring was observed for the dinuclear $\mathbf{11_{Yb}}$, which was obtained under two forms, with indolyl groups in *trans* (major) or *cis* (minor) position from each other (Fig. 6, right).

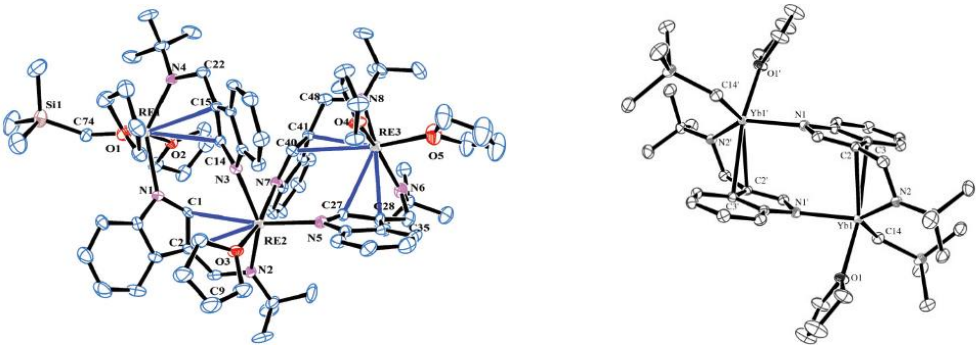

Fig. 6 Molecular structure of $[\eta^2{:}\eta^1{-}\mu{-}\eta^1$-3-(^{t}BuNCH$_2$)Ind$]_4Ln_3(THF)_5$(CH$_2$SiMe$_3$) $\mathbf{10_{Ln}}$ (RE = Ln = Y, Er, Dy, left)[42] and of complex *trans*-[{μ-$\eta^2{:}\eta^1{:}\eta^1$-3-(^{t}BuNCH$_2$)Ind}Yb(THF)(CH$_2$SiMe$_3$)]$_2$ $\mathbf{11_{Yb}}$ (right).[43] Thermal ellipsoids are set at the 30% probability level. Reprinted with the authorization of the Royal Society of Chemistry and Wiley-VCH Verlag GmbH.

In parallel, dinuclear species $\mathbf{12_{Ln}}$ were prepared from the one-pot treatment of 3-(^{t}BuNH-CH$_2$)C$_8$H$_5$NH proligand and [Ln(CH$_2$SiMe$_3$)$_3$(THF)$_2$] in the presence of [(2,6-^{i}Pr$_2$C$_6$H$_3$)N=CHNH-(C$_6$H$_3{}^i$Pr$_2$-2,6)] amidine (Ln = Er, Y, Scheme 5).

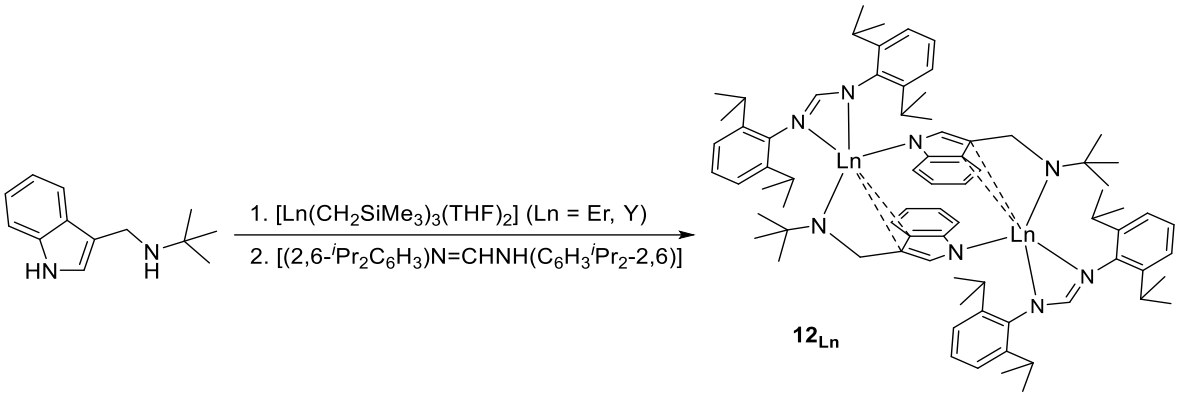

Scheme 5 Synthesis of dinuclear complexes **12$_{Ln}$**

The X-ray molecular structure revealed that in **12$_{Ln}$** the metal center is also coordinated to the carbon of the indolyl ring in η^2-mode and the nitrogen atom in η^1-fashion (Fig. 7).

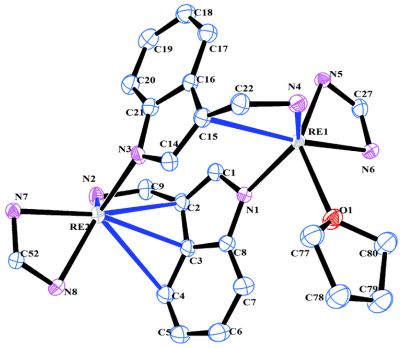

Fig. 7 Molecular structure of [η^1-μ–η^1:η^1-3-(^{t}BuNCH$_2$)Ind][η^1-μ–η^1:η^3-3-(^{t}BuNCH$_2$)Ind]RE$_2$(THF)[(η^3-2,6-^{i}Pr$_2$C$_6$H$_3$)NCHN(C$_6$H$_3$^{i}Pr$_2$-2,6)]$_2$ [**12$_{Ln}$**] (RE = Ln = Er, Y, ellipsoid are drawn at the 30% probability level). Reprinted with the authorization of the Royal Society of Chemistry.[42]

Following the same strategy as for the synthesis of complexes **9$_{Ln}$** (scheme 3), but using 3-(^{t}BuN=CH)C$_8$H$_5$NH as proligand, afforded the dinuclear lanthanide complexes [*trans*-[{μ-η^2:η^1:η^1-3-{^{t}BuNCH(CH$_2$SiMe$_3$)}Ind}Ln(THF)(CH$_2$SiMe$_3$)]$_2$] [**13$_{Ln}$**] (Ln = Y, Dy, Yb), where *trans* represents the orientation of six membered rings of the indolyl ligands in opposite directions. According to X-ray analysis, dinuclear rare-earth metal alkyl complexes with central symmetry were isolated as dianionic species bridges with two metal alkyl units in μ-η^2:η^1:η^1 bonding mode (Figure 8).[43]

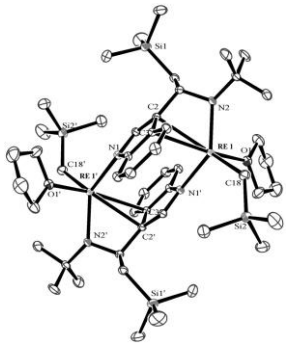

Fig. 8 Representative molecular structure of [*trans*-[{μ-η^2:η^1:η^1-3-{^{t}BuNCH(CH$_2$SiMe$_3$)}Ind}Ln(THF)(CH$_2$SiMe$_3$)]$_2$] [**13$_{Ln}$**] (RE = Ln = Y, Dy, Yb, ellipsoid are drawn at the 30% probability level). Reprinted with the authorization of the Royal Society of Chemistry.[43]

In a more recently published work by Trifonov and coworkers, divalent benzhydryl Ln(II) derivatives of the formula [(*p*-^{t}Bu-C$_6$H$_4$)$_2$CH]$_2$Ln(L)$_n$ (**14$_{Sm}$**, Ln = Sm, L = DME, n = 2; **14'$_{Ln}$**, Ln = Sm, Yb, L = TMEDA, n

= 1) were synthesized.[44] The complexes display structural peculiarities: X-ray diffraction studies showed that the benzhydryl ligands are bound to the metal center in an η^2-coordination mode in **14$_{Sm}$**, where short contacts between Sm(II) ion and the *ipso*-carbon atom of one of the phenyl rings were detected, whereas **14'$_{Yb}$** displays η^3-coordination of the benzhydryl moieties to the metal center (Fig. 9). In **14'$_{Sm}$**, one benzhydryl is η^3-coordinated while the second one is η^4-coordinated to the Sm(II) ion. Theoretical calculations were carried out in order to get more details on the nature of M–L bonding, which corroborates the presence of short interactions between the metal center and the *ortho*- and *ipso*-carbons of the benzhydryl ligands, highlighting the variety of hapticities observed.

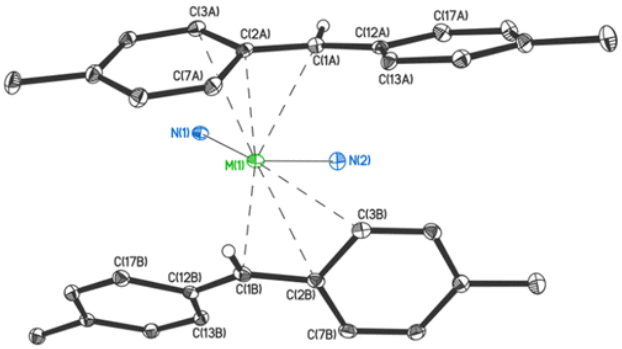

Fig. 9 Molecular structure of a representative complex [(*p*-^{t}Bu-C$_6$H$_4$)$_2$CH]$_2$Ln(L)$_n$ (**14'$_{Ln}$**, M = Ln = Sm, Yb). Ellipsoids are set at the 30% probability, hydrogen atoms, methyl groups of ^{t}Bu-substituents, and carbon atoms of TMEDA molecules are omitted for clarity. Reprinted with the authorization of the American Chemical Society.[44]

Substitution of one benzhydryl ligand by *tert*-butylcarbazol-9-yl (^{t}Bu$_4$Carb) or 2,7-di-*tert*-butyl-fluoren-9-trimethylsilyl (^{t}Bu$_2$FluTMS) was also performed later by the same group.[45] The molecular structure of the DME adducts of samarium and ytterbium [^{t}Bu$_4$Carb]Ln[(*p*-^{t}Bu-C$_6$H$_4$)$_2$CH](DME) [**15$_{Sm}$**, **15$_{Yb}$**] revealed an η^3- coordination mode of the benzhydryl ligand to the metal (Fig. 10, left and right, respectively) while the ytterbium complex [^{t}Bu$_2$FluTMS]Yb[(*p*-^{t}Bu-C$_6$H$_4$)$_2$CH](TMEDA) bearing TMEDA ligand [**16$_{Yb}$**] shows an η^1- coordination mode.

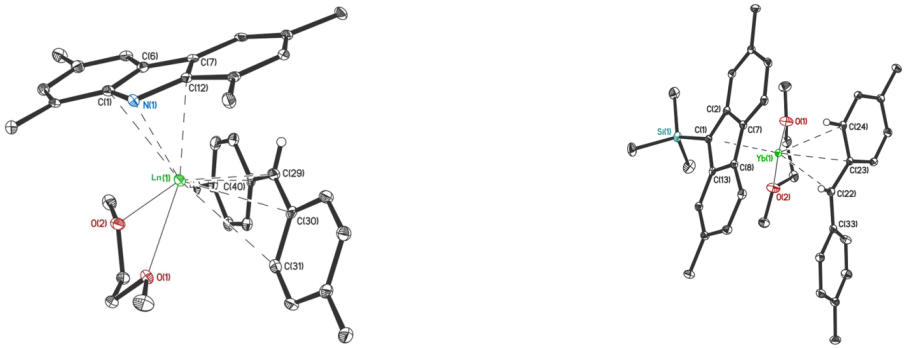

Fig. 10 Molecular structure of the half-sandwich complexes **15$_{Sm}$** (left) and **15$_{Yb}$** (right). Methyl fragments of ^{t}Bu groups and all hydrogen atoms except the methine hydrogen are omitted for clarity. Ellipsoids are given at 30% of the probability level. Reprinted with the authorization of the American Chemical Society.[45]

Following the synthesis of [(*p*-^{t}Bu-C$_6$H$_4$)$_2$CH]$_2$Ln(L)$_n$, Trifonov and coworkers prepared a series of Ln(III) (Ln = La, Nd and Y) complexes supported by three benzhydryl ligands, **17$_{Ln}$**, from salt metathesis of [(*p*-^{t}Bu-C$_6$H$_4$)$_2$CH]Na in presence of 1/3 equiv. of LnX$_3$(THF)$_{3.5}$ (X = Cl, I) (Scheme 6).[46]

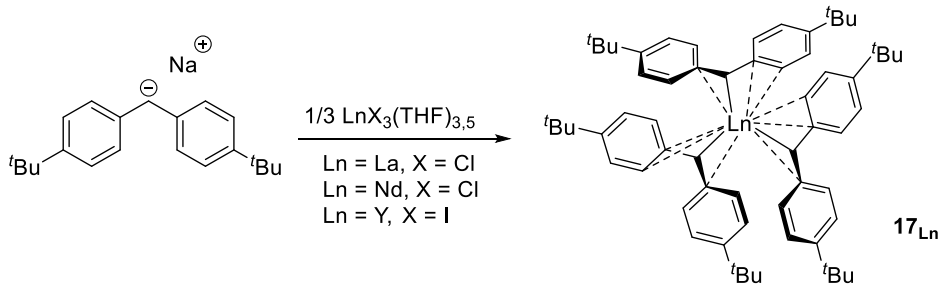

Scheme 6 Synthesis of complexes **17$_{Ln}$**

Single crystals of **17$_{Ln}$** suitable for X-ray diffraction studies revealed that, for each lanthanide element, the benzhydryl ligand is rather coordinated in an η^4-mode to the metal center with one covalent bond between Ln and the methanide carbon as well as short contacts with two *ipso* and one *ortho*-phenyl carbons of the benzhydryl part (Figure 11).

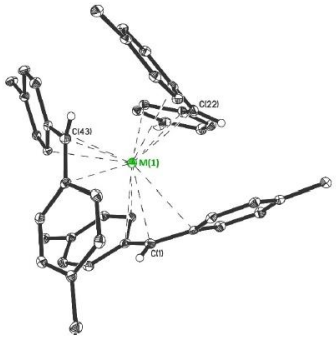

Fig. 11 Molecular structure of complexes **17$_{Ln}$** (M = Ln = La, Nd, Y). Thermal ellipsoids are given at the 30% probability level. Methyl groups of *tert*-butyl substituents and hydrogen atoms except bonded with methanide carbons were omitted for clarity. Reprinted with the permission of Wiley-VCH GmbH.[46]

Upon reaction of the potassium salt {[2,2-(4-MeC$_6$H$_3$NMe$_2$)$_2$CH]K(THF)}$_2$ with LnI$_2$(THF)$_2$(Ln = Yb and Sm), the replacement of the ^{t}Bu substituent on the *para* position of the benzhydryl ligand by NMe$_2$ group led to the formation of the homoleptic [2,2-(4-MeC$_6$H$_3$NMe$_2$)$_2$CH]$_2$Ln [**18$_{Ln}$**] (Scheme 7).[47]

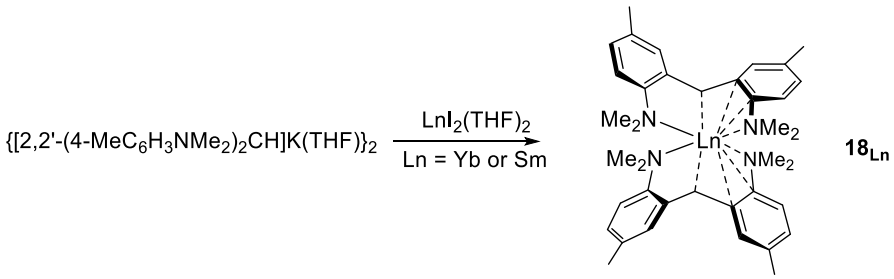

Scheme 7 Synthesis of complexes **18$_{Ln}$**

The X-ray diffraction studies revealed that, in both cases, the divalent lanthanide centers in **18$_{Ln}$** are coordinated by two [2,2-(4-MeC$_6$H$_3$NMe$_2$)$_2$CH]$^-$ ligands through the carbon of the methanido group as well as two additional nitrogen atoms of the NMe$_2$ substituents (Fig. 12), although, the coordination mode of both [2,2-(4-MeC$_6$H$_3$NMe$_2$)$_2$CH]$^-$ ligands was shown to be different. Upon closer examination of the distances and angles between the metals and the ligands, it was observed that one ligand coordinates in κ^1-N mode while the other revealed a short contact between *ipso*- and *ortho*-carbons of one phenyl substituent, resulting in an η^4-CCCN coordination mode with the metal.

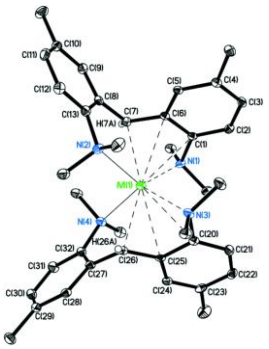

Fig. 12 Molecular structure of **18$_{Ln}$** (M = Yb and Sm) with a 30% thermal ellipsoid probability level. All hydrogen atoms except that of M–CH are omitted for clarity. Reprinted with the permission of the Royal Society of Chemistry.[47]

Long *et al.* described the preparation of two half-sandwich complexes of the type (Cp*)Dy(2,6-^{i}Pr$_2$C$_6$H$_3$N−CMe=CMe−NC$_6$H$_3$^{i}Pr$_2$−2,6)(THF) [**19$_{Dy}$**] and [Li(THF)$_3$][Dy(2,6-^{i}Pr$_2$C$_6$H$_3$N−CMe=CMe−NC$_6$H$_3$ ^{i}Pr$_2$−2,6)(Cp*)Cl] (Cp* = C$_5$Me$_5$) [**19'$_{Dy}$**] by treatment of DyCl$_3$ with [K(THF)$_x$(2,6-^{i}Pr$_2$C$_6$H$_3$N−CMe=CMe−NC$_6$H$_3$^{i}Pr$_2$−2,6)K(THF)$_x$] in the presence of either KCp* or LiCp*, respectively (Scheme 8).[48]

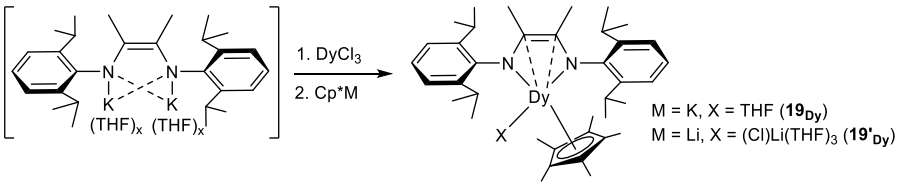

Scheme 8 Synthesis of **19$_{Dy}$** and **19'$_{Dy}$** starting from potassium or lithium reagent, respectively

In both cases, the X-ray diffraction measurement revealed that the metal centers of both **19$_{Dy}$** and **19'$_{Dy}$** are coordinated to one dianionic NC=CN ligand, one Cp* ligand and one THF or (Cl)Li(THF)$_3$ moiety, respectively (Fig. 13). The weak interaction of the Dy(III) cation with the carbon atoms of the NC=CN part is consistent with an η^2-coordination mode of the carbon double bond to the metal center.

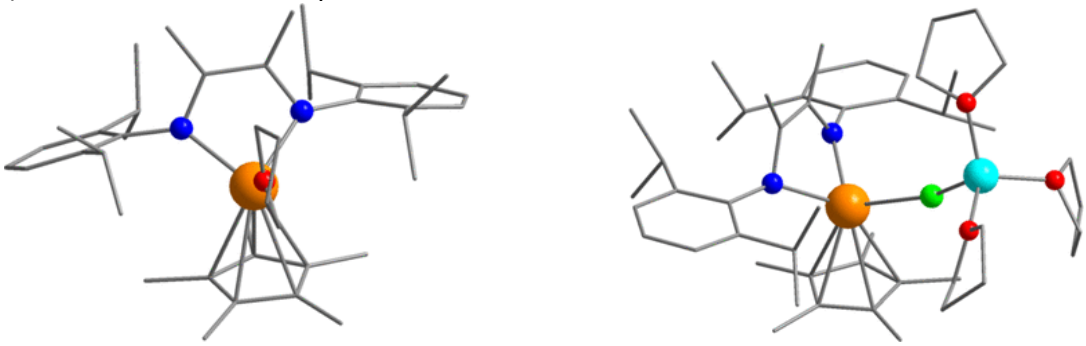

Fig. 13 Structure of **19$_{Dy}$** (left) and **19'$_{Dy}$** (right). Color code: orange, Dy; red, O; gray, C; green, Cl; light blue, Li. Hydrogen atoms have been omitted for clarity. Reprinted with the permission of the American Chemical Society.[48]

Table 1 Structural and analytical data of alkene and alkyl complexes (in brackets for relevant complexes only, otherwise for all complexes)

Compound number	**Molecular Formula**	**X-ray data** Typical Ln-C (alkene or alkyl) distances (Å)	**NMR data**	**References**

1_{Y}	$[(Cp^*)_2Y(\eta^1{:}\eta^5\text{-}CH_2CH_2CR_2CR'{=}CH_2)]$	-	^1H, ^1H NOESY, ^{13}C, VT ^1H and ^{13}C NMR, ^1H-^{13}C HMQC	26 - 34
2_{Yb}	$[(Cp^*)_2Yb(\mu\text{-}\eta^2{:}\eta^2\text{-}C_2H_4)Pt(PPh_3)_2]$	Yb-C = 2.770(3), 2.793(3)	^1H, ^{31}P	35
3_{Yb}	$[[Yb\{\eta^1{:}\eta^2\text{-}C(SiMe_3)_2SiMe_2CH{=}CH_2\}\{OEt_2\}]_2(\mu\text{-}I)_2]$	Yb-C = 2.50(2)	^1H attempts (broad signals/ rearrangements)	36
4_{Yb}	$[Yb(C_5Me_4CH_2CH_2CH{=}CH_2)_2]$	Yb-C = 2.941(7), 3.132(7) 2.881(7), 3.032(7)	^1H, ^{13}C	38, 39
5_{Sm}, 5_{Eu}, 5_{Yb}	$[Ln\{(C_5Me_4)SiMe_2(CH_2\text{-}CH{=}CH_2)]_2\}]$ (Ln = Sm, Eu, Yb)	Sm-C = 3.249(4), 3.004(3) Eu-C = 3.293(4), 3.008(3) Yb-C = 3.182(3), 2.905(3)	^1H, ^{13}C (**5_{Yb}**)	37
6_{La}, 6_{Ce}, 6_{Nd}, 6_{Er}, 6_{Yb}, 6_{Y}	$[\{Ln[DALP]_2\}_2[\mu\text{-}DALP]_2]$ (Ln = La, Ce, Nd, Er, Yb, Y)	Nd-C = 3.122(6), 3.024(5), 3.185(6), 3.256(5) Er-C = 3.122(6), 2.928(5), 3.186(6), 3.126(5) Y-C = 3.128(5), 2.970(5), 3.187(5), 3.153(5)	^1H, ^{13}C for (**6_{Nd}**, **6_{Y}**)	40
7_{La}, 7_{Sm}, 7_{Y}	$[\{Ln[MALP]_2\}_2[\mu\text{-}MALP]_2]$ (Ln = La, Sm, Y)	Sm-C = 3.120(4), 3.099(3), 3.149(4), 3.252(3) Y-C = 3.090(3), 3.140(4), 3.123(3), 3.288(4)	^1H	40
8_{Yb}, 8_{Sm}, 8_{Eu}	$[(Cp^{Bn5})_2Ln]$ ($Cp^{Bn5} = C_5(CH_2Ph)_5$, Ln = Yb, Sm, Eu)	Yb-C = 2.952(2), 3.197(2) Sm-C = 2.996(2), 3.161(2) Eu-C = 2.991(2), 3.163(2)	^1H, ^{13}C (**8_{Yb}**, **8_{Eu}**)	41
8_{Sm}'	$[(Cp^{Bn5})_2Sm]_2[\mu\text{–}\eta^3{:}\eta^3\text{-}(C_{12}H_8N_2)]]$	Sm-C = 2.869(2), 2.901(2)	^1H, ^{13}C	41
9_{Yb}, 9_{Er}, 9_{Y}	$[\{[\eta^2{:}\eta^1\text{–}\mu\text{–}\eta^1\text{-}3\text{-}(CyNCH(CH_2SiMe_3))Ind]Ln(THF)(CH_2SiMe_3)\}_2]$ (Cy = cyclohexyl, Ind = indolyl, Ln = Yb, Er, Y)	Yb-C = 2.675(6), 2.811(7) Er-C = 2.717(6), 2.825(5) Y-C = 2.709(5), 2.816(5)	^1H (**9_{Y}**), ^{13}C (**9_{Y}**)	42
10_{Y}, 10_{Er}, 10_{Dy}	$[\eta^2{:}\eta^1\text{–}\mu\text{–}\eta^1\text{-}3\text{-}(^t BuNCH_2)Ind]_4Ln_3(THF)_5(CH_2SiMe_3)$ Ln = Y, Er, Dy	Y-C = 2.963(3), 3.044(3) Er-C = 2.969(6), 3.026(5) Dy-C = 2.989(5), 3.027(6)	^1H (**10_{Y}**), ^{13}C (**10_{Y}**)	42
11_{Yb}	*trans*-$[\{\mu\text{-}\eta^2{:}\eta^1{:}\eta^1\text{-}3\text{-}(^t BuNCH_2)Ind\}Yb(THF)(CH_2SiMe_3)]_2$	Yb-C = 2.681(4), 2.787(5)	-	43
12_{Er}, 12_{Y}	$[[\eta^1\text{-}\mu\text{–}\eta^1{:}\eta^1\text{-}3\text{-}(^t BuNCH_2)Ind][\eta^1\text{-}\mu\text{–}\eta^1{:}\eta^3\text{-}3\text{-}(^t BuNCH_2)Ind]Ln_2(THF)[(\eta^3\text{-}2,6\text{-}{}^i Pr_2C_6H_3)NCHN(C_6H_3{}^i Pr_2\text{-}2,6)]_2]$ (Ln = Er, Y)	Er1-C = 2.794(7), Er2-C = 2.733(8), 2.712(7), 3.031(6) ; Y1-C = 2.825(6), Y2-C = 2.759(7), 2.738(7), 3.022(7)	^1H(**12_{Y}**), ^{13}C (**12_{Y}**)	42
13_{Y}, 13_{Dy}, 13_{Yb}	[*trans*-$[\{\mu\text{-}\eta^2{:}\eta^1{:}\eta^1\text{-}3\text{-}\{^t BuNCH(CH_2SiMe_3)\}Ind\}Ln(THF)(CH_2SiMe_3)]_2]$	Y-C = 2.725(4), 2.810(4) Dy-C = 2.745(3), 2.775(3) Yb-C = 2.636, 2.838(3)	^1H(**13_{Y}**), ^{13}C (**13_{Y}**)	43

	(Ln = Y, Dy, Yb)			
14$_{Sm}$, 14'$_{Yb}$, 14'$_{Sm}$	[[(*p*-^{t}Bu-C$_6$H$_4$)$_2$CH]$_2$Ln(L)$_n$] (**14$_{Sm}$**, Ln = Sm, L = DME, n = 2; **14'$_{Ln}$**, Ln = Sm, Yb, L = TMEDA, n = 1)	**14$_{Sm}$**: Sm-C = 2.863(2), 2.662(2), 2.701(2), 2.944(2), 2.963(2), 3.060(2) **14'$_{Yb}$**: Yb-C = 2.668(2), 2.555(2), 2.617(2), 2.853(2), 2.889(2), 2.895(2) No R-Xay for **14'$_{Sm}$**	^{1}H, ^{13}C (**14$_{Sm}$**, **14$_{Yb}$**)	44
15$_{Sm}$, 15$_{Yb}$	[[^{t}Bu$_4$Carb]Ln[(*p*-^{t}Bu-C$_6$H$_4$)$_2$CH](DME)] (Ln = Sm, Yb)	Sm-C = 2.670(4), 2.904(3), 3.220(4), 3.125(4) Yb-C = 2.540(4), 2.806(4), 3.084(4), 3.350(4)	^{1}H (**15$_{Sm}$**), ^{13}C (**15$_{Sm}$**)	45
16$_{Yb}$	[(^{t}Bu$_2$FluTMS)Yb[(*p*-^{t}Bu-C$_6$H$_4$)$_2$CH](DME)]	Yb–C = 2.589(2), 2.721(2), 2.737(2)	^{1}H, ^{13}C	45
17$_Y$, **17$_{La}$**, **17$_{Nd}$**	[Ln[(*p*-^{t}Bu-C$_6$H$_4$)$_2$CH]$_3$] (Ln = Y, La, Nd)	Y-C$_{ipso}$ = 2.720(2) to 2.844(2) Y-C$_{ortho}$ = 2.812(2), 2.814(2), 2.814(2) La-C$_{ipso}$ = 2.841(2) to 2.915(2) La-C$_{ortho}$ = 2.948(2), 2.958(2), 2.971(2) Nd-C$_{ipso}$ = 2.795(3) to 2.867(3) Nd-C$_{ortho}$ = 2.905(3), 2.918(3), 2.920(3)	^{1}H (**17$_Y$**, **17$_{La}$**), ^{13}C (**17$_Y$**, **17$_{La}$**)	46
18$_{Yb}$, **18$_{Sm}$**	[Ln[2,2-(4-MeC$_6$H$_3$NMe$_2$)$_2$CH]$_2$] (Ln = Yb, Sm)	Yb-C = 2.576(4), 2.585(4), 2.730(4), 2.742(4), 2.852(3), 2.864(4) Sm-C = 2.710(2), 2.728(2), 2.779(2), 2.804(2), 2.854(2), 2.883(2)	^{1}H, ^{13}C	47
19$_{Dy}$	(Cp*)Dy(2,6-^{i}Pr$_2$C$_6$H$_3$N−CMe=CMe−NC$_6$H$_3$^{i}Pr$_2$−2,6)(THF)	Dy-C = 2.837(2), 2.845(2)	-	48
19'$_{Dy}$	[Li(THF)$_3$][Dy(2,6-^{i}Pr$_2$C$_6$H$_3$N−CMe=CMe−NC$_6$H$_3$^{i}Pr$_2$−2,6)(Cp*)Cl]	Dy-C = 2.764(2), 2.769(2)	-	48

2.2 Alkenyl and alkynyl complexes

The reactivity of lanthanide complexes with unsaturated hydrocarbon substrates has been the subject of numerous investigations in the 1980s, but it was only in 1990 that the group of Evans succeeded in identifying the first examples of an η^2-alkene lanthanide complexes [(Cp*)$_2$Sm]$_2$(μ-η^2:η^4-CH$_2$CHPh) [**20$_{Sm}$**] and [(Cp*)$_2$Sm]$_2$(μ-η^2:η^4-PhCHCHPh) [**20'$_{Sm}$**] by reduction of styrene and stilbene precursors, respectively, in the presence of divalent (Cp*)$_2$Sm.[9] A decade later, the same group extended the reactivity of the decamethylsamarium with isoprene and myrcene to produce the bimetallic [(Cp*)$_2$Sm]$_2$[μ-η^2:η^4-CH$_2$CHC(Me)CH$_2$] [**21$_{Sm}$**] and [(Cp*)$_2$Sm]$_2$[μ-η^2:η^4-CH$_2$CHC(CH$_2$)CH$_2$CH$_2$CHCMe$_2$] [**21'$_{Sm}$**] complexes, respectively.[49] In addition, the coordination chemistry of yttrium was also explored by reacting YCl$_3$ with tetraphenylethylenyl M[PhCCPh$_2$] (M = Na or K) to form complexes of the type [M(THF)$_x$][Y(Ph$_2$CCPh$_2$)$_2$] [**22$_Y$**].[50]

The extension of the chemistry of alkenyl lanthanides was at the same period pursued by Floriani and coworkers by reacting the *meso*-octaethylporphyrinogen (oepg) lanthanide complexes, {(oepg)Ln}Na(THF)$_2$ (Ln = Pr, Nd) with $NaC_{10}H_8$ in an ethylene atmosphere in the presence of 18-crown-6 in THF that yields dimeric species of formula [{(oepg)Ln}Na(THF)$_2$(μ-η^2:η^2-C_2H_4)]$_2$ [**23$_{Ln}$**] where the metals are bridged by the $[C_2H_4]^-$ moiety.[51] According to the X-ray crystal structure of the Nd derivative **23$_{Nd}$**, the $[C_2H_4]^-$ unit is side-on bonded to the two metal atoms (Fig. 14, left). In the presence of acetylene and sodium metal, the resulting acetylido complexes were formed where the two metal centers in [{(oepg)Ln}(Na)$_2$(μ-η^2:η^2-C_2)]$_2$ [**24$_{Ln}$**] are bridged by the C_2^{2-} μ-η^2:η^2-bonded anion as shown in the X-ray structure of **24$_{Pr}$** (Fig. 14, right).

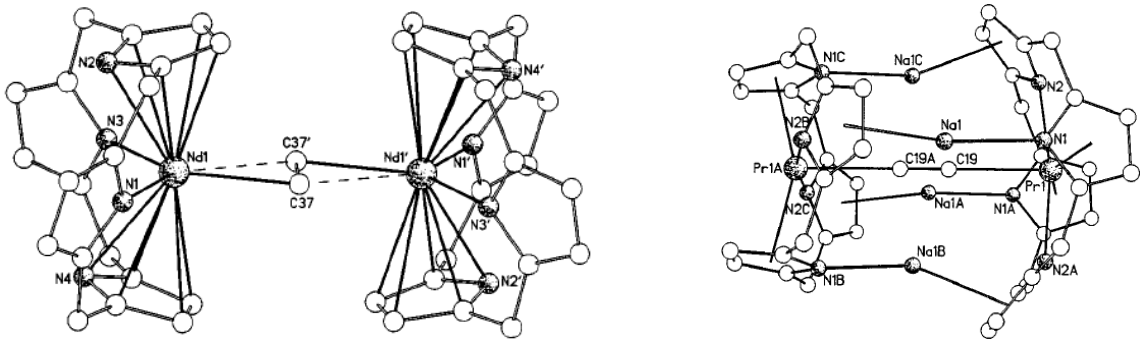

Fig. 14 Molecular structure of **23$_{Nd}$** (left, Na(THF)$_2$ and counter-cationic part and *meso*-ethyl groups omitted for clarity) and **24$_{Pr}$** (right, *meso*-ethyl groups omitted for clarity). Reprinted with the permission of the Royal Society of Chemistry.[51]

[(Cp"$_2$Sc)$_2$-(μ-η^2:η^2-C_2H_4)] [**25$_{Sc}$**] was isolated in low yield (< 5%) from the tentative reduction of (Cp")$_2$ScI with lipophilic reducing agent [K(18-crown-6)]$_2$[C_6H_2($SiMe_3$)$_4$-1,2,4,5] (Cp" = [η^5-C_5H_3($SiMe_3$)$_2$-1,3]). This compound was suspected to arise from transient Sc(II)- induced cleavage of the crown ether.[52] The X-ray structure (Fig. 15) features a centrosymmetric ethylene-bridged binuclear scandium compound where the Sc-C(ethylene) distances of 2.314(3) Å are comparable to previously observed.[53]

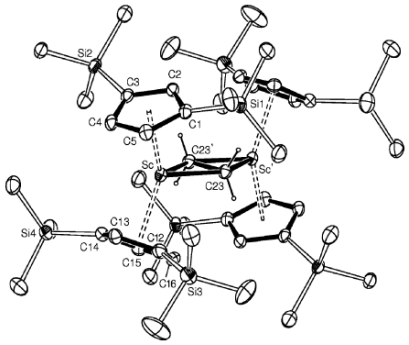

Fig. 15 Molecular structure of **25$_{Sc}$**. Thermal ellipsoids are drawn at the 30% probability level. Hydrogen atoms except H_2C= are omitted for clarity. Reprinted with the authorization of the American Chemical Society. [52]

In 2014, Diaconescu and coworkers reported that the reduction of (*E*)-stilbene using (NNTBS)LnI(THF)$_2$ (NNTBS = 1,1-Fc(NSi^{t}BuMe$_2$)$_2$, Ln = Y and La, Fc = ferrocene) in presence of potassium graphite KC_8 resulted in the formation of [(NNTBS)Ln(THF)]$_2$[μ-η^3:η^3-(E)-PhCHCHPh] (**26$_{Ln}$**) as illustrated in Scheme 9.[54]

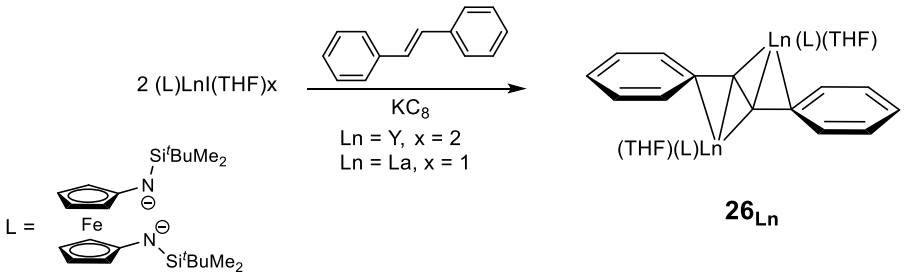

26$_{Ln}$

Scheme 9 Synthesis of complexes **26$_{Ln}$**

The molecular structure of **26$_Y$** was determined by X-ray diffraction analysis and revealed that the bridging stilbene coordinates to the metal center in an η^3-fashion through the central C-C bond and one *ipso*-carbon (Fig. 16).

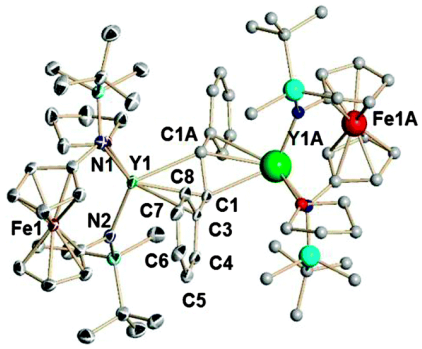

Fig. 16 Molecular structure of **26$_Y$**. Thermal ellipsoids are drawn at the 50% probability level. Hydrogen atoms and disordered counterparts are omitted for clarity. Reprinted with the authorization of the Royal Society of Chemistry.[54]

The three-decker Yb(II) complex [Cp^{Bn5}Yb(DME)]$_2$[μ-C$_{10}$H$_8$] (**27$_{Yb}$**) (Cp^{Bn5} = pentabenzylcyclopentadienyl, C$_{10}$H$_8$ = naphtalene) was synthesized by reacting [Cp^{Bn5}Yb(DME)(μ-I)]$_2$ with 2 molar equiv. of [C$_{10}$H$_8$]K or [YbI(DME)$_2$]$_2$[μ-C$_{10}$H$_8$] in the presence of Cp^{Bn5}K in a 1:2 molar ratio in DME (Scheme 10).[55] This complex contained a dianionic μ–η^4:η^4 naphthalene bridge between the two metal centers. Upon oxidation with 1,4-diphenyl-buta-1,3-diene, the three-decker [Cp^{Bn5}Yb(DME)]$_2$(μ–η^4:η^4-PhCHCHCHCHPh) Yb (II) complex **27'$_{Yb}$**, where the dianionic diphenylbutadiene replaced the naphthalene moiety, was isolated. Both complexes were structurally characterized and the peculiar nature of the bonding in their bridging unit was additionally investigated by DFT studies.

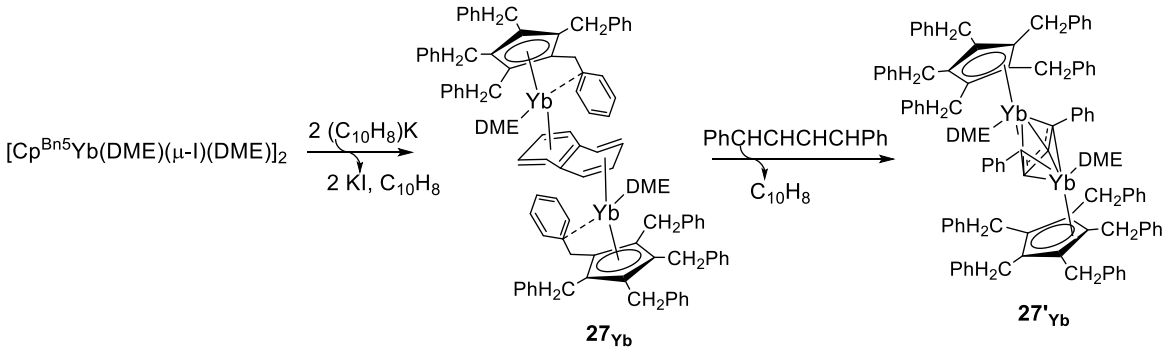

27$_{Yb}$ **27'$_{Yb}$**

Scheme 10 Successive steps of the synthesis of **27$_{Yb}$** and **27'$_{Yb}$** [55]

The *sp*^{2} C-H activation of the ligand 1-R-3-(2,6-^{i}Pr$_2$C$_6$H$_3$N=CH)C$_8$H$_5$N (R = Bn or Me) in the presence of 0.5 equiv. of Ln(CH$_2$SiMe$_3$)$_3$(THF)$_2$ (Ln = Y, Er, Dy) resulted in the formation of the σ-bonded indolyl-

supported rare earth complexes of the type [1-R-3-(2,6-$^{i}Pr_2C_6H_3N$=C)C_8H_5N]$_2$Ln(CH_2SiMe_3) [**28$_{Ln}$**, R = Bn; **28'$_{Ln}$**, R = Me], while a single ligand coordinates to the smaller ytterbium precursor to yield the [1-Bn-3-(2,6-$^{i}Pr_2C_6H_3N$=C)C_8H_5N]Yb(CH_2SiMe_3)$_2$(THF)$_2$ complex [**29$_{Yb}$**] (Scheme 11).[56]

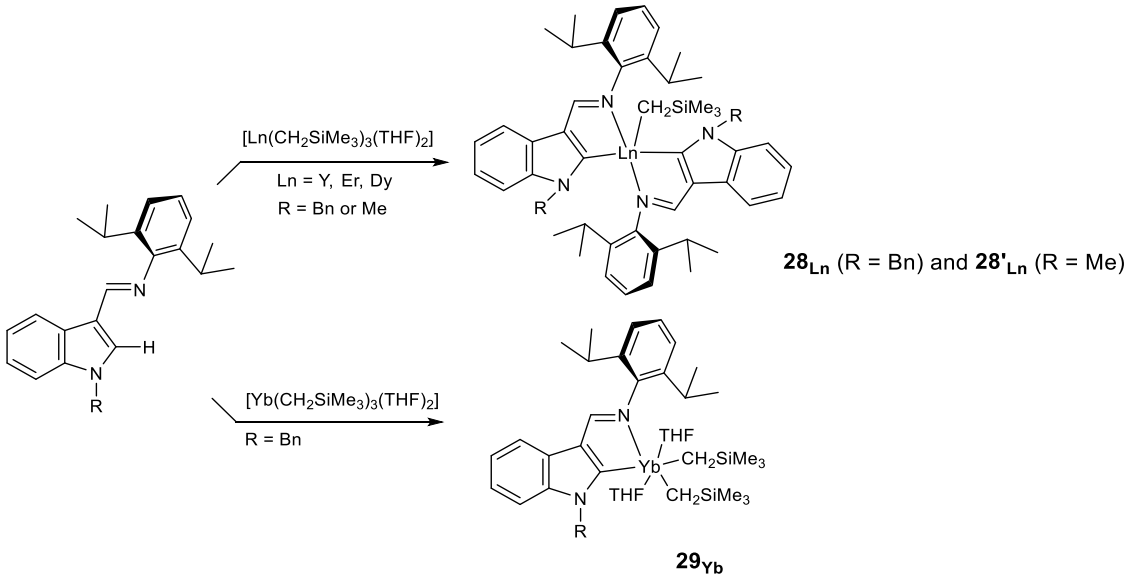

Scheme 11 Synthesis of bis-indolyl **28$_{Ln}$** and **28'$_{Ln}$** and mono-indolyl **29$_{Yb}$**

The X-ray diffraction analysis of the yttrium complexes **28$_{Y}$** and **28'$_{Y}$** indicated a rather similar five-coordinate distorted trigonal bipyramidal geometry around the metal center with Csp^2-Y bond distances in the same range (2.48 – 2.47 Å) (Fig. 17, left, **28'$_{Y}$**). On the other hand, the ytterbium complex **29$_{Yb}$** showed a six-coordinate octahedral geometry around the metal center (Fig. 17, right).

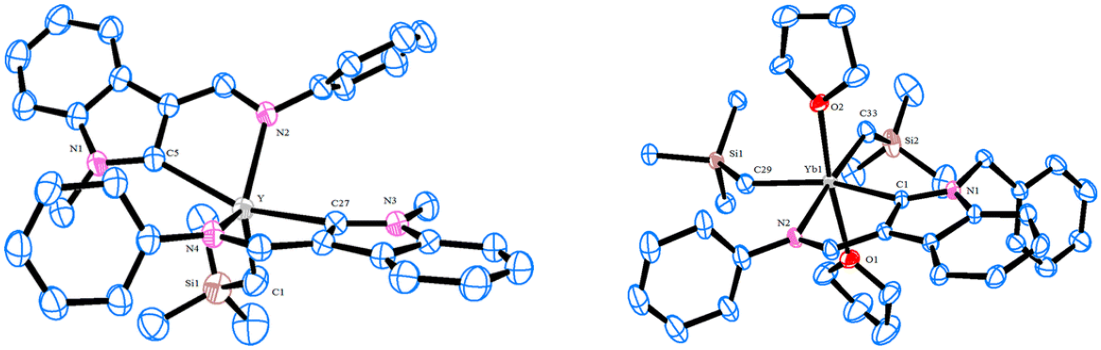

Fig. 17 Molecular structure of **28'$_{Y}$** (left) and of **29$_{Yb}$** (right) with thermal ellipsoids drawn at the 30% probability level. All hydrogen atoms and isopropyl groups are omitted for clarity. Reprinted with the permission of the American Chemical Society.[56]

Zhu *et al.* reported recently that the dinuclear pyrrolyl-functionalized β-diketiminato erbium alkynyl complex [MeC(NDipp)CHC(Me)N$CH_2CH_2NC_4H_2$-2,5-Me_2]Er(CH_2SiMe_3)(μ-C≡CPh)]$_2$ (**30$_{Er}$**, Dipp = 2,6-$^{i}Pr_2C_6H_3$) is obtained by the reaction of the lanthanide dialkyl precursor with phenylacetylene (Scheme 12).[57] According to the authors, activation of the terminal *sp*C-H bond in the alkyne takes place to afford dinuclear alkynyl **30$_{Er}$**.

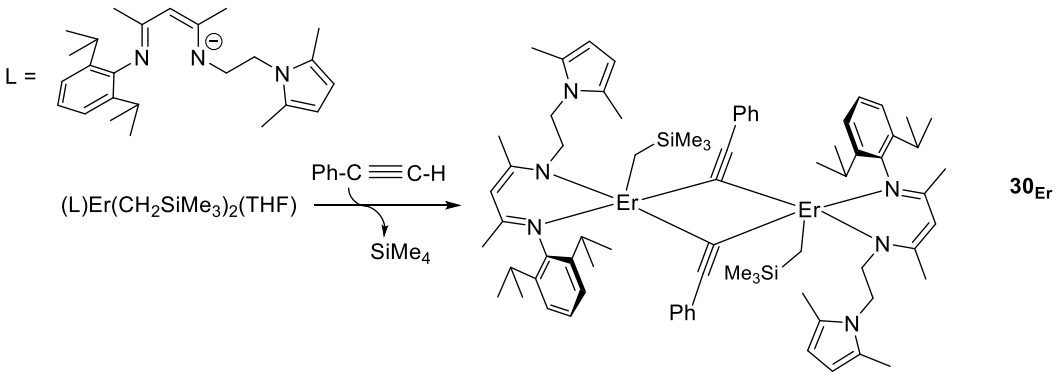

Scheme 12 Synthesis of alkynyl complex **30$_{Er}$**

From XRD, it was established that the alkynyl complex **30$_{Er}$** exhibits a centrosymmetric structure with phenylacetylene as a bridge bonded to the erbium ions, and the core of the molecule is a four-membered ring (Fig. 18).

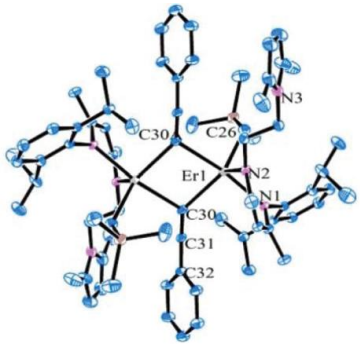

Fig. 18 Molecular structure of **30$_{Er}$** (hydrogen atoms and isopropyl groups are omitted for clarity). Reprinted with the authorization of the Royal Society of Chemistry.[57]

The group of Wang described the synthesis of {(R-C≡C)Ln[2-(^{t}BuN=CH)C$_8$H$_5$N]$_2$}$_2$ complexes (**31$_Y$**, Ln = Y, R = Ph; **31'$_{Yb}$**, Ln = Yb, R = SiMe$_3$) starting from [2-(^{t}BuN=CH)C$_8$H$_5$N]Ln[N(SiMe$_3$)$_2$]$_2$ combined with R-C≡CH (Scheme 13) that were prepared with the aim to study the mechanism of the catalytic addition of terminal alkynes on carbodiimide substrates.[58]

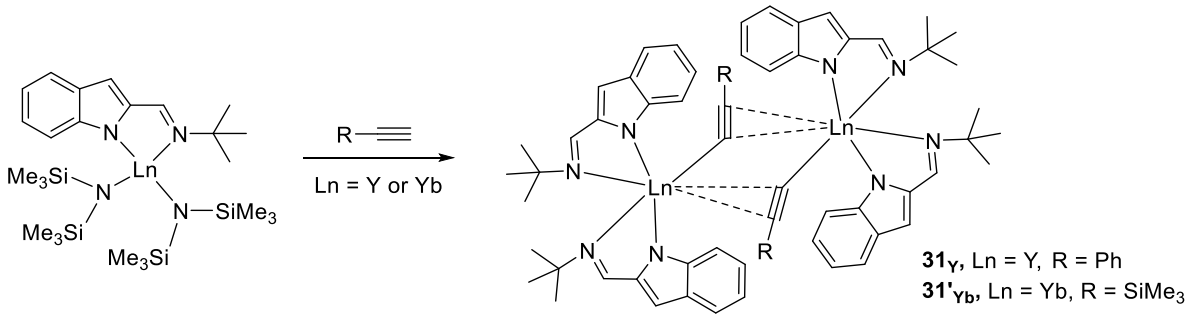

Scheme 13 Synthesis of alkynyl complexes **31$_Y$** and **31'$_{Yb}$**

The X-ray diffraction analysis on single-crystals of **31$_Y$** and **31'$_{Yb}$** revealed the formation of dimeric structures, with the alkynyl ligand being coordinated to the metal center in μ–η^1:η^2 haptic mode (Fig. 19).

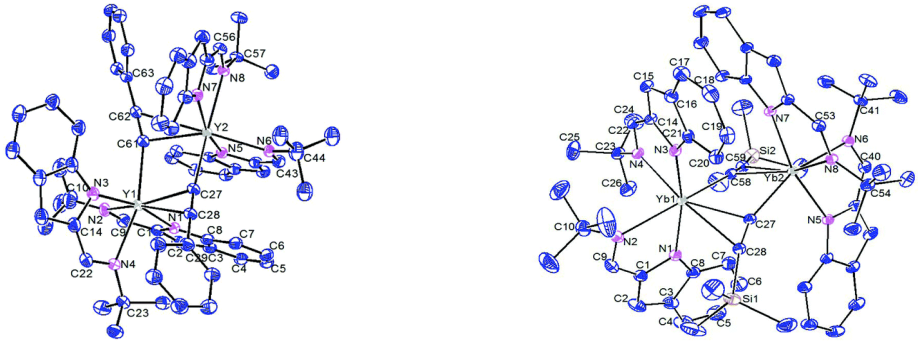

Fig. 19 Molecular structures of **31**$_{Y}$ (left) and **31'**$_{Yb}$ (right) with thermal ellipsoids set at the 15% probability level. All hydrogen atoms are omitted for clarity. Reprinted with the permission of the Royal Society of Chemistry.[58]

The addition of 1 equiv. of phenylacetylene to the monoalkyl (Tp^{Me2})Gd(THF)(Cp)(CH$_2$Ph) (Tp^{Me2} = tri(3,5-dimethylpyrazolyl)borate) in toluene afforded the corresponding phenylacetylide gadolinium complex [**32**$_{Gd}$] (Scheme 14 and Fig. 20).[59]

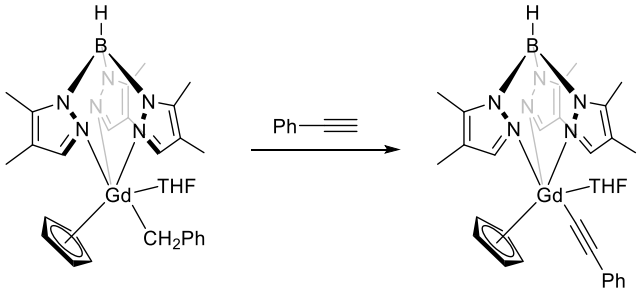

32$_{Gd}$

Scheme 14 Synthesis of alkynyl complex **32**$_{Gd}$

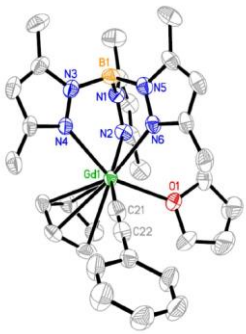

Fig. 20 Molecular structure of **32**$_{Gd}$ with 30% probability thermal ellipsoids. All hydrogen atoms are omitted for clarity. Reprinted with the permission of the American Chemical Society.[59]

Table 2 Structural and analytical data of alkenyl and alkynyl complexes (in brackets only the relevant complexes only, otherwise for all complexes)

Compound number	**Molecular Formula**	**X-ray data** Typical Ln-C (alkenyl or alkynyl) distances (Å)	**NMR data**	**References**

20$_{Sm}$, 20'$_{Sm}$	[(Cp*)$_2$Sm]$_2$(μ-η^2:η^4-CH$_2$CHPh); [(Cp*)$_2$Sm]$_2$(μ-η^2:η^4-PhCHCHPh)	not available	-	9
21$_{Sm}$, 21'$_{Sm}$	[(Cp*)$_2$Sm]$_2$[μ-η^2:η^4-CH$_2$CHC(Me)CH$_2$]; [(Cp*)$_2$Sm]$_2$[μ-η^2:η^4-CH$_2$CHC(CH$_2$)CH$_2$CH$_2$CHCMe$_2$]	Sm-C = 2.544(9), 2.674(9); Sm-C = 2.5294(4), 2.672(4)	^{1}H, ^{13}C	49
22$_Y$	[M(THF)$_x$][Y(Ph$_2$CCPh$_2$)$_2$] (M = Na, K)	Y-C = 2.518(6)	-	50
23$_{Nd}$, 23$_{Pr}$	[{(oepg)Ln}Na(THF)$_2$(μ-η^2:η^2-C$_2$H$_4$)]$_2$ (Ln = Nd, Pr)	Nd-C = 2.497(7), 2.790(7)	-	51
24$_{Nd}$, 24$_{Pr}$	[{(oepg)Ln}(Na)$_2$(μ-η^2:η^2-C$_2$)]$_2$ (Ln = Nd, Pr)	Pr-C = 2.670(4)	-	51
25$_{Sc}$	[(Cp''$_2$Sc)$_2$-(μ-η^2:η^2-C$_2$H$_4$)]	Sc-C = 2.314(3)	-	52
26$_{La}$, 26$_Y$	[(NNTBS)Ln(THF)]$_2$[μ–η^3:η^3-(E)-PhCHCHPh] (Ln = La, Y)	Y-C = 2.603(4), 2.581(5) and 2.741(7)	^{1}H, ^{13}C	54
27$_{Yb}$, 27'$_{Yb}$	[(Cp^{Bn5})Yb(DME)]$_2$[μ-C$_{10}$H$_8$]; [(Cp^{Bn5})Yb(DME)]$_2$(μ–η^4:η^4-PhCHCHCHCHPh) (Cp^{Bn5} = pentabenzylcyclopentadienyl, C$_{10}$H$_8$ = naphtalene)	Yb-C = 2.687(2), 2.681(2), 2.695(2), 2.720(2); Yb-C = 2.726(6), 2.745(6), 2.789(6), 2.821(4)	^{1}H, ^{13}C	55
28$_Y$, 28$_{Er}$, 28$_{Dy}$, 28'$_Y$, 28'$_{Er}$, 28'$_{Dy}$, 28'$_{Yb}$	[1-R-3-(2,6-^{i}Pr$_2$C$_6$H$_3$N=C)C$_8$H$_5$N]$_2$Ln(CH$_2$SiMe$_3$) (R = Bn, Ln = Y, Er, Dy; R = Me, Ln = Y, Er, Dy, Yb)	Y-C = 2.483(2), Er-C = 2.468(3), Dy-C = 2.489(3) ; Y-C = 2.473(4), Er-C = 2.466(4), Dy-C = 2.472(4), Yb-C = 2.422(3)	^{1}H (**28$_Y$**, **28'$_Y$**), ^{13}C (**28$_Y$**, **28'$_Y$**)	56
29$_{Yb}$	[1-Bn-3-(2,6-^{i}Pr$_2$C$_6$H$_3$N=C)C$_8$H$_5$N]Yb(CH$_2$SiMe$_3$)$_2$(THF)$_2$	Yb-C = 2.522(4)	-	56
30$_{Er}$	[MeC(NDipp)CHC(Me)NCH$_2$CH$_2$NC$_4$H$_2$-2,5-Me$_2$]Er(CH$_2$SiMe$_3$)(μ-C≡CPh)]$_2$	Er-C = 2.521(5)	-	57
31$_Y$, 31'$_{Yb}$	{(R-C≡C)Ln[2-(^{t}BuN=CH)C$_8$H$_5$N]$_2$}$_2$ (**31$_Y$**, Ln = Y, R = Ph; **31'$_{Yb}$**, Ln = Yb, R = SiMe$_3$)	Y-C = 2.502(8), 2.524(8) Yb-C = 2.483(4), 2.488(4)	^{1}H (**31$_Y$**), ^{13}C (**31$_Y$**)	58
32$_{Gd}$	(Tp^{Me2})Gd(THF)(Cp)(C≡PhC) (Tp^{Me2} = tri(3,5-dimethylpyrazolyl)borate)	Gd-C = 2.519(8)	-	59

3 Allyl complexes of the lanthanides

3.1 Homoleptic allyl complexes

3.1.1 Bis-allyl complexes

The substituted-allyl complexes of ytterbium under the form of THF adducts ([1-(SiMe$_3$)C$_3$H$_4$]$_2$Yb(THF)$_2$ [**33$_{Yb}$**] and [1-(SiPh$_3$)-3-(SiMe$_3$)C$_3$H$_3$]$_2$Yb(THF) [**34$_{Yb}$**] and terpyridine adducts [1,3-(SiMe$_3$)$_2$C$_3$H$_3$]$_2$Yb(tpy) [**35$_{Yb}$**], [1,3-(SiMe$_3$)$_2$C$_3$H$_3$]$_2$Yb(tpyCN), [**35'$_{Yb}$**] [1,3-(SiMe$_3$)$_2$C$_3$H$_3$]$_2$Yb(tpy(CN)$_2$

[**35''$_{Yb}$**], [1-(SiMe$_3$)C$_3$H$_4$]$_2$Yb(tpyCN) [**33'$_{Yb}$**] and [1-(SiPh$_3$)-3-(SiMe$_3$)C$_3$H$_3$]$_2$Yb(tpyCN) [**34'$_{Yb}$**] were synthesized (Scheme 15) and studied regarding the effect of allyl ligands on the internal charge-transfer process. The two allyl ligands are η^3-coordinated in the THF complexes according to their crystal structures and ^{1}H NMR data.[60]

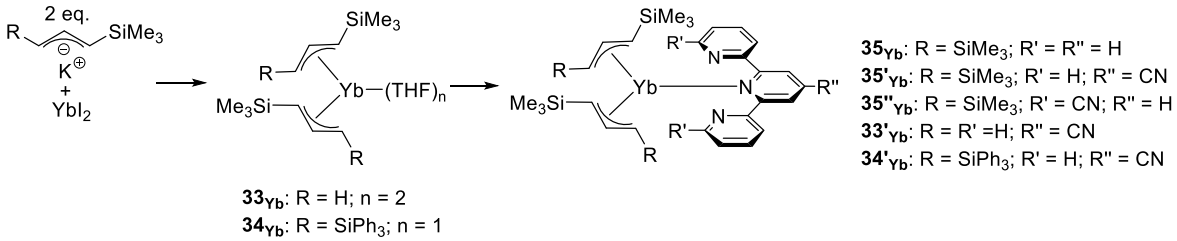

Scheme 15 Synthesis of bis(allyl) ytterbium complexes and their terpyridine adducts

The X-ray structure of **35$_{Yb}$** displays η^3-coordinated allyl ligands and shorter Yb-C distances (2.52(2) to 2.62(2) Å) than previously noticed in divalent [1,3-(SiMe$_3$)$_2$C$_3$H$_3$]$_2$Yb(THF)$_2$, which was explained by the +III oxidation state of Yb in the tpy adduct (Fig. 21).[61]

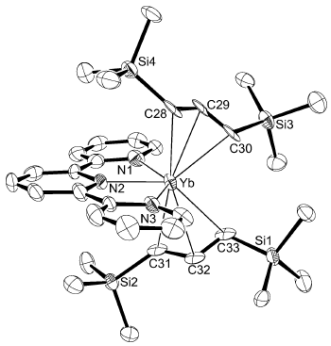

Fig. 21 Thermal ellipsoid representation of **35$_{Yb}$** (50% probability ellipsoids). H atoms have been omitted for clarity. Reprinted with the permission of the American Chemical Society.[61]

3.1.2 Tris-allyl complexes

The tris-allyl complexes of the group 3 metals and the lanthanides are known since the seminal work of Taube's research group,[3,4] later completed by Bochmann.[5]

In another study published in 2005, Bochmann and coworkers, trying to generalize the synthetic route to the tris-allyl derivatives of lanthanides, isolated the mixed lanthanide/magnesium derivatives **36$_{Ln}$** where Ln = La, Y, whereas anionic allyl species were obtained with neodymium and samarium (see further).[62] These compounds **36$_{Ln}$**, which were afforded in moderate yields, resulted from the reaction of LnI$_3$(THF)$_n$ with (allyl)magnesium iodide according to Scheme 16. From ^{1}H NMR analysis, it was deduced that the allyl moiety is η^3-coordinated to the lanthanide atom and η^1-bonded to Mg.

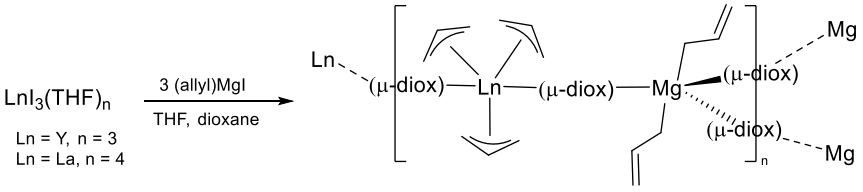

36$_{Ln}$

Scheme 16 Synthesis of [Ln(η^3-C$_3$H$_5$)$_3$(μ-dioxane)Mg(η^1-C$_3$H$_5$)$_2$(μ-dioxane)$_{1.5}$]$_\infty$ (**36$_{Ln}$**, Ln = La, Y)

From X-ray studies, the mode of coordination of the allyl groups was confirmed and it was also established that these complexes are coordination polymers, featuring sheets of parallel zigzag –[Mg-(μ-dioxane)-Mg-(μ-dioxane)]$_n$- chains, linked by –[(μ-dioxane)-Ln(η^3-C_3H_5)$_3$-(μ-dioxane)-Ln(η^3-C_3H_5)$_3$]$_n$- units as shown in Fig. 22 (for Ln = Y).

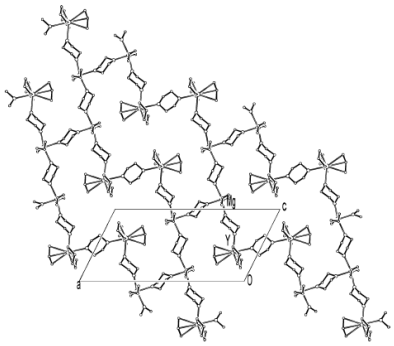

Fig. 22 Projection of the planar polymeric chains down the *b*-axis in **36$_Y$**. Reprinted with the authorization of the American Chemical Society. [62]

A few years later, Okuda brought an important contribution with the isolation of the tris-allyl complex [{Ce(η^3-C_3H_5)$_3$(diox)}$_2$(μ-diox)] [**37$_{Ce}$**] that was obtained by recrystallization in neat dioxane of [Ce(η^3-C_3H_5)$_3$(diox)] (diox = 1,4-dioxane) synthesized according to the published procedure (reaction of $LnCl_3$ with 3 equiv. of (allyl)MgCl, *vide infra*). From XRD analysis (Fig. 23, left), the geometry around the cerium center in **37$_{Ce}$** was found to be best described as distorted trigonal bipyramidal. In turn, recrystallization of [Ln(η^3-C_3H_5)$_3$(diox)] (Ln = Ce, Pr) in THF/pentane afforded the bis-THF adducts [Ln(η^3-C_3H_5)$_3$(THF)$_2$] [**37'$_{Ln}$**] as crystals suitable for X-ray diffraction studies. In the molecular structure of **37'$_{Ce}$**, two allyl groups and a THF molecule are found in the equatorial plane, with the third allyl group and an additional THF molecule occupying the apical positions (Fig. 23, right).[6]

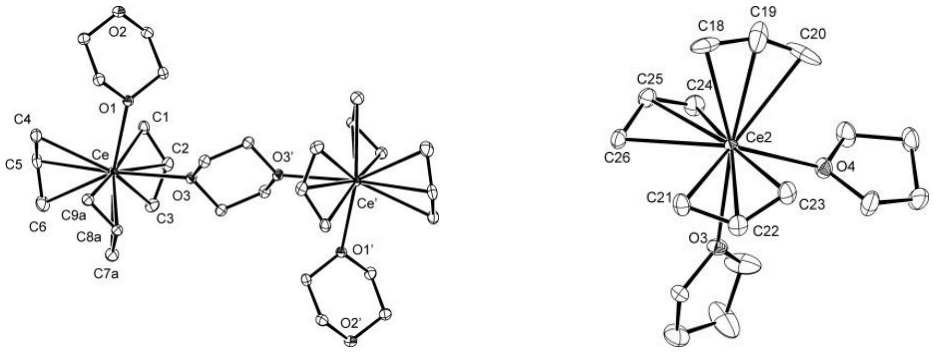

Fig. 23 Molecular structures of **37$_{Ce}$** (left) and **37'$_{Ce}$** (right). Thermal ellipsoids are drawn at the 30% probability level, hydrogen atoms are omitted for clarity. Reprinted with the authorization of Wiley-VCH Verlag GmbH.[6]

Quite surprisingly, it is only in 2011 that the tris(allyl)scandium compounds [Sc(C_3H_5)$_3$(THF)$_n$] (n = 0, 2) were obtained, by the simple reaction of anhydrous $ScCl_3$ with three equivalents of allylpotassium or 1.5 equivalents of bis(allyl)calcium in THF at 0 °C (Scheme 17).[63]

$$ScCl_3(THF)_n \xrightarrow[\text{or } 3/2\ Ca(C_3H_5)_2]{3\ K(C_3H_5)} \underset{\mathbf{37'_{Sc}}}{Sc(\eta^3\text{-}C_3H_5)_2(\eta^1\text{-}C_3H_5)(THF)_2} \xrightarrow{\text{vacuum}} \underset{\mathbf{37''_{Sc}}}{Sc(C_3H_5)_3}$$

Scheme 17 Synthesis of **37'$_{Sc}$** followed by subsequent vacuum treatment affording **37''$_{Sc}$**

Drying *in vacuo* of the bis-THF adduct **37'$_{Sc}$** afforded the homoleptic uncoordinated $Sc(C_3H_5)_3$ (**37''$_{Sc}$**). X-ray diffraction studies on crystals isolated from THF solution revealed that, in the bis-THF adduct **37'$_{Sc}$**, two allyl ligands are coordinated in an η^3-fashion while one allyl ligand is in the η^1-mode, consistent with the formula $Sc(\eta^1\text{-}C_3H_5)_3(\eta^3\text{-}C_3H_5)_2(THF)_2$ (Fig. 24). This structural arrangement is in good agreement with the *ab initio* calculations carried out by the group of Schaefer, in which the theoretical study performed on divalent and trivalent homoleptic allyl complexes $Sc(C_3H_5)_2$ and $Sc(C_3H_5)_3$ suggested that in both complexes, the allyl groups are bonded as fluxional trihapto to the Sc metal.[64]

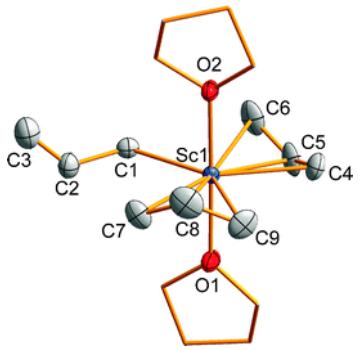

Fig. 24 Molecular structure of **37'$_{Sc}$** (ellipsoids are set at the 50% probability level, hydrogen atoms are omitted for clarity). Reprinted with the permission of the Royal Society of Chemistry. [63]

In 2006, Hanusa and coworkers attempted the synthesis of a non-solvated tris-allyl derivative of lanthanide bearing the bis-trimethylsilylallyl ligand. They carried out the reaction with an holmium precursor, a metal of small ionic radius among the lanthanides family (thus belonging to the *late* sub-group of lanthanides),[65] since THF-adducts $Ln[1,3\text{-}(SiMe_3)_2C_3H_3]_3(THF)$ were formed with lanthanides of larger ionic radius (belonging to the *early* sub-group of lanthanides). [6161] Instead of the presumably formed tris-allyl derivative, the isolated holmium compound was a dimeric complex of formula $\{[1,3\text{-}(SiMe_3)_2C_3H_3]Ho[CH(SiMe_3)CHCHSiMe_2\text{-}\mu\text{-}CH_2]\}_2$ [**38$_{Ho}$**] in which hydrogen abstraction from a trimethylsilyl group has occurred on two allyl ligands, resulting in the formation of dimethylsilylene units that bridge the holmium atoms (Fig. 25, left).[66]

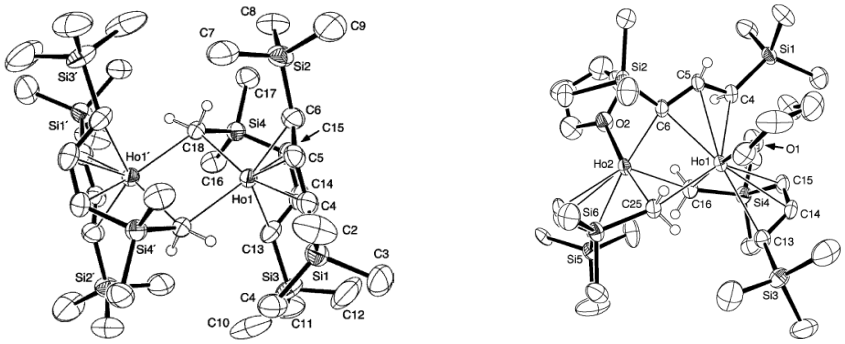

Fig. 25 Molecular structure of **38$_{Ho}$** (left) and **39$_{Ho}$** (right) (ellipsoids are set at the 50% probability level, hydrogen atoms of the dimethylsilylene and allylidene bridges are omitted for clarity). Reprinted with the permission of the American Chemical Society. [66]

Furthermore, when the reaction time was prolonged, a second and different product was isolated and structurally characterized, $\{(THF)Ho[CH(SiMe_3)CHCHSiMe_2\text{-}\mu\text{-}CH_2]\}_2[\mu\text{-}\eta^1,\eta^3\text{-}C(SiMe_3)CHCHSiMe_3]$ [**39$_{Ho}$**], in which, in addition to two dimethylsilylene bridges, the metal centers are joined with a μ-η^1,η^3-allylidene ligand (Fig. 25, right). Evidence for delocalized bonding in the allylidene fragment was provided from both crystallographic and computational studies. A tentative explanation of the successive formation of the two compounds, due to the presence of residual water in the starting holmium triflate material, is given in scheme 18.

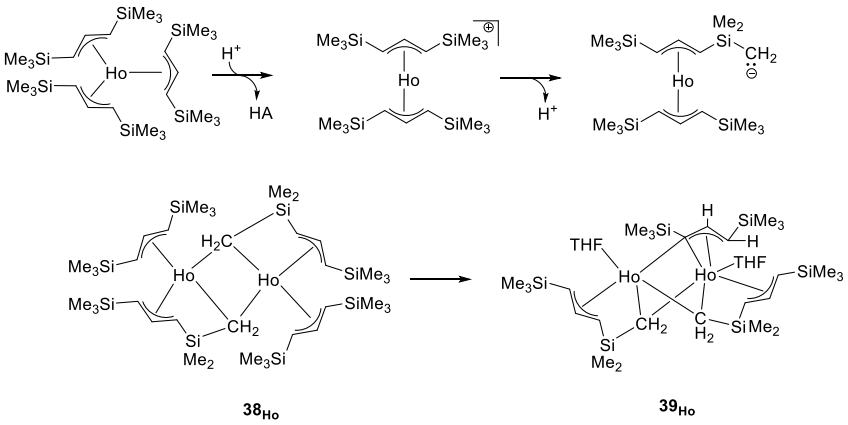

Scheme 18 Proposed explanation for the formation of bis(trimethylsilyl)allyl holmium complexes **38$_{Ho}$** and **39$_{Ho}$**[66]

A generalization about the strategy of synthesis of allyl complexes of the lanthanides with [1,3-bis(trimethylsilyl)allyl] ligand was then proposed by Hanusa and coworkers in 2007.[67] The authors succeeded in the preparation in good yields (> 75%) of tris-allyl lanthanide Ln[1,3-$(SiMe_3)_2C_3H_3]_3$ complexes **40$_{Ln}$**, by starting from rigorously anhydrous triflates $Ln(OTf)_3$ (Ln = Dy, Ho, Er, Tm, Lu) with 3 equiv. of K[1,3-$(SiMe_3)_2C_3H_3$] in THF (scheme 19).

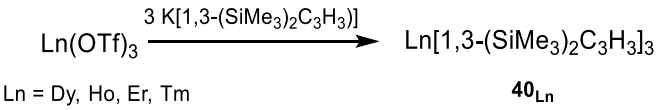

Scheme 19 Straightforward synthesis of tri-[(bistrimethylsilyl)allyl] complexes **40$_{Ln}$** using the potassium allyl reagent as starting material

All complexes in this small ionic radius lanthanide series were found to be non-solvated. The thulium compound Tm[1,3-$(SiMe_3)_2C_3H_3]_3$ (**40$_{Tm}$**) could be crystallographically characterized (Fig. 26), showing the three allyl ligands η^3-bounded to the metal and the Tm–C bond distances range from 2.326(2) to 2.606(2) Å, with an average of 2.53(1) Å.

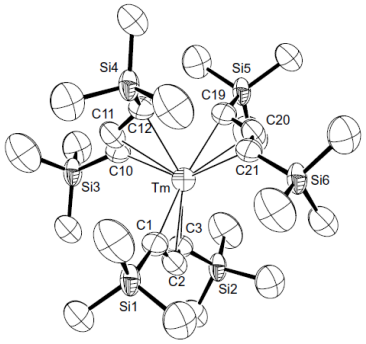

Fig. 26 Molecular structure of **40$_{Tm}$** (ellipsoids are set at the 50% probability level, hydrogen atoms are omitted for clarity). Reprinted with the permission of Elsevier.[67]

Starting from the trichlorides with Ln = Ho or Er, the (bistrimethylsilyl)allyl complexes were isolated as well, whether with two or three equivalents of allyl ligand as starting material, as same as previously observed with yttrium.[68] The same tris(allyl) product **40$_{Ho}$** was isolated in the case of starting with HoI_3 as precursor. However, this was an unexpected result, as anionic "ate" complexes of formula [Ln[1,3-$(SiMe_3)_2C_3H_3]_3I]^-$ were previously shown to be formed in the dysprosium and erbium series when the triiodides were used as precursors.[69] To isolate the tetra-allyl lanthanate holmium complex **41$_{Ho}$**, the

authors found that it was necessary to carry out the reaction from the lithium allyl reagent (Scheme 20). Unfortunately, they could not obtain X-ray quality crystals of that complex.

$$Ho(OTf)_3 \xrightarrow[THF]{3\ Li[1,3\text{-}(SiMe_3)_2C_3H_3)]} [Ho[1,3\text{-}(SiMe_3)_2C_3H_3]_3I]^-[Li(THF)_4]^+$$

41$_{Ho}$

Scheme 20 Synthesis of tetra-[(bistrimethylsilyl)allyl] "ate" complex **41$_{Ho}$** starting from the lithium allyl reagent.

It was not until 2014 that the tris-allyl scandium complex Sc[1,3-(SiMe$_3$)$_2$C$_3$H$_3$]$_3$ [**42$_{Sc}$**] comprising the same bulky tris[1,3-bis(trimethylsilyl)allyl] groups was prepared, by mechanochemical synthesis *via* ionic metathesis between $ScCl_3$ and the potassium salt of the allyl anion. The X-ray crystal structure of this hexane-soluble compound revealed monomeric compound having three π-bound η^3-allyl ligands (Fig. 27), which was confirmed by ^{1}H NMR analysis in solution.[70]

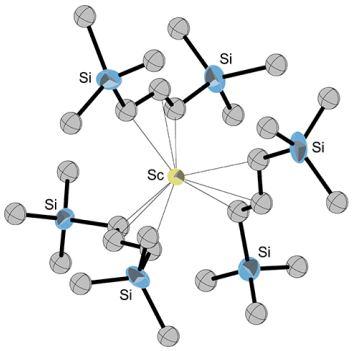

Fig. 27 Molecular structure of **42$_{Sc}$** with the thermal ellipsoids drawn at the 50% probability level, hydrogen atoms are excluded for clarity. Reprinted with the authorization of the American Society of Chemistry.[70]

3.1.3 Bis-allyl cationic complexes

The lanthanum and the neodymium [Ln(allyl)$_2$][B(C$_6$F$_5$)$_4$] ionic pairs were briefly described and assessed as single-component catalysts for butadiene polymerization in 1999.[71] It is however a decade later that Okuda and co-workers reported the full synthesis of a series of mono-cationic bis-allyl complexes [Ln(η^3-C$_3$H$_5$)$_2$(THF)$_3$]$^+$[B(C$_6$F$_5$)$_4$]$^-$ (**43$_{Ln}$**, Ln = Y, La, Nd), by reacting the tris-allyl complexes Ln(η^3-C$_3$H$_5$)$_3$(diox), described by Taube, with one equivalent of [HNMe$_2$Ph][B(C$_6$F$_5$)$_4$] in THF (Scheme 21).[6] The mono-cationic bis-allyl analogues, bearing a non-perfluorinated counteranion [Ln(η^3-C$_3$H$_5$)$_2$(THF)$_3$]$^+$[BPh$_4$]$^-$ (**43'$_{Ln}$**, Ln = Y, La, Nd) were prepared similarly using [HNEt$_3$][BPh$_4$].

$$Ln(C_3H_5)_3(diox) \xrightarrow{[HNR_3][B(C_6X_5)_4]} [Ln(\eta^3\text{-}C_3H_5)_2(THF)_3]^+[B(C_6X_5)_4]^-$$

43$_{Ln}$, $NR_3 = NMe_2Ph$, X = F, Ln = Y, La, Nd
43'$_{Ln}$, $NR_3 = NEt_3$, X = H, Ln = Y, La, Nd, Ce, Pr

Scheme 21 Synthesis of ionic pairs **43$_{Ln}$** and **43'$_{Ln}$** by protonation of the tris-allyl precursors with ammonium borates.

An X-ray crystal study of the mono-cationic yttrium complex **43'$_Y$** showed that all three allyl ligands are η^3- coordinated with similar bond lengths between each allyl ligand and yttrium metal (Fig. 28). The neodymium and lanthanum analogues (the cerium and praseodymium complexes were not analyzed) were found to contain a fourth THF molecule. Shorter metal-allyl bonds were noticed in these complexes by comparison with the neutral tris-allyl parent complexes, revealing a higher Lewis acidity of the rare earth metal from neutral to cationic species.

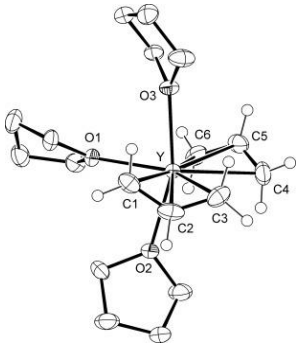

Fig. 28 Molecular structure of **43'$_Y$** with displacement ellipsoids set at the 50% probability level (the counter-anion and hydrogen atoms are omitted for the sake of clarity). Reprinted with permission of WILEY-VCH Verlag GmbH.[6]

The ^{1}H NMR analysis of both yttrium complexes **43$_Y$** and **43'$_Y$** displayed two signals (1H/4H relative ratio) for the allyl group, corresponding to fast *syn*/*anti* exchange on the NMR timescale. In contrast, three distinct signals were seen for the lanthanum and neodymium ones, typical of slow *syn*/*anti* exchange.

Upon reaction of the tris-allyl precursors with a Lewis acid ER_3 ($Al(CH_2SiMe_3)_3$ or BPh_3), allyl abstraction took place, affording the ion pair $[Ln(\eta^3\text{-}C_3H_5)_2(THF)_3]^+[ER_3(\eta^1\text{-allyl})]^-$ (**43''$_Y$**, E = Al, Ln = Y; **43'''$_{Ln}$**, E = B, Ln = Y, La), where the abstracted allyl group is found η^1-coordinated to the E element (Scheme 22).

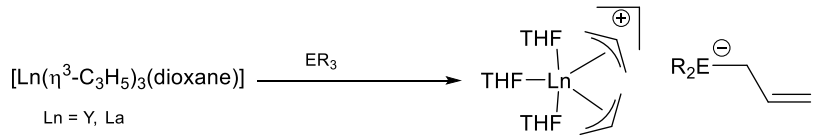

43"$_Y$: Ln = Y, E = Al, R = CH_2SiMe_3
43"'$_{Ln}$: Ln = Y, La, E = B, R = Ph

Scheme 22 Synthesis of ionic pairs **43''$_Y$** and **43'''$_{Ln}$** by allyl abstraction with a Lewis acid.

Interestingly, it was found that benzophenone inserts into the La-C(allyl) bond of **43'$_{La}$** to form the bis(alkoxy) complex $[La\{OCPh_2(CH_2CH{=}CH_2)\}_2(THF)_3]^+[BPh_4]^-$ (**44$_{La}$**). It is noteworthy that, however, the yttrium derivative **43'$_Y$** failed to react under the same conditions.

The bis-allyl cation $[Sc(\eta^3\text{-}C_3H_5)_2(THF)_3]^+$ was isolated two years after the other lanthanide counterparts, upon protonation of the tris-allyl scandium **37'$_{Sc}$** with a Brønsted acid similarly as shown in Scheme 21. Depending on the acid reagent, three ionic pairs of formula $[Sc(\eta^3\text{-}C_3H_5)_2(THF)_3]^+[B(C_6X_3Z_2)_4]^-$ (**43'$_{Sc}$**: X = Z = H; **43''''$_{Sc}$**: X = H, Z = Cl; **43$_{Sc}$**: X = Z = F) could be isolated. The X-ray structure of **43'$_{Sc}$** showed that the allyl ligands are η^3-coordinated. The ^{1}H NMR analysis indicated dynamic behavior of the allyl ligand.[63] This cationic complex was also isolated by the reaction of two equiv. of Brønsted acid with tetraanionic $K[Sc(C_3H_5)_4]$ (*vide supra*).

The bis-allyl mono-cationic complexes **43$_{Ln}$** were found to be active towards the polymerization of 1,3-butadiene when combined with $Al(^iBu)_3$ as co-catalyst.[6,63] Among the resulting catalytic combinations, the yttrium catalyst was found to be the most active (TOF 10,000 h^{-1}) leading to the formation of polybutadiene (PB) with the highest 1,4-*cis* stereoregularity of 90% in rare contradiction of the well-known "neodymium effect", where neodymium exhibits the best performances along the rare earths family for this kind of polymerization catalysis.[12] The addition of one extra equivalent of $[NPhMe_2H][B(C_6F_5)_4]$ to the mono-cationic **43$_Y$**/$Al(^iBu)_3$ catalyst system in the butadiene polymerization mixture led to an increase in both the activity (up to TOF - 12,000 h^{-1}) and the selectivity (92.5% of 1,4-*cis* PB). The *in situ* formation of mono-allyl di-cationic species was likely to be responsible for the better

reactivity according to the authors.[6] In the case of scandium, the complex displayed low activity (TOF 95 h^{-1}) in styrene polymerization to afford atactic PS, with little improvement when $[HNMe_2Ph][B(C_6F_5)_4]$ was added in the reaction mixture.[63]

3.1.4 Mono-allyl dicationic complexes

The first examples of mono-allyl di-cationic complexes of the early lanthanides La and Nd $[Ln(\eta^3\text{-}C_3H_5)(THF)_6]^{2+}[BPh_4]_2^-$ [**45$_{Ln}$**] could be prepared by protonation of their tris-allyl precursors with two equivalents of $[HNEt_3][BPh_4]$. The same products were isolated from the single protonation of the mono(allyl) cationic complexes **43'$_{Ln}$** with one equivalent of acid (Scheme 23).[6]

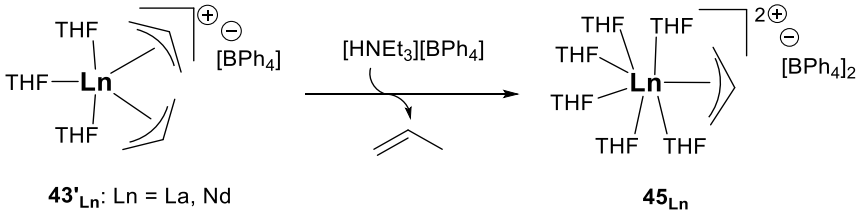

43'$_{Ln}$: Ln = La, Nd

45$_{Ln}$

Scheme 23 Protonation of the mono-cationic precursors **43'$_{Ln}$** with ammonium borates leading to di-cationic **45$_{Ln}$** complexes

X-ray quality crystals were obtained for the lanthanum complex [**45$_{La}$**], where a distorted pentagonal-bipyramidal coordination geometry was observed, with the remaining allyl group occupying the axial position.

Slow reaction with pyridine indicated a rather inertness of the remaining allyl group in these di-cationic **45$_{Ln}$** ion pairs (Ln = La, Nd), in contrast to what was expected from the reactivity observed in butadiene polymerization where the *in situ* formation of similar species was postulated (*vide infra*).

3.1.5 Tetra-allyl anionic complexes

When $[Sc(C_3H_5)_3(THF)_2]$ [**37'$_{Sc}$**] was treated with one equivalent of allylpotassium, the "ate" complex $K[Sc(C_3H_5)_4]$ [**46$_{Sc}$**] was obtained, which could also be synthesized directly by treating $ScCl_3$ with four equivalents of allylpotassium (Scheme 24). The ^{1}H NMR spectrum of this complex shows a doublet and a quintet for the allyl groups, indicating fluxional behavior of the allyl moiety in solution.[63]

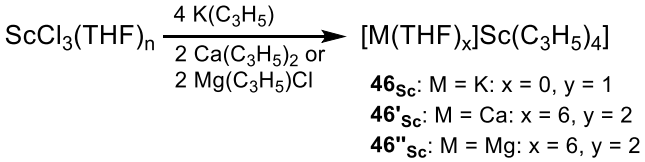

46$_{Sc}$: M = K: x = 0, y = 1
46'$_{Sc}$: M = Ca: x = 6, y = 2
46''$_{Sc}$: M = Mg: x = 6, y = 2

Scheme 24 Synthesis of tetra-allyl ionic scandium complexes

When $ScCl_3$ was treated with two equivalents of bis(allyl)calcium, $[Ca(THF)_6][Sc(C_3H_5)_4]_2$ [**46'$_{Sc}$**] was obtained, while the reaction of $ScCl_3$ with two equivalents of (allyl)MgCl afforded X-ray quality crystals of the adduct $[Mg(THF)_6][Sc(C_3H_5)_4]_2$ [**46''$_{Sc}$**]. In this latter complex, two allyl ligands are found η^1- and the two others are η^3–coordinated to the scandium center (Fig. 29).

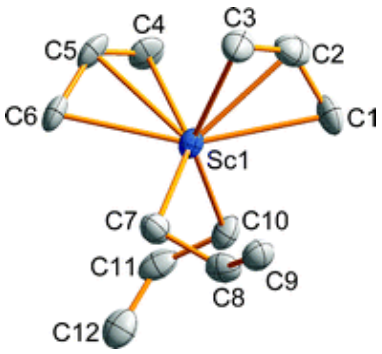

Fig. 29 Molecular structure of **46''$_{Sc}$**. The cationic counter-cation and hydrogen atoms are omitted for clarity. Thermal ellipsoids drawn at the 50% probability level. Reprinted with the authorization of the Royal Society of Chemistry.[63]

Tetra-allyl ionic compounds of the larger lanthanides were prepared some years before these scandium derivatives.[62] The heterobimetallic trinuclear {[Mg(THF)$_6$][Nd(η^3-C$_3$H$_5$)$_4$]$_2$(THF)$_2$} [**46''$_{Nd}$**] was isolated from the room temperature reaction between NdI$_3$(THF)$_{3.5}$ and 3 equiv. of (allyl)MgI in a THF/dioxane mixture. On the other hand, under the same experimental conditions, the tetra-allyl samarium complex was first isolated as {[Mg(THF)$_6$][Sm$_2$(η^3-C$_3$H$_5$)$_6$(μ-η^3:η^3-C$_3$H$_5$)]$_2$(toluene)} [**47$_{Sm}$**], which yielded {[Mg(THF)$_6$][Sm(η^3-C$_3$H$_5$)$_4$]$_2$(THF)$_2$} [**46''$_{Sm}$**] after reaction in hot THF with the diketimine ArN=C(Me)CH=C(Me)NHAr (Ar = 2,6-C$_6$H$_3$^{i}Pr$_2$), along with the previously reported allyl(diketiminate)Sm(η^3-C$_3$H$_5$)$_2${HC-(MeCNAr)$_2$} [5] and the known Sm(η^3-C$_3$H$_5$)$_3$.

X-ray crystal analysis of **47$_{Sm}$** showed a binuclear anion [Sm$_2$(η^3-C$_3$H$_5$)$_7$]$^-$ that involves two samarium centers in distorted tetrahedral arrangements, with three terminal and one bridging η^3-allyl ligand (Fig. 30). The X-Ray structure of **46''$_{Nd}$** was also elucidated, featuring the tetra-allyl anion [Nd(η^3-C$_3$H$_5$)$_4$]$^-$ of the type already discussed in details by Taube in [Li(dioxane)$_{1.5}$][Ln(η^3-C$_3$H$_5$)$_4$] (Ln = La, Nd).[3]

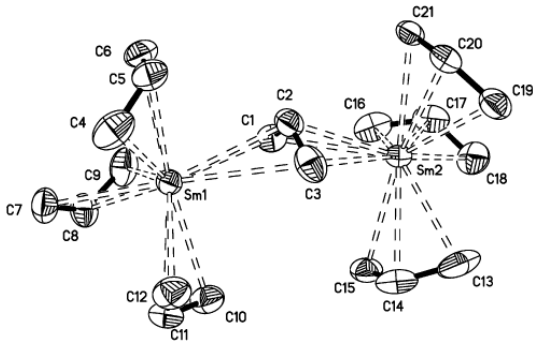

Fig. 30 X-ray molecular structure of **47$_{Sm}$**. The cationic Mg counter-cation and hydrogen atoms are omitted for clarity. Thermal ellipsoids drawn at the 50% probability level. Reprinted with the authorization of the American Chemical Society.[62]

Table 3 Structural and analytical data of homoleptic allyl complexes (in brackets only the relevant complexes only, otherwise for all complexes)

Compound number	**Molecular Formula**	**X-ray data** Ln-C(allyl) distances (Å)	**NMR data**	**References**
33$_{Yb}$, **33'$_{Yb}$**	[1-(SiMe$_3$)C$_3$H$_4$]$_2$Yb(L)$_2$ (L = THF, tPyCN)	**35'$_{Yb}$**: Yb-C = 2.52(2) to 2.62(2)	^{1}H	60,61
34$_{Yb}$, **34'$_{Yb}$**	[1-(SiPh$_3$)-3-(SiMe$_3$)C$_3$H$_3$]$_2$Yb(L) (L = THF, tPyCN)			

35$_{Yb}$,35'$_{Yb}$, 35''$_{Yb}$	[1,3-(SiMe$_3$)$_2$C$_3$H$_3$]$_2$Yb(L) (L = THF, tPyCN, tPy(CN)$_2$)			
36$_{Y}$, 36$_{La}$	[Ln(η^3-C$_3$H$_5$)$_3$(μ-dioxane)Mg(η^1-C$_3$H$_5$)$_2$(μ-dioxane)$_{1.5}$]$_\infty$	Y-C = 2.600(8), 2.589(8), 2.525(11); 2.770(9), 2.704(9), 2.686(8); 2.622(5), 2.645(5), 2.709(5); Mg-C = 2.188(8); 2.189(8) La-C = 2.794(6), 2.827(6), 2.756(6); 2.815(7), 2.8068, 2.739(6); 2.731(6), 2.783(6), 2.763(6); Mg-C = 2.197(6), 2.195(6)	^{1}H, ^{13}C	62
37$_{Ce}$	[{Ce(η^3-C$_3$H$_5$)$_3$(diox)}$_2$(μ-diox)]	Ce-C = 2.765(3), 2.780(3), 2.719(3)	-	6
37'$_{Ce}$, 37'$_{Pr}$	[Ln(η^3-C$_3$H$_5$)$_3$(THF)$_2$] (Ln = Ce, Pr)	-	^{1}H, ^{13}C	6
37'$_{Sc}$,	[Sc(η^1-C$_3$H$_5$)(η^3-C$_3$H$_5$)$_2$(THF)$_2$]	η^1-C$_3$H$_5$: Sc-C = 2.373(4); η^3-C$_3$H$_5$: Sc-C = 2.434(4), 2.479(4), 2.557(4), 2.493(4), 2.485(4), 2.447(4)	^{1}H, ^{13}C	63
37''$_{Sc}$	[Sc(η^3-C$_3$H$_5$)$_3$]	-	-	63, 64
38$_{Ho}$	{[1,3-(SiMe$_3$)$_2$C$_3$H$_3$]Ho[CH(SiMe$_3$)CHCHSiMe$_2$-μ-CH$_2$]}$_2$	Ho-C = 2.603(4), 2.617(4), 2.510(4)	-	66
39$_{Ho}$	{(THF)Ho[CH(SiMe$_3$)CHCHSiMe$_2$-μ-CH$_2$]}$_2$[μ-η^1,η^3-C(SiMe$_3$)CHCHSiMe$_3$]	Ho-C = 2.564(5), 2.645(5), 2.500(5)	-	66
40$_{Dy}$, 40$_{Ho}$, 40$_{Er}$, 40$_{Tm}$, 40$_{Lu}$	Ln[1,3-(SiMe$_3$)$_2$C$_3$H$_3$]$_3$ (Ln = Dy, Ho, Er, Tm, Lu)	Tm-C = 2.326(2) to 2.606(2)	-	67
41$_{Ho}$	[Ho[1,3-(SiMe$_3$)$_2$C$_3$H$_3$]$_3$I]$^-$ [Li(THF)$_4$]$^+$	-	-	67
42$_{Sc}$	Sc[1,3-(SiMe$_3$)$_2$C$_3$H$_3$]$_3$	Sc−C = 2.38(3) average distance	^{1}H	70
43$_{Y}$, 43$_{La}$, 43$_{Nd}$	[Ln(η^3-C$_3$H$_5$)$_2$(THF)$_3$]$^+$[B(C$_6$F$_5$)$_4$]$^-$ (Ln = Y, La, Nd)	-	^{1}H, ^{13}C, ^{11}B, ^{19}F	6
43'$_{Y}$, 43'$_{La}$, 43'$_{Ce}$, 43'$_{Pr}$, 43'$_{Nd}$	[Ln(η^3-C$_3$H$_5$)$_2$(THF)$_3$]$^+$[BPh$_4$]$^-$ (Ln = Y, La, Ce, Pr, Nd)	Y-C = 2.617(3), 2.597(3), 2.515(3), 2.584(3), 2.608(3), 2.593(3) La-C = 2.783(4), 2.757(4), 2.711(4), 2.753(4), 2.798(4), 2.772(4) Nd-C = 2.704(17), 2.747(16), 2.725(16), 2.689(18), 2.691(18), 2.729(17)	^{1}H, ^{13}C (**43'$_{La}$**, **43'$_{Ce}$**, **43'$_{Pr}$**, **43'$_{Nd}$**) ^{11}B (**43'$_{La}$**, **43'$_{Ce}$**, **43'$_{Pr}$**, **43'$_{Nd}$**)	6
43''$_{Y}$, 43'''$_{Y}$, 43'''$_{La}$	[Ln(η^3-C$_3$H$_5$)$_2$(THF)$_3$]$^+$[ER$_3$(η^1-allyl)]$^-$ (E = Al, Ln = Y; E = B, Ln = Y, La)	-	^{1}H, ^{13}C, ^{27}Al (**43''$_{Y}$**) ^{11}B (**43'''$_{Y}$**, **43'''$_{La}$**)	6
44$_{La}$	[La{OCPh$_2$(CH$_2$CH=CH$_2$)}$_2$(THF)$_3$]$^+$[BPh$_4$]$^-$	-	^{1}H, ^{13}C, ^{11}B	6

43'$_{Sc}$, 43''''$_{Sc}$, 43$_{Sc}$	[Sc(η^3-C_3H_5)$_2$(THF)$_3$][B($C_6X_3Z_2$)$_4$] (X = Z = H; X = H, Z = Cl; X = Z = F)	**43'$_{Sc}$**: Sc-C = 2.5071(16), 2.4662(16), 2.4117(16), 2.3854(16), 2.474(2), 2.486(6), 2.5870(17)	^{1}H (**43'$_{Sc}$**)	63
45$_{La}$, 45$_{Nd}$	[Ln(η^3-C_3H_5)(THF)$_6$]$^{2+}$[BPh_4]$_2^-$ (Ln = La, Nd)	**45$_{La}$**: distorted structure	^{1}H, ^{13}C, ^{11}B	6
46$_{Sc}$	K[Sc(C_3H_5)$_4$]	-	^{1}H	63
46'$_{Sc}$	[Ca(THF)$_6$][Sc(C_3H_5)$_4$]$_2$	-	^{1}H, ^{13}C	63
46''$_{Sc}$	[Mg(THF)$_6$][Sc(η^1-C_3H_5)$_2$(η^3-C_3H_5)$_2$]$_2$	η^3-C_3H_5: Sc-C = 2.450(5), 2.436(6), 2.450(6); Sc-C = 2.488(5), 2.453(5), 2.424(5) η^1-C_3H_5: Sc-C = 2.271(5), 2.277(5)	^{1}H, ^{13}C	63
46''$_{Nd}$, 46''$_{Sm}$	{[Mg(THF)$_6$][Ln(η^3-C_3H_5)$_4$]$_2$(THF)$_2$}	Sm-C = 2.761(5), 2.708(4), 2.648(4); 2.673(4), 2.712(5), 2.751(5); 2.739(5), 2.738(4), 2.734(4); 2.709(4), 2.736(4), 2.743(4)		62
47$_{Sm}$	{[Mg(THF)$_6$][Sm$_2$(η^3-C_3H_5)$_6$(μ-η^3:η^3-C_3H_5)]$_2$(toluene)}	Bridging allyl: Sm(1)-C = 2.793(6), 2.762(6), 2.977(6); Sm(2)-C = 2.774(6), 2.765(6), 2.972(6) η^3-allyl: Sm(1)-C = 2.675(5), 2.700(5), 2.680(5); 2.725(5), 2.710(5), 2.651(5); 2.713(5), 2.701(5), 2.623(5); Sm(2)-C = 2.699(5), 2.712(5); 2.712(5); 2.655(5), 2.717(5), 2.712(6); 2.632(5), 2.691(5), 2.673(5)	-	62

3.2 Mono-substituted bis-allyl complexes: (Allyl)$_2$LnX compounds

3.2.1 (Allyl)$_2$LnX compounds with halide ligand

In 2006, Carpentier and coworkers extended the family of heterobimetallic bis-allyl derivatives of formula Ln(allyl)$_2$Cl(MgCl$_2$)$_2$(THF)$_4$ to Ln = Y and La [**48$_{Ln}$**], after the pioneering synthesis of their neodymium congener by Porri and coworkers.[72] All complexes were synthesized from LnCl$_3$(THF)$_n$ and (allyl)MgCl in THF (Scheme 25). Two sets of broadened resonances for two inequivalent allyl groups were observed by ^{1}H NMR spectroscopy.[73]

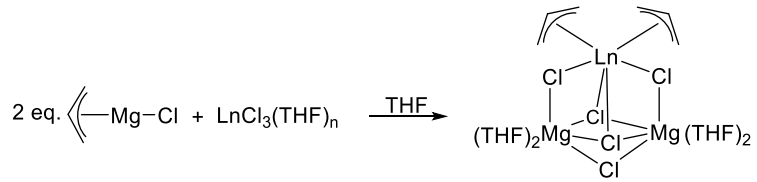

48$_{Ln}$ (Ln = Y, La)

Scheme 25 Synthesis of mixed chloro-bis(allyl) complexes **48$_{Ln}$**

All three complexes (Nd, Y, La) were assessed as precatalysts towards isoprene polymerization, they were found to be active only when activated with an alkylaluminum or MAO, along with good control over macromolecular data. The Nd(allyl)$_2$Cl(MgCl$_2$)$_2$(THF)$_4$/MAO combination gave high 1,4-*cis* selectivity (> 96%) along with high activity (TOF up to 50,000 h^{-1}). Reversal in stereoregularity was

observed with **48**$_Y$ when this bis-allyl derivative was associated with $AlEt_3$ or Al*i*Bu_3, affording PI with up to 91% 1,4-*trans* content (TOF *ca.* 100 h^{-1}), while MAO as co-catalyst lead to 75% 1,4-*cis* PI.

3.2.2 (Allyl)$_2$LnX compounds with amide and related N-donor ligands

The preparation and characterization of a series of neutral solvent-free bis(allyl) rare-earth metal complexes [Ln(Me_3TACD)(η^3-C_3H_5)$_2$] (**49**$_{Ln}$, Ln = Y, La, Ce, Pr, Nd, Sm) supported by the 1,4,7-trimethyl-1,4,7,10-tetraazacyclododecane anion (Me_3TACD^-) have been reported by Okuda and coworkers.[74] These complexes were synthesized by the clean reaction of the proligand (Me_3TACD)H with the tris(allyl) [Ln(η^3-C_3H_5)$_3$(diox)] precursors (Scheme 26).

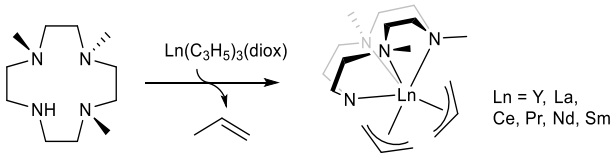

Scheme 26 Synthesis of mixed amido-bis(allyl) complexes **49**$_{Ln}$ by reaction of the tris(allyl) derivatives with (Me_3TACD)H

X-ray diffraction studies on single crystals of the complexes **49**$_{Ln}$ (Ln = Y, La, Pr, and Sm) show similar arrangement around the metal center, which can be described as a square antiprism formed by the nitrogen atoms of the ligand and the terminal carbon atoms of both allyl ligands. ^{1}H NMR investigations in solution of **49**$_{La}$, conducted in the temperature range -80 to +80 °C, established that the allyl ligands retain the η^3-binding mode on the NMR timescale.

Upon treatment with Brønsted acids, the series of monocationic mono-allyl complexes [Ln(Me_3TACD)(η^3-C_3H_5)(THF)$_2$][B(C_6X_5)$_4$] (**50**$_{La}$, X = F; **50'**$_{Ln}$, Ln = La, Ce, Nd, X = H) were isolated and characterized (Scheme 27).

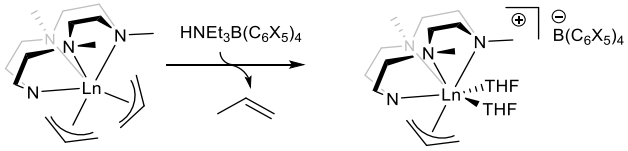

Scheme 27 Synthesis of mixed amido-mono(allyl) ionic complexes **50**$_{Ln}$ and **50'**$_{Ln}$ by reaction of the bis(allyl) precursors **49**$_{Ln}$ with Bronsted acids

The cerium compound **50'**$_{Ce}$ was found to crystallize as a separated ion pair without close interactions between the cation and anion. The comparison of the structural parameters (distances and angles) in neutral [Ce(Me_3TACD)(η^3-C_3H_5)$_2$] [**50**$_{Ce}$] and cationic [Ce(Me_3TACD)(η^3-C_3H_5)(THF)$_2$][B(C_6X_5)$_4$] [**50'**$_{Ce}$] compounds in the solid state did not reveal significant difference, in relation with the higher Lewis acidity of the metal center in the cationic cerium analogue, as same as already observed when comparing the pure allyl Ce(η^3-C_3H_5)$_3$(THF)$_3$ and [Ce(η^3-C_3H_5)$_2$(THF)$_4$][BPh_4] derivatives.[6]

Hydrogenolysis of **49**$_{Ln}$ with H_2 afforded the hydride complexes [Ln(Me_3TACD)H_2]$_n$ (Ln = Y, La, Sm, n = 3-4), which crystallize under a tetrameric form for the lanthanum complex (Scheme 28). Allyl complexes of the lighter lanthanides can therefore be considered as a valuable alternative to the commonly used alkyl precursors for the synthesis of hydrido compounds.

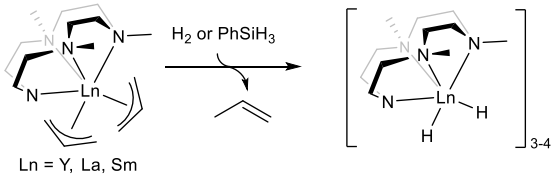

49$_{Ln}$

Scheme 28 Hydrogenolysis of mixed amido-(allyl) **49$_{Ln}$** affording the Me_3TACD-supported dihydride complexes

Further reactivity studies of mixed amido-bis(allyl) complexes **49$_{Ln}$** towards furan derivatives were reported in the same article, *i.e.* hydrosilylation of furfural and hydrodeoxygenation of furan and 2-methylfuran. The active species was proposed to be the dihydride complex formed by hydrogenation of the neutral bis(allyl) moiety. [6]

3.2.3 (Allyl)$_2$LnX compounds with Cyclopentadienyl/Indenyl ligands

The half-sandwich bis-allyl scandium complexes ($C_5Me_4SiMe_3$)Sc(η^3-C_3H_5)$_2$ [**51$_{Sc}$**], (C_5Me_5)Sc(η^3-C_3H_5)$_2$ [**52$_{Sc}$**] and (C_5Me_5)Sc(η^3-2-MeC_3H_4)$_2$ [**53$_{Sc}$**] were synthesized in 2008 by Hou and coworkers from the straightforward reaction of $ScCl_3$ with the cyclopentadienyl lithium derivatives and allyl magnesium chlorides, as described in Scheme 29 for complex **51$_{Sc}$**. [75]

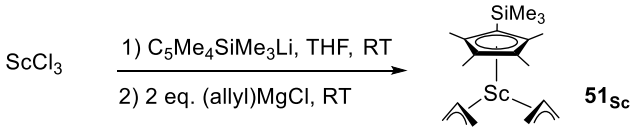

51$_{Sc}$

Scheme 29 Synthesis of half-sandwich bis(allyl) scandium complex **51$_{Sc}$**

All three scandium complexes were isolated as base-free and were structurally characterized. They displayed similar characteristics in the solid state, but whereas one allyl ligand is found prone and the other supine in the two C_5Me_5 complexes **52$_{Sc}$** and **53$_{Sc}$**, the two allyl groups are all prone in **51$_{Sc}$** (Fig. 31). All three complexes were found to be fluxional in solution from ^{1}H NMR studies in deuterated toluene, the two allyl units being non-equivalent at very low temperature (-80 °C).

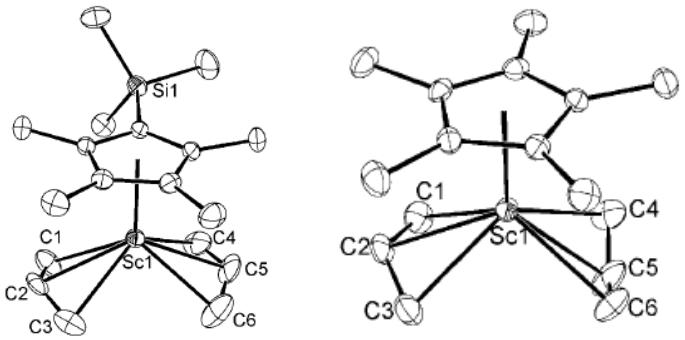

Fig. 31 ORTEP drawings of **51$_{Sc}$** (left) and of **52$_{Sc}$** (right). Displacement ellipsoids are set at the 30% probability level and the hydrogen atoms are excluded for clarity. Reprinted with the permission of WILEY-VCH Verlag GmbH. [75]

When combined with [$HNMe_2$][$B(C_6F_5)_4$], the bis(allyl) derivative **51$_{Sc}$** was found to be active towards the polymerization of isoprene and its copolymerization with norbornene. [75]

One year later, the reaction of the neutral tris-allyl complexes Ln(η^3-C_3H_5)$_3$(diox) (Ln = Y, La) with the proligand $HC_5Me_4SiMe_3$ was used by Okuda to cleanly prepare the half-sandwich bis(allyl)

complexes ($C_5Me_4SiMe_3$)Ln(η^3-C_3H_5)$_2$(THF) [**51'$_{Ln}$**] with propene release (Scheme 30), where the allyl group was noted as fluxional by ^{1}H NMR analysis.[6]

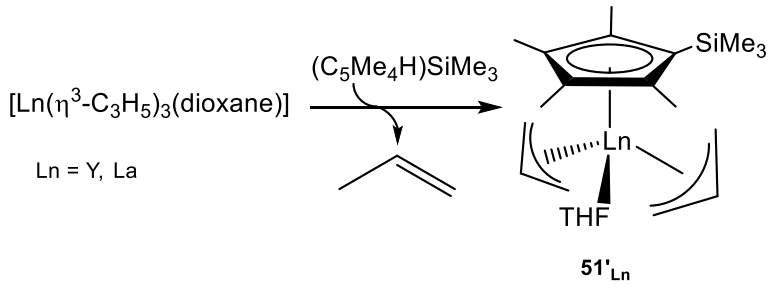

Scheme 30 Synthesis of half-sandwich bis(allyl) complexes **51'$_{Ln}$**

The syntheses of a series of rare earth bis(allyl) complexes with constrained geometry ($C_5Me_4C_6H_4$-*o*-NMe_2)Ln(η^3-C_3H_5)$_2$ (**54$_{Ln}$**, Ln = Y, Nd, Gd, Dy, Lu), ($C_5Me_4C_6H_4$-*o*-PPh_2)Ln(η^3-C_3H_5)$_2$ (**55$_{Ln}$**, Ln = Y, Gd), ($C_9H_6C_6H_4$-*o*-NMe_2)Ln(η^3-C_3H_5)$_2$ (**56$_{Ln}$**, Ln = Y, Dy), ($C_9H_6C_6H_4$-*o*-PPh_2)Ln(η^3-C_3H_5)$_2$ (**57$_{Ln}$**, Ln = Y, Gd) (Fig. 32) were mentioned in a patent in 2010.[76] Upon combination with an alkylaluminum reagent and an organic boron activator, all these complexes showed high catalytic performances in 1,4-*cis* selective polymerization of conjugated dienes (isoprene and butadiene) along with full conversion. The polymerization reaction displayed the characteristics of a living polymerization.

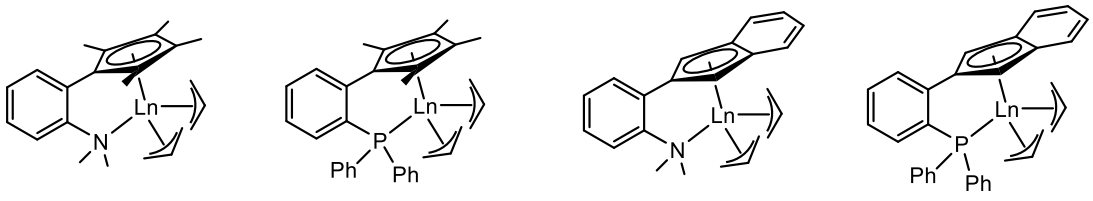

Fig. 32 Constrained geometry bis(allyl) complexes **54$_{Ln}$**, **55$_{Ln}$**, **56$_{Ln}$**, **57$_{Ln}$**

The preparation of the lanthanide aminophenyl-Cp bis(allyl) complexes **54$_{Ln}$** (Ln = Y, Nd, Gd, Dy) was described in further details in a communication reported in 2010 [77] and two years later in a full paper for the lutetium derivative,[78] by the sequential metathesis reactions of $LnCl_3$ with (C_5Me_4-C_6H_4-*o*-NMe_2)Li and (C_3H_5)MgCl (Scheme 31).

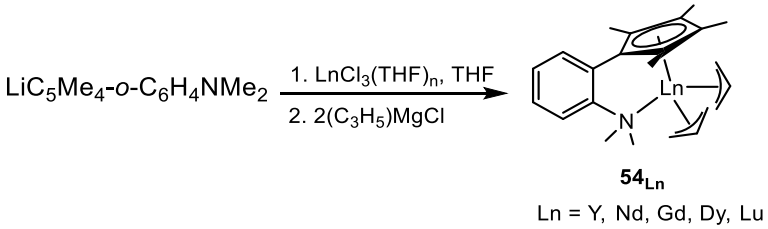

Scheme 31 Synthesis of the aminophenyl-Cp bis(allyl) complexes **54$_{Ln}$**

Thanks to ^{1}H NMR studies, the allyl group in the yttrium complex [**54$_Y$**] was found fluxional with the typical 1H/4H resonances. The yttrium, gadolinium, and dysprosium complexes (**54$_Y$**, **54$_{Gd}$**, **54$_{Dy}$**, respectively) were characterized by X-ray crystallography as solvent-free—even though the reaction was performed in THF solvent—isostructural complexes and it was shown that both allyl moieties coordinate in the η^3-mode. The molecular structure of the lutetium complex **54$_{Lu}$** was also later deduced from X-ray studies, in which both of the allyl groups, in the solid state as well as in solution, coordinated to the metal center in classical trihapto η^3- mode (Fig. 33). The coordination of the amino moiety corroborated the absence of additional solvent in the molecule.

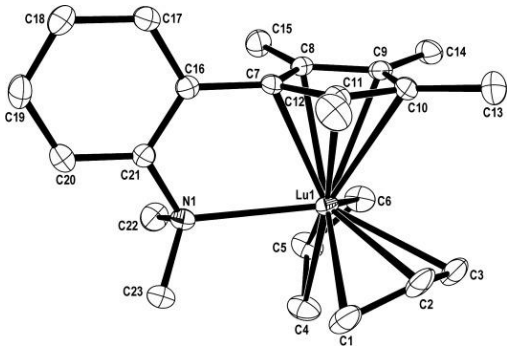

Fig. 33 ORTEP plot of **54$_{Lu}$**. Displacement ellipsoids are set at the 40% probability level and the hydrogen atoms are excluded for clarity. Reprinted with the permission of WILEY-VCH Verlag GmbH.[78]

The yttrium- and scandium–bis (allyl) complexes, (C_5Me_4-C_5H_4N)Ln(η^3-C_3H_5)$_2$ (**58$_{Ln}$**, Ln = Y, Sc), which contained pyridyl-Cp, another electron-withdrawing ligand, were obtained following a similar two-step procedure as described in the same publication (Scheme 32, left).[78] A more-crowded environment in **54$_{Lu}$** -due to this aminophenyl-Cp- than in the pyridyl-Cp lutetium bis(allyl) complex (C_5Me_4-C_5H_4N)Lu(η^3-C_3H_5)$_2$ (**58$_{Lu}$**), which was published separately,[79] was advanced to explain the lower reactivity of the former complex (see further).

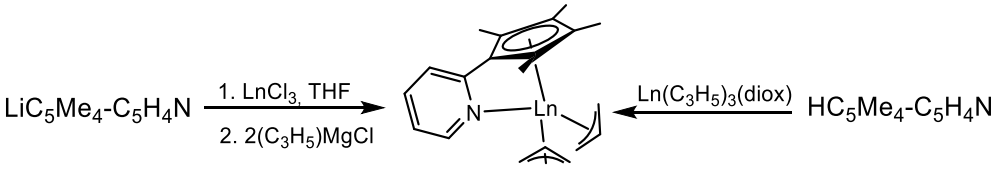

58$_{Ln}$

Ln = Y, Sc, Lu

Scheme 32 Two synthetic approaches for the preparation of complexes **58$_{Ln}$**

Alternatively, these compounds **58$_{Ln}$** were prepared, including their lutetium congener, by protonolysis reaction of Ln(allyl)$_3$(diox) with the proligand HC_5Me_4-C_5H_4N (Scheme 32, right).[78,79] The ^{1}H NMR analysis of the yttrium complex **58$_Y$** suggested slow *syn/anti* exchange of the allylic protons, in contrast to what was observed in previously mentioned **54$_Y$**[77] and ($C_5Me_4SiMe_3$)Y(η^3-C_3H_5)$_2$(THF).[6] On the other hand, in the case of the scandium analogue **58$_{Sc}$**, only two allyl signals (1H/4H) were observed, as for its lutetium analog. All three complexes **58$_{Ln}$** (Ln = Y, Sc, Lu) displayed the same solvent-free monomeric arrangement in which the ligand generates a CGC configuration with the two allyl units bounded in η^3-fashion to the metal and one allyl group prone while the other supine (Fig. 34, only shown here for **58$_{Lu}$**).[79]

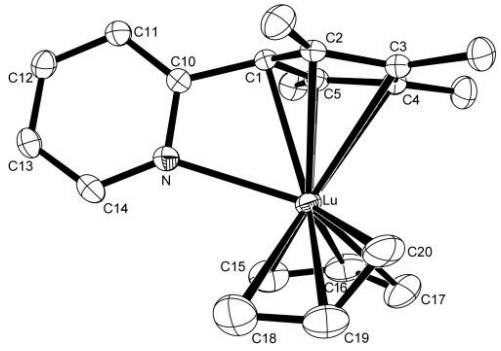

Fig. 34 ORTEP plot of constrained geometry Cp-Pyridyl bis(allyl) **58$_{Lu}$**. Displacement ellipsoids are set at the 40% probability level and the hydrogen atoms are excluded for clarity. Reprinted with the permission of WILEY-VCH Verlag GmbH.[79]

Upon activation with $[Ph_3C][B(C_6F_5)_4]$, the electron withdrawing pyridine-Cp-based lutetium complex **58$_{Lu}$** afforded highly active catalyst towards butadiene polymerization (TOF 60,000 h^{-1}), which was also *cis*-1,4-selective, up to 97%. Moreover, the three **58$_{Ln}$** complexes in the same pyridine-Cp-based series (Y, Lu, Sc), in particular the scandium complex, exhibited outstanding activity (TOF 60,000 h^{-1}) for styrene polymerization, when combined with trityl borate as activator, to give perfectly syndiotactic polystyrene (*s*PS). As such, the scandium and the lutetium complexes in this series are among the rare examples of precatalysts having a dual ability in both syndiotactic styrene polymerization and *cis*-selective 1,3-diene polymerization.[80] In contrast, the amino-phenyl Cp yttrium and lutetium complexes $(C_5Me_4\text{-}C_6H_4\text{-}o\text{-}NMe_2)Ln(\eta^3\text{-}C_3H_5)_2$ **54$_{Ln}$** failed to polymerize styrene under the same conditions of activation. This result was explained in terms of bite angle, which hinders the coordination and insertion of the styrene monomer, while being more favorable for Cp-pyridine complexes.

In combination with tritylborate $[Ph_3C][B(C_6F_5)_4]$, **58$_{Lu}$** afforded as well a highly active catalyst (TOF up to 5,100 h^{-1}) for the statistical and the sequenced copolymerization of butadiene and styrene. Copolymers having highly *cis*-1,4-PB and syndiotactic PS segments, along with high molecular weight and narrow dispersity were obtained. Kinetic studies demonstrated that in the presence of a mixture of the two monomers butadiene was consumed first, followed by the growing of the syndiotactic PS sequence, finally affording diblock styrene-butadiene copolymers in all cases. The same kind of copolymer was isolated from sequenced butadiene/styrene copolymerization.[79]

The pyridine-cyclopentadienyl bis(allyl) complex $(C_5Me_4C_5H_4N)Lu(\eta^3\text{-}C_3H_5)_2$ (**58$_{Lu}$**) was also used as precatalyst for the copolymerization of isoprene with styrene, in combination with $[Ph_3C][B(C_6F_5)_4]$.[81] The resulting Ip/St copolymers displayed multiblock microstructure with high *cis*-1,4-polyisoprene (PI) units (80%) and crystalline *s*PS sequences. The terpolymerization of styrene with isoprene and butadiene with the same catalytic combination gave unprecedented terpolymers that were composed of perfect *s*PS blocks, high *cis*-1,4-PI units and almost pure *cis*-1,4-PB sequences arranged in multiblock mode, with excellent control over the regio- and stereoregularity as well as the composition (Scheme 33).

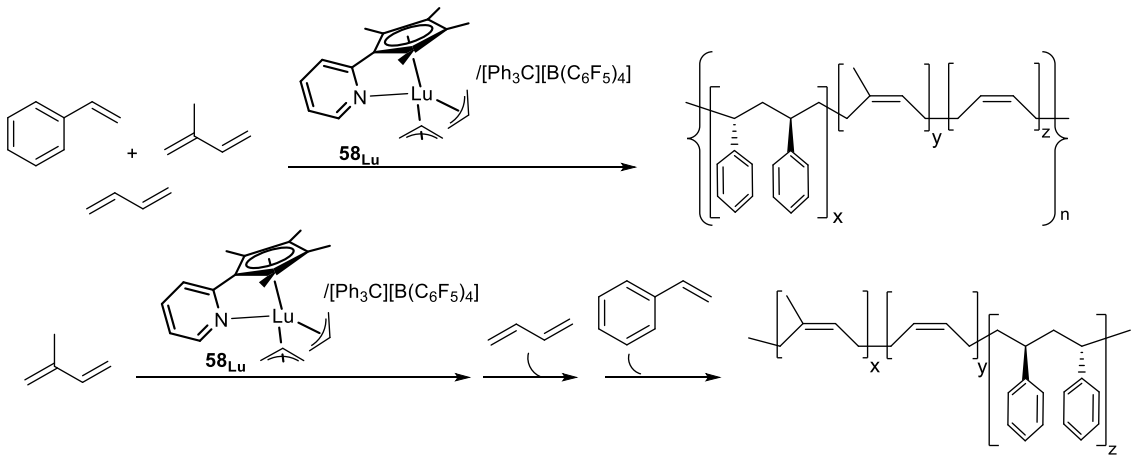

Scheme 33 Terpolymerization experiments performed with **58$_{Lu}$**-based catalyst

The activity of the bis(allyl) complexes **54$_{Ln}$** (Ln = Y, Nd, Gd, Dy) was assessed towards the polymerization of isoprene in the presence of AlR_3 (mainly $Al(^iBu)_3$) and $[PhMe_2NH][B(C_6F_5)_4]$ in toluene at 20 °C. The neodymium complex had the highest activity (TOF 3,000 h^{-1}). The gadolinium complex afforded the highest *cis*-1,4 regular PI at 99.2% (at 0 °C) along with the living character of the polymerization. It was observed that when the Al/Gd ratio was increased, a typical catalyzed chain

growth (CCG) process was operating, with systematic decrease of the molecular weight of the PI while the molecular weight distribution remained unchanged. Again, upon activation with $[Ph_3C][B(C_6F_5)_4]/Al(^iBu)_3$, $(C_5Me_4–C_6H_4\text{-}o\text{-}NMe_2)Gd(\eta^3\text{-}C_3H_5)_2$ (**54$_{Gd}$**) afforded, *via* sequential monomer addition of isoprene and butadiene, unprecedented *cis*-PI-*b*-*cis*-PB and *cis*-PI-*b*-*cis*-PB-*b*-*cis*-PI block copolymers. This was possible thanks to the living polymerization process occurring through reversible Gd/Al chain transfer.[77]

More recently, Anwander and coworkers synthesized the allyl half-sandwich complexes of the heavier lanthanides, $Cp^{NMe2}Ln(\eta^3\text{-}C_3H_5)_2$ (**59$_{Ln}$**, Ln = Y, Ho, Lu; Cp^{NMe2} = $C_5Me_4CH_2CH_2NMe_2$) having a more flexible N-functionalized cyclopentadienyl ligand than in the aminophenylCp complexes **54$_{Ln}$**.[82] The reaction was conducted in two steps by first reacting $LnCl_3(THF)_x$ with $Cp^{NMe2}Li$ at room temperature, and then adding two equivalents of the Grignard reagent C_3H_5MgCl (Scheme 34).

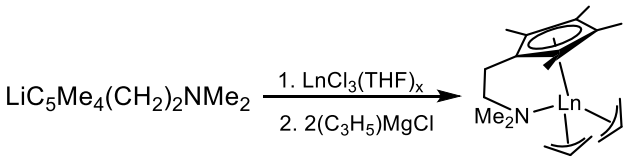

Ln = Y, Ho, Lu

59$_{Ln}$

Scheme 34 Synthesis of constrained-geometry allyl complexes **59$_{Ln}$**

X-ray analysis showed that the three complexes were under a bis-allyl half-sandwich monomeric form and were all isostructural, in an overall arrangement similar to that found for complexes **54$_{Ln}$**. One of the allyl groups showed similar bond lengths between terminal and central carbon atoms, while the second allyl group showed a significantly longer bond length between the rare earth metal and the terminal carbon. The ^{1}H NMR spectra of diamagnetic yttrium [**59$_Y$**] and lutetium [**59$_{Lu}$**] complexes showed the typical quintet (1H)/doublet (4H) set of signals characteristic of dynamic exchange of the allylic protons, along with splitting of the quintet in the case of the yttrium derivative, due to the coupling with ^{89}Y.

An [Allyl]/[Cl] exchange was observed when yttrium and holmium complexes reacted with $AlEt_2Cl$, leading to multi(μ-chlorido) hexametallic $[Ln_6Cl_{12}]$ clusters, consistent with the absence of any reactivity towards isoprene polymerization when adding $AlEt_2Cl$. When activated with either $[Ph_3C][B(C_6F_5)_4]$ or $[PhNMe_2H][B(C_6F_5)_4]$ borates, only the lutetium half-sandwich displayed a noticeable activity (TOF 500 h^{-1}) towards the polymerization of isoprene, affording non stereo-regular PI. However, in the presence of 10 additional equiv. Al^iBu_3, all three **59$_{Ln}$**-based catalysts displayed improved activity (TOF 1,000-2,000 h^{-1}). A decrease in the polymer molecular weights with narrow dispersities was also noticed, which indicated chain transfer to aluminum.

The pyrrolidine-functionalized half-sandwich complexes $(C_5Me_4SiMe_2NC_4H_8)Ln(\eta^3\text{-}C_3H_5)_2$ (**60$_{Ln}$**, Ln = Sc, Y, Lu) were synthesized by Luo and coworkers by reacting $LnCl_3$ with one equivalent of $C_5Me_4SiMe_2\text{-}NC_4H_8Li$ followed by the addition of two equivalents of $(C_3H_5)MgCl$ in THF at room temperature (Scheme 35).[83]

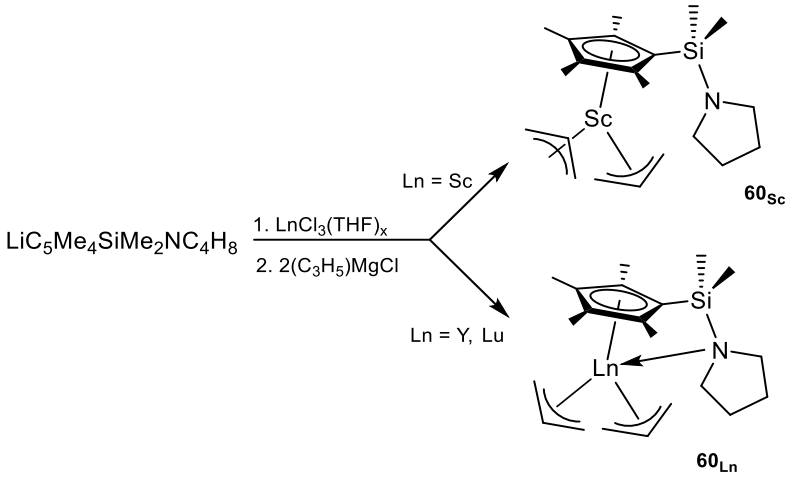

Scheme 35 Synthesis of half-sandwich allyl complexes **60$_{Ln}$**

The ^{1}H NMR spectra of the three **60$_{Ln}$** complexes indicated the fluxional allyl ligand in solution, with the typical doublet signal for the terminal allylic protons and one multiplet for the central allylic protons. X-ray analysis showed that the pendant pyrrolidine moiety coordinates to the metal center in the yttrium and lutetium complexes (Fig. 35, left), where this coordination is absent for the scandium complex due to smaller size of the scandium cation (Fig. 35, right).[65] In the three complexes, the two allyl moieties were coordinated to the central metal in an η^3-mode, but with one allyl group prone and the other supine in the case of the scandium complex.

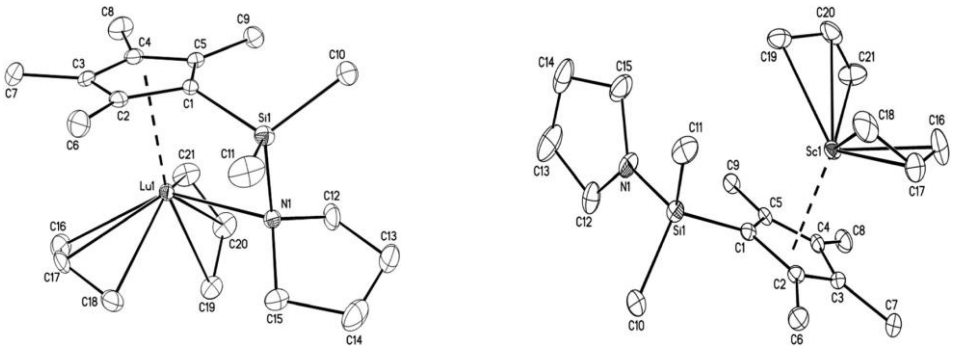

Fig. 35 ORTEP plot of ($C_5Me_4SiMe_2NC_4H_8$)Ln(η^3-C_3H_5)$_2$ (**60$_{Ln}$**, Ln = Lu, left and Sc, right). Thermal ellipsoids are drawn at the 10% probability level and the hydrogen atoms are excluded for clarity. Reprinted with the permission of the Royal Society of Chemistry.[83]

The half-sandwich scandium complex **60$_{Sc}$** was found to be highly active towards styrene polymerization when activated with one equivalent of [Ph_3C][$B(C_6F_5)_4$], producing pure *s*PS at room temperature (TOF 250 h^{-1}). When Al(^{i}Bu)$_3$ was added in excess, the activity increased drastically (TOF 1500 h^{-1}). On the other hand, yttrium and lutetium complexes proved to be much less active.

Table 4 Structural and analytical data of monosubstituted bis(allyl) complexes (in brackets only the relevant complexes only, otherwise for all complexes)

Compound number	Molecular Formula	X-ray data Ln-C(allyl) distances (Å)	NMR data	References
48$_Y$, 48$_{La}$	Ln(allyl)$_2$Cl($MgCl_2$)$_2$(THF)$_4$ (Ln = Y, La)	-	^{1}H	73
49$_Y$, 49$_{La}$, 49$_{Ce}$, 49$_{Pr}$, 49$_{Nd}$, 49$_{Sm}$	[Ln(Me_3TACD)(η^3-C_3H_5)$_2$] (Ln = Y, La, Ce, Pr, Nd, Sm)	Y-C = 2.641(3), 2.684(4)*, 2.610(8)*, 2.754(4); 2.740(3), 2.698(3), 2.697(3)	^{1}H, ^{13}C	74

		La-C = 2.808(4), 2.859(4), 2.837(4); 2.791(4), 2.918(4), 2.887(4) Pr-C = 2.782(5), 2.751(7), 2.744(5) ; 2.824(14)*, 2.83(2)* Sm-C = 2.743(3), 2.700(5), 1.337(4); 2.716(3), 2.779(9)*, 2.758(15)*		
50$_{La}$, 50'$_{La}$, 50'$_{Ce}$, 50'$_{Nd}$	[Ln(Me_3TACD)(η^3-C_3H_5)$(THF)_2$][B(C_6X_5)$_4$] (X = F, Ln = La ; X = H, Ln = La, Ce, Nd)	Ce-C = 2.822(3), 2.816(3), 2.792(3)	^{1}H, ^{13}C	74
51$_{Sc}$ **52$_{Sc}$** **53$_{Sc}$**	($C_5Me_4SiMe_3$)Sc(η^3-C_3H_5)$_2$ (C_5Me_5)Sc(η^3-C_3H_5)$_2$ (C_5Me_5)Sc(η^3-2-MeC_3H_4)$_2$	**51$_{Sc}$:** Sc-C = 2.419(4) to 2.466(5) **52$_{Sc}$:** Sc-C = 2.415(3) to 2.460(3) **53$_{Sc}$:** Sc-C = 2.397(2) to 2.512(3)	^{1}H, ^{13}C	75
51'$_Y$, 51'$_{La}$	Ln($C_5Me_4SiMe_3$)(η^3-C_3H_5)$_2$(THF) (Ln = Y, La)	-	^{1}H, ^{13}C	6
54$_Y$, 54$_{Nd}$, 54$_{Gd}$, 54$_{Dy}$, 54$_{Lu}$	(C_5Me_4-C_6H_4-*o*-NMe_2)Ln(η^3-C_3H_5)$_2$ (Ln = Y, Nd, Gd, Dy, Lu)	Gd-C = 2.648(4), 2.674(4) Dy-C= 2.612(3), 2.637(3) Lu–C = 2.579(3), 2.582(3) (average distances)	^{1}H, ^{13}C (**54$_Y$**, **54$_{Lu}$**)	76,77,78
55$_Y$, 55$_{Gd}$	($C_5Me_4C_6H_4$-*o*-PPh_2)Ln(η^3-C_3H_5)$_2$ (Ln = Y, Gd)	_	_	76
56$_Y$, 56$_{Dy}$	($C_9H_6C_6H_4$-*o*-NMe_2)Ln(η^3-C_3H_5)$_2$ (Ln = Y, Dy)	_	_	76
57$_Y$, 57$_{Gd}$	($C_9H_6C_6H_4$-*o*-PPh_2)Ln(η^3-C_3H_5)$_2$ (Ln = Y, Gd)	_	_	76
58$_{Sc}$, 58$_Y$, 58$_{Lu}$	(C_5Me_4-C_5H_4N)Ln(η^3-C_3H_5)$_2$ (Ln = Sc, Y, Lu)	Sc–C = 2.483(4), 2.476(4) Y–C = 2.600(3), 2.617(3) Lu-C = 2.567(4), 2.603(3) (average distances)	^{1}H, ^{13}C	78,79
59$_Y$, 59$_{Ho}$, 58$_{Lu}$	Cp^{NMe2}Ln(η^3-C_3H_5)$_2$ (Cp^{NMe2} = $C_5Me_4CH_2CH_2NMe_2$; Ln = Y, Ho, Lu)	Y-C = 2.590(5) to 2.663(7) Ho-C = 2.587(7) to 2.660(13) Lu - C = 2.534(4) - 2.633(9)	^{1}H (**59$_Y$**, **59$_{Lu}$**)	82
60$_{Sc}$, 60$_Y$, 60$_{Lu}$	($C_5Me_4SiMe_2NC_4H_8$)Ln(η^3-C_3H_5)$_2$ (Ln = Sc, Y, Lu)	Sc–C = 2.418(8), 2.431(7), 2.395(7); 2.438(7), 2.414(7), 2.428(8) Y–C = 2.625(3), 2.617(3), 2.600(3); 2.656(3), 2.637(3), 2.554(3) Lu–C = 2.596(4), 2.564(4), 2.539(5); 2.633(4), 2.592(4), 2.506(4)	^{1}H, ^{13}C	83

* distorted

3.3. Bis-substituted Mono-allyl complexes: (Allyl)LnX_2 compounds

3.3.1 (Allyl)LnX_2 compounds with borohydride ligands

Recently, Fadlallah *et al.* synthesized the first lanthanide complexes bearing both allyl and borohydride ligands, Ln(BH_4)$_2$(η^3-C_3H_5)$(THF)_3$ (**61$_{Ln}$**, Ln = Nd, Sm) from the reaction of the precursor

$Ln(BH_4)_3(THF)_3$ with half an equivalent of $Mg(C_3H_5)_2(L)_n$ (L = THF, dioxane) at room temperature in THF solution.[84] This family of complexes, which are the counterparts of the $LnCl_2(allyl)(THF)_2$ in chloride series,[85] was a little later extended to yttrium, lanthanum and scandium, the latter being isolated as a bis-THF adduct (Scheme 36).[86]

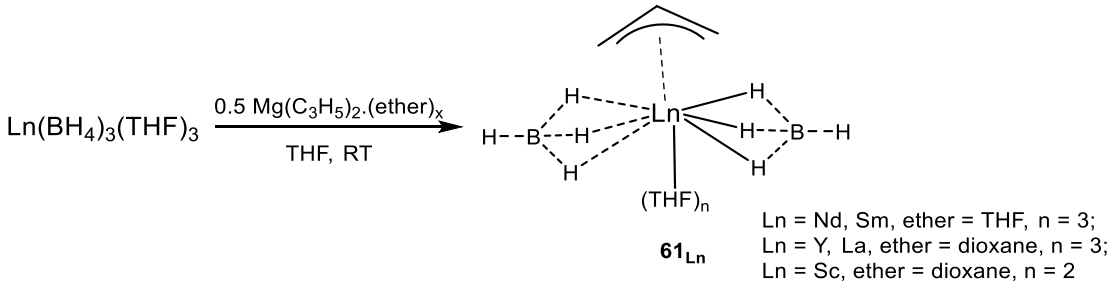

Scheme 36 Synthesis of mixed allyl-borohydride **61$_{Ln}$** complexes

From ^{1}H NMR analysis, the allyl moiety appeared as a 1H/2H/2H set of resonances for the complexes made with the larger lanthanides (La, Nd and Sm), revealing no dynamic behavior at the ^{1}H NMR timescale. In contrast, the allyl group was found to be fluxional (1H/4H pattern by ^{1}H NMR spectroscopy) in the case of the smaller yttrium and scandium. All complexes **61$_{Ln}$** displayed a monomeric structure according to X-ray studies. Complex **61$_{Sc}$** is the only one to crystallize as a bis-THF adduct. Among the five complexes, **61$_{Y}$** stands out, with one borohydride trihapto and the other dihapto, while for the other four complexes the ligands are coordinated in tridentate mode to the metal. In all five complexes, the allyl moiety binds the metal in an η^3-mode (Fig. 36).

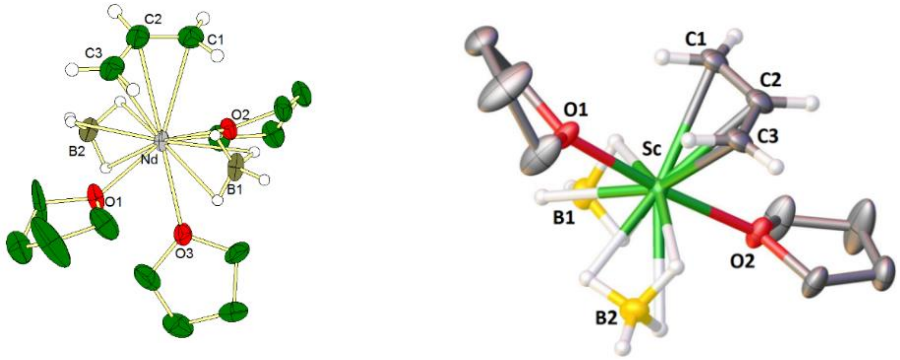

Fig. 36 ORTEP plot of **61$_{Nd}$** (left) and **61$_{Sc}$** (right). Hydrogen atoms are partially omitted for clarity. Reprinted with the permission of WILEY-VCH Verlag Gm and the American Chemical Society, respectively.[84,86]

The neodymium derivative **61$_{Nd}$** was the only one in the series to be active towards the polymerization of isoprene (TOF 177-1,000 h^{-1}), either on its own, due to the presence of the Nd-allyl bond, or combined with various alkylating reagents among which $Mg(^nBu)(Et)$, $Al(^iBu)_3$ or MAO (Methylaluminoxane). In every case, the selectivity of the reaction was 1,4-*trans*, up to 95.5%. In turn, all five complexes **61$_{Ln}$** were found very active towards the Ring-Opening Polymerization (ROP) of ε-caprolactone (TOF up to 700,000 h^{-1} with neodymium), *L*-lactide (TOF up to 1,300 h^{-1} with neodymium), and statistical copolymerization of both monomers. It is noteworthy that the initiation of the polymerization was demonstrated to take place *via* the borohydride rather than the allyl moiety by means of ^{1}H NMR spectroscopy end-group analysis. This experimental result was just recently corroborated by DFT studies, where the peculiar reactivity of the borohydride *vs*. the allyl group was explained by the lower stability of the product resulting from monomer insertion into Ln-allyl rather than Ln-(BH_4) in **61$_{Ln}$** complexes.[87] In contrast, the metal-allyl bond was found to be more reactive than

the metal-borohydride one towards the insertion of benzophenone, as expected from the literature,[6] and towards the protonation reaction with $[HNMe_2Ph][B(C_6F_5)_4]$ and HC_5Me_4R (R = Me, Et, Scheme 37).

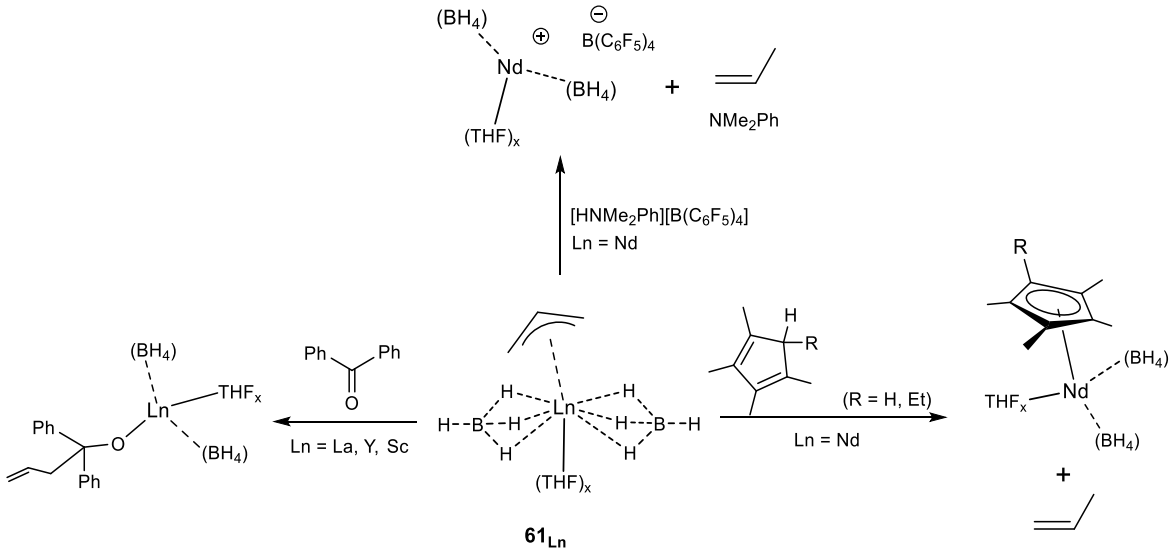

Scheme 37 Reactivity of complexes **61$_{Ln}$** towards various reagents[87]

3.3.2 (Allyl)LnX$_2$ compounds with amide and related N-donor ligands

In 2013, Okuda and coworkers used a dianionic (L_4X_2)-type surrogate for the bis(cyclopentadienyl) scaffold to synthesize the mono(allyl) complexes $[(1,7\text{-}Me_2TACD)Ln(\eta^3\text{-}C_3H_5)]_2$ (**62$_{Ln}$**, Ln = Y , La) by the acid-base 1:1 reaction of the protio form of the macrocyclic ligand $(1,7\text{-}Me_2TACD)H_2$ ($1,7\text{-}Me_2TACD$ = 1,7-dimethyl-1,4,7,10-tetraazacyclododecane, $1,7\text{-}Me_2[12]aneN_4$) with $[Ln(\eta^3\text{-}C_3H_5)_3(diox)]$ in THF (Scheme 38, left). [88]

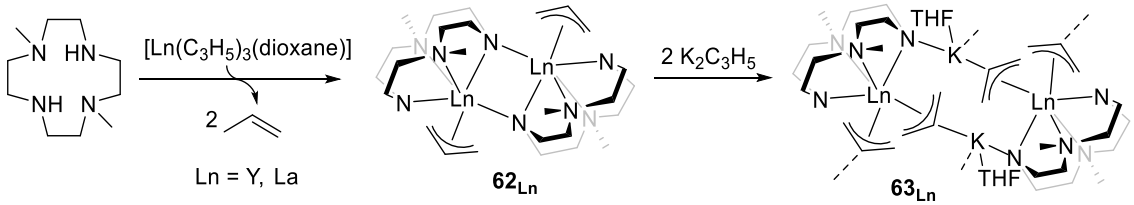

Scheme 38 Synthetic scheme for the preparation of allyl complexes of the series **62$_{Ln}$** and **63$_{Ln}$**

From XRD studies, it was established that the lanthanum congener **62$_{La}$** is a centrosymmetric dimer with lanthanum atoms bridged by one of the two amido nitrogen atoms (Fig. 37). The average La–C(allyl) bond length was found similar to the value found in the mono substituted bis-allyl $(Me_3TACD)La(\eta^3\text{-}C_3H_5)_2$ [**49$_{La}$**] [74] and in $La(\eta^3\text{-}C_3H_5)_3(TMEDA)$.[89]

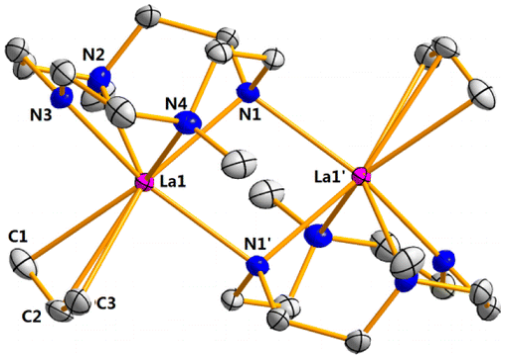

Fig. 37 ORTEP plot of dimeric **62$_{La}$**. Displacement parameters are set at 50% probability level and the hydrogen atoms are omitted for clarity. Reprinted with the authorization of the American Chemical Society.[88]

By subsequent reaction of complexes **62$_{Ln}$** with K(allyl), the corresponding heterometallic allyl "ate" complexes [(1,7-Me_2TACD)Ln(η^3-C_3H_5)$_2$K(THF)]$_n$ (**63$_{Ln}$**, Ln = Y, La) were isolated (Scheme 38, right), which were found to be both polymeric in the solid state *via* allyl bridges according to X-ray analysis. One allyl ligand is nearly symmetrically η^3- bonded to the potassium ion, while the other is η^3- bonded in an unsymmetrical fashion (Fig. 38).

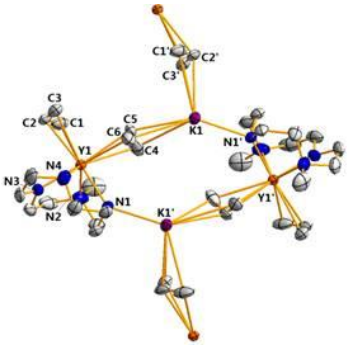

Fig. 38 Molecular structure of **63$_{Y}$**. Displacement parameters are set at the 50% probability level and the hydrogen atoms are omitted for clarity. Reprinted with the authorization of the American Chemical Society.[88]

In terms of reactivity, hydrogenolysis of the yttrium/potassium compound **63$_{Y}$** afforded the heterobimetallic hydrido complex [(1,7-Me_2TACD)$_2$$Y_2H_3K(THF)_2$]$_2$. In turn, upon the same treatment, **63$_{La}$** led to the formation of the heptanuclear La_3K_4 heptahydrido complex [(1,7-Me_2TACD)$_3$$La_3H_7K_4(THF)_7$].

The same research group prepared one year later, similarly as for its yttrium and lanthanum counterparts, the scandium mono(allyl) complex (1,7-Me_2TACD)Sc(η^3-C_3H_5) [**62$_{Sc}$**] from the diamino diamine (1,7-Me_2TACD)H_2 and (C_3H_5)$_3$Sc(THF)$_2$ [**37'$_{Sc}$**] in THF (Scheme 39).[90]

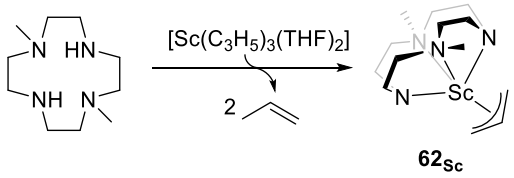

62$_{Sc}$

Scheme 39 Synthesis of diamino-diamido(allyl) **62$_{Sc}$**

Unlike its dinuclear yttrium and lanthanum homologues, **62$_{Sc}$** was readily soluble in hydrocarbon solvents. Its monomeric nature as well as the η^3-coordination mode of the allyl group was confirmed by variable temperature NMR spectroscopy studies, where the allyl group was shown to be fluxional in solution.

Hydrogenolysis of **62$_{Sc}$** with H_2 in THF gave the bimetallic hydride ionic complex [(1,7-Me_2TACD)$_3$$Sc_3H_2$][(1,7-$Me_2$TACD)$_3$$Sc_3H_4$]. Interestingly, monitoring this reaction in THF-d_8 indicated the formation of mixed allyl–hydrido intermediates, leading to the production of the hydride as the main compound after two days.

Mixed allyl-hydrido complexes could be obtained in the Me_3TACD series previously discussed: [Ln(Me_3TACD)(η^3-C_3H_5)(μ-H)]$_2$ dimeric complexes (**64$_{Ln}$**, Ln = Nd, Sm) were isolated from the reaction of the neutral bis(allyl) compounds **49$_{Ln}$** with phenylsilane but only in the case of neodymium and samarium (Scheme 40). It is interesting to note that the same reaction afforded the bis(hydride) [Ln(Me_3TACD)(μ-H)$_2$]$_4$ when Ln = Ce, Pr.[91]

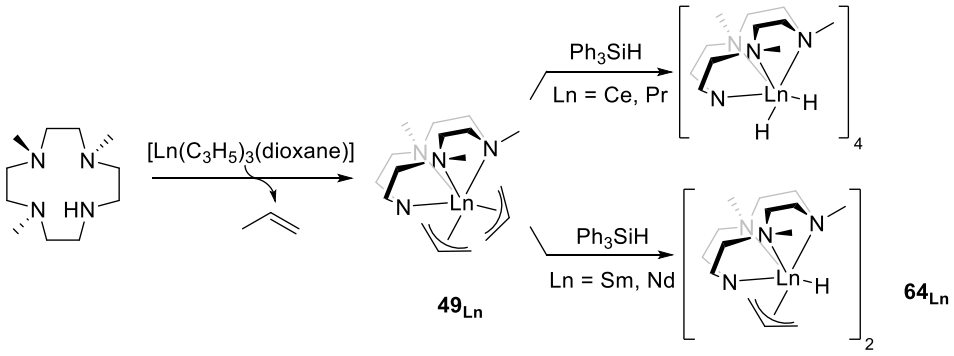

Scheme 40 Reaction of complexes **49$_{Ln}$** with triphenylsilane yielding mixed (allyl)(hydride) **64$_{Ln}$**

These exceptional mixed allyl-hydride complexes **64$_{Ln}$** were structurally characterized by X-ray analysis, showing that the allyl moiety coordinates in a η^3-bonding mode to the metal center (Fig. 39). So far, these complexes are the only rare-earth metal hydride compounds that possess an allyl moiety.

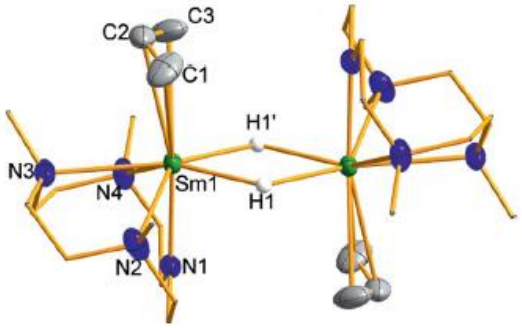

Fig. 39 ORTEP plot of **64$_{Sm}$**. Thermal ellipsoids of the Sm, N and C atoms are set at the 50% probability level. Hydrogen atoms of the Me_3TACD and allyl ligands are omitted for clarity. Reprinted with the authorization of WILEY-VCH Verlag GmbH.[91]

In the same article, it was found that the mixed allyl-hydride complexes **64$_{Ln}$** are able to promote the copolymerization of cyclohexene oxide with CO_2. As usually observed for such polymerization,[92] TON of order of magnitude of *ca*. 100 and broad dispersities of copolymers are noticed, which possess an alternating, atactic microstructure.

In 2020, the tridentate amidine 2-[$Ph_2P(O)$]C_6H_4NHC(^{t}Bu)=N(2,6-$Me_2C_6H_3$) containing the side-chain donor group Ph_2P=O was introduced by Trifonov and coworkers in the chemistry of lanthanide allyls. The reaction of the tris-allyl precursor Nd(C_3H_5)$_3$(diox)$_2$ with this tridentate ligand in a 1:2 molar ratio gave the bis(amidinate)mono(allyl) neodymium complex {2-[$Ph_2P(O)$]C_6H_4NC(^{t}Bu)N(2,6-$Me_2C_6H_3$)}$_2$Nd(C_3H_5) (**65$_{Nd}$**). This complex was alternatively prepared by the reaction between the monochloride complex {2-[$Ph_2P(O)$]C_6H_4NC(^{t}Bu)N(2,6-$Me_2C_6H_3$)}$_2$NdCl and allylmagnesium bromide (C_3H_5)MgBr (Scheme 41).[93]

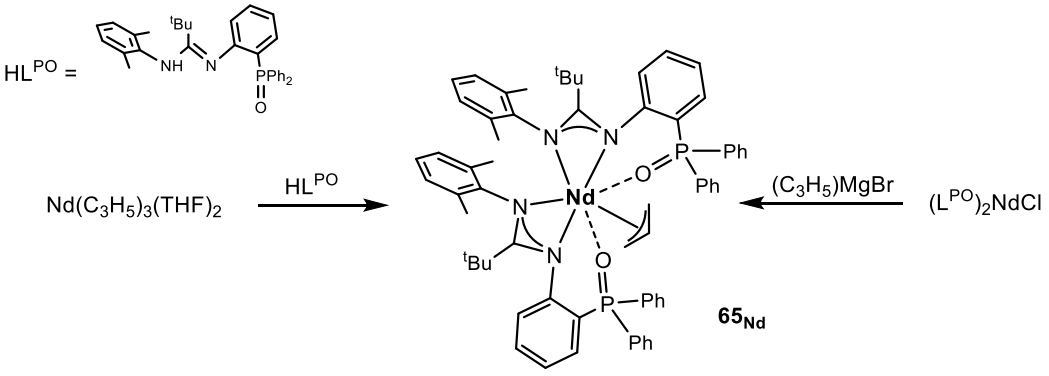

Scheme 41

X-ray studies revealed that complex **65$_{Nd}$** crystallizes as a solvate with 3.5 molecules of dioxane per Nd in the asymmetric unit (Fig. 40). The η^3-coordination mode of the allyl ligand was deduced by the CH_2-CH bond lengths in the complex that have similar values. It was also established that the Nd—C(allyl) bond lengths are slightly longer than the corresponding ones in the heteroleptic cyclopentadienyl neodymium allyl chloride complex [$CpNMe_2Nd(\eta^3$-$C_3H_5)(\mu$-$Cl)]_2$, where $CpNMe_2$ is 1-[2-(N,N-dimethylamino)ethyl]-2,3,4,5-tetramethylcyclopentadienyl (see further),[82] but are to some extent smaller than the Nd—C(allyl) distances in the allyl-hydride complex **64$_{Nd}$**,[91] providing an overview of the steric/electronic properties of this amidino phosphine-oxide ligand.

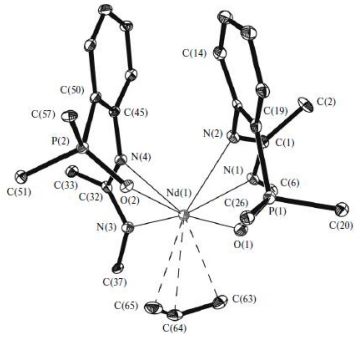

Fig. 40 ORTEP plot of {2-[Ph_2P(O)]$C_6H_4NC(^tBu)N$(2,6-$Me_2C_6H_3$)}$_2$Nd(C_3H_5) [**65$_{Nd}$**]. The displacement ellipsoids are drawn at the 30% probability level. Hydrogen atoms, methyl groups of the ^{t}Bu substituent, 2,6-$Me_2C_6H_3$ moieties and aryl substituents of Ph_2P=O are omitted for clarity. Reprinted with the permission of Springer.[93]

Allyl complexes of the lanthanides are known to initiate the Ring Opening Polymerization (ROP) of cyclic esters, although such studies are rather scarce in the literature.[94,95,96,5,97,88] The monoallyl complex **65$_{Nd}$** was as well found efficient towards *rac*-lactide and ε-caprolactone, exhibiting higher activity compared to the neodymium diketiminate bis(allyl) complex Ln(η^3-$C_3H_5)_2\{\kappa^2$-HC(MeCNAr)$_2\}$ (Ar = 2,6-^{i}Pr$_2C_6H_3$) previously described by Bochmann and coworkers,[5] but the process was rather uncontrolled with both monomers.

3.3.3. (Allyl)LnX$_2$ compounds with alkoxide ligands

A series of non-metallocene allyl complexes of early lanthanide containing a 1,ω-dithiaalkenediyl-bridged bis(phenolate) ligand [Ln(L)(η^3-C_3H_5)(THF)$_{1\text{-}2}$] (**66$_{Ln}$**, L = tbbp, Y, La; **67$_{Ln}$**, L = etbbp, La, Ce, Nd, Sm) (Fig. 41) were synthesized by Okuda and coworkers by reacting the tris(allyl) complex Ln(η^3-$C_3H_5)_3$(diox) with the corresponding bis(phenol) through propene elimination.[98] The (OSO)-type bisphenolate tbbp ligand was best suited for yttrium and lanthanum, whereas the larger lanthanides lanthanum, cerium, neodymium and samarium accommodated the tetradentate (OSSO)-type bis(phenolate) etbbp ligand.

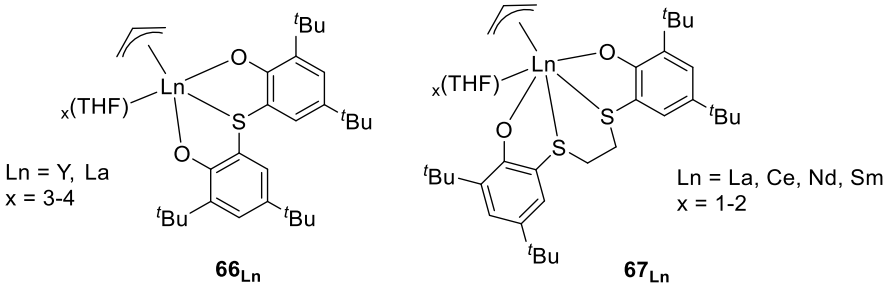

Fig. 41 1,ω-dithiaalkenediyl-bridged bis(phenolate) [Ln(L)(η^3-C_3H_5)(THF)$_{1\text{-}2}$] complexes (**66$_{Ln}$**, L = tbbp, Y, La; **67$_{Ln}$**, L = etbbp, La, Ce, Nd, Sm)

Variable-temperature ^{1}H NMR spectroscopy of the lanthanum complex [**67$_{La}$**] showed the typical fluxional behavior for the allyl protons at room temperature, while the *syn* and *anti* H resonances could be observed at lower temperature (-30 °C). The tbbp-yttrium [**66$_Y$**] (Fig. 42) and etbbp- lanthanum [**67$_{La}$**] and cerium [**67$_{Ce}$**] complexes were obtained as suitable single-crystals for further X-ray structure determination.

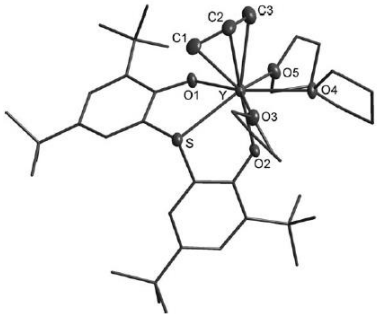

Fig. 42 ORTEP diagram of [{Y(tbbp)(η^3-C_3H_5)$(THF)_3$}.THF] [**66$_Y$**]. Thermal ellipsoids are drawn at the 30% probability level. Hydrogen atoms as well as the non-coordinated THF solvent molecules are omitted for clarity. Reprinted with the permission of WILEY-VCH Verlag GmbH.[98]

The (OSSO)-type complexes **67$_{Ln}$** were found very efficient and versatile catalysts towards the hydrosilylation of various olefins. According to the authors, lanthanum and cerium compounds were among the most active and regioselective homogeneous rare-earth metal catalysts for the hydrosilylation of styrene.[98]

3.3.4. Cationic (Allyl)LnX compounds with Cyclopentadienyl or related ligands

The reaction of complex ($C_5Me_4SiMe_3$)Sc(η^3-C_3H_5)$_2$ (**51$_{Sc}$**, *vide infra*, section 3.2.3), with [$HNMe_2Ph$][$B(C_6F_5)_4$] cleanly afforded the N,N-dimethylaniline-coordinated cationic mono-(η^3-allyl) complex [($C_5Me_4SiMe_3$)Sc(η^3-C_3H_5)(η^6-$PhNMe_2$)][$B(C_6F_5)_4$] [**68$_{Sc}$**]. Upon treatment with the trityl reagent [Ph_3C][$B(C_6F_5)_4$], complex **51$_{Sc}$** yielded the separated ion pair [($C_5Me_4SiMe_3$)Sc(η^3-C_3H_5)(η^6-PhMe)][$B(C_6F_5)_4$] [**68'$_{Sc}$**], whereas the same starting complex afforded the contact ion pair ($C_5Me_4SiMe_3$)Sc(η^3-C_3H_5)(μ,η^6-Ph)BPh_3] [**68''$_{Sc}$**] when reacted with [$HNMe_2Ph$][BPh_4] (Scheme 42).[75,75]

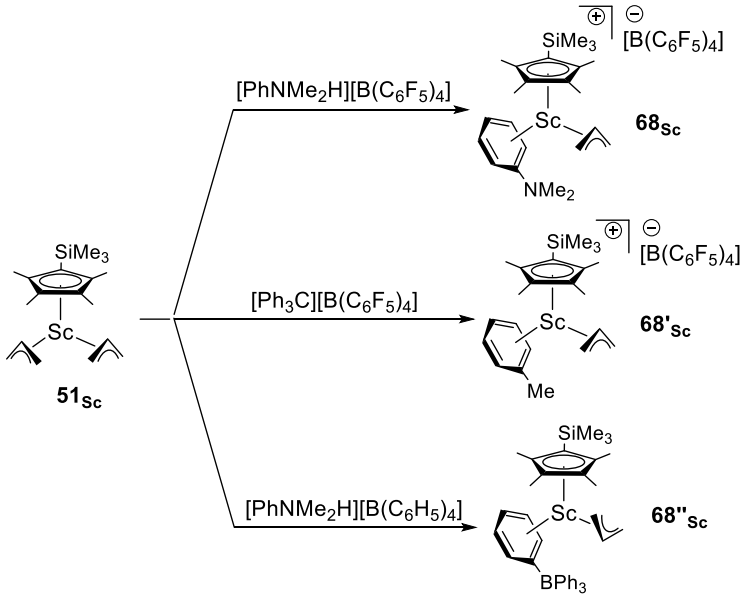

Scheme 42 Synthesis of allyl cationic scandium complexes

These cationic allyl complexes were found to be fluxional in solution from ^{1}H NMR analysis. They were all three isolated as X-ray suitable crystals and hence structurally characterized. Among them, **68$_{Sc}$** was the first example of a crystallographically characterized N,N-dimethylaniline-coordinated cationic metal complex, especially in allyl series. The isolation of the Lewis base free contact-ion-pair complex **68''$_{Sc}$** was an illustration that BPh_4 is more strongly coordinating than $B(C_6F_5)_4$, where one of the four Ph groups in BPh_4 showed bonding interactions with the Sc atom in an η^6 manner (Fig. 43). From recrystallization of the latter complexes in THF, THF-separated ion pairs $[(C_5Me_4SiMe_3)Sc(\eta^3\text{-}C_3H_5)(THF)_2][B(C_6F_5)_4]$ and $[(C_5Me_4SiMe_3)Sc(\eta^3\text{-}C_3H_5)(THF)_2][BPh_4]$ were isolated.

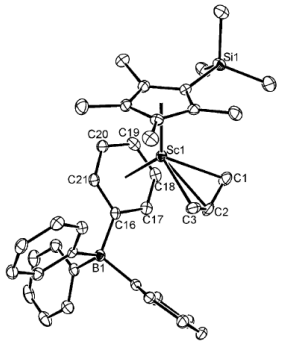

Fig. 43 ORTEP diagram of $[(C_5Me_4SiMe_3)Sc(\eta^3\text{-}C_3H_5)][BPh_4]$ [**68''$_{Sc}$**]. Thermal ellipsoids are drawn at the 30% probability level. Hydrogen atoms are omitted for clarity. Reprinted with the permission of WILEY-VCH Verlag GmbH.[75]

The THF-free ionic complexes **68$_{Sc}$** and **68'$_{Sc}$** were found to be highly active, without addition of any borate activator, towards the polymerization of isoprene and its copolymerization with norbornene.[75]

In a no less remarkable paper, Okuda and coworkers reported, shortly after these above mentioned studies of the Hou's group on scandium, that acid treatment of the half-sandwich bis-allyl complexes $Ln(C_5Me_4SiMe_3)(\eta^3\text{-}C_3H_5)_2(THF)$ (**51'$_{Ln}$**) with $[NEt_3H][BPh_4]$ or $[HNMe_2Ph][B(C_6F_5)_4]$ afforded the mono-allyl mono-cations $[(C_5Me_4SiMe_3)Ln(\eta^3\text{-}C_3H_5)(THF)_2]^+[B(C_6X_5)_4]^-$ (Ln = Y, La; **68$_{Ln}$**: X = F, **68'$_{Ln}$**: X = H) (Scheme 43).[6]

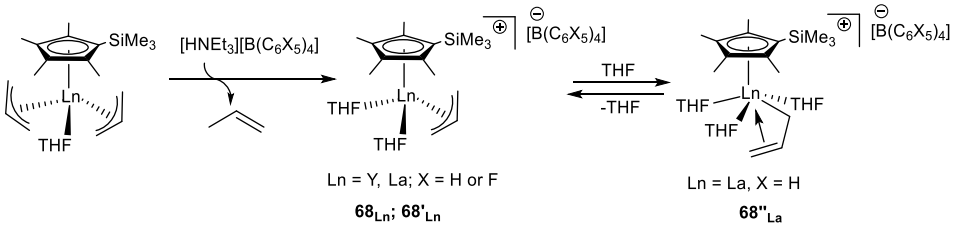

Scheme 43 Synthesis of half-sandwich allyl cationic complexes **68$_{Ln}$** and formation of related THF adducts in THF solution.

In the molecular structure of the lanthanum derivative **68''$_{La}$**, which was determined from X-ray quality crystals obtained in THF, one shorter C-C bond within the allyl ligand was found opposite to the Cp ligand, indicating an increased double-bond character (Fig. 44). ^{1}H NMR spectroscopy revealed little rigidity for the allyl group of the lanthanum complexes **68$_{La}$** and **68'$_{La}$**, whereas the yttrium derivatives **68$_{Y}$** and **68'$_{Y}$** displayed higher fluxionality with fast *syn/anti* exchange.

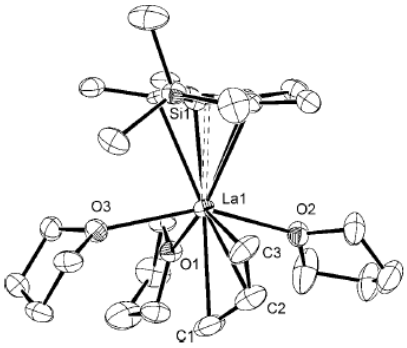

Fig. 44 ORTEP view of the cationic part of one of the two independent sets of ion pairs in **68''$_{La}$**. Thermal ellipsoids are set at the 50% probability level. Hydrogen atoms are omitted for clarity. Reprinted with the permission of WILEY-VCH Verlag GmbH.[6]

1,3-Butadiene polymerization was assessed with the monocationic half-sandwich allyl complexes **68$_{La}$** and **68$_{Y}$** in the presence of Al^{i}Bu$_3$. The yttrium-based catalyst **68$_{Y}$** showed much higher activity (TOF 12,000 h^{-1}), in comparison to the lanthanum one (TOF 1,600 h^{-1}) at room temperature in toluene with fair selectivity (86% 1,4-*cis*).

In a recently published joint experimental/theoretical study,[99] cationic Sc-allyl active species are described as intermediates that are formed during the uncommon ethylene/*cis*-1,4 butadiene copolymerization by means of catalysts issued from specially designed half-sandwich thiophene-fused cyclopentadienyl scandium complexes (see Fig. 45, **A** and **A'**).[100] From DFT calculations, it is proposed that it is the open coordination sphere of the scandium active species that facilitates butadiene η^4-*cis* coordination/insertion to give 1,4-*cis* regularity *via* the *anti* Sc-π-allyl intermediate.

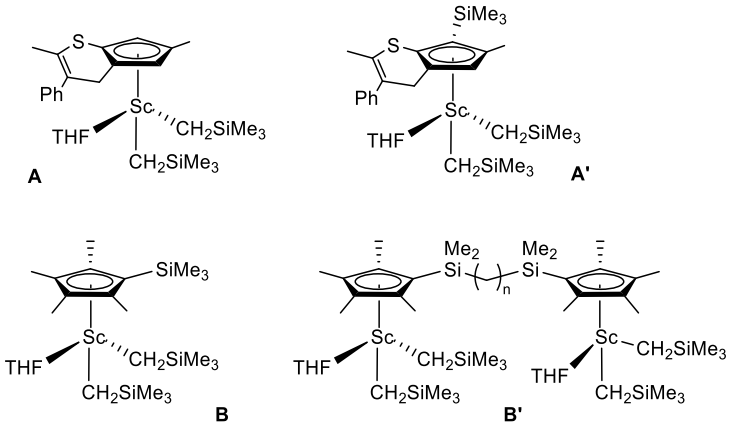

Fig. 45 Structures of thiophene-fused Cp and mononuclear/binuclear scandium complexes

At the same time, the Marks' group has prepared mononuclear and binuclear half-scandocenes (see Fig. 45, **B**) to study the impact of both pre-catalyst and co-catalyst nuclearity on the selectivity of isoprene (co-)polymerization. They concluded that the isomerization of allyl active species during the polymerization process was related to this nuclearity, which explained the different selectivities obtained.[101]

3.3.5. (Allyl)LnX$_2$ compounds with Cyclopentadienyl ligands

The mono(allyl)metallocene of scandium (C$_5$Me$_4$H)$_2$Sc(η^3-C$_3$H$_5$) [**69$_{Sc}$**] was synthesized similarly as described by Tsutsui in the pioneer studies related to mono(allyl) lanthanidocenes in the C$_5$H$_5$ series,[102] by the simple ionic metathesis between (C$_5$Me$_4$H)$_2$ScCl(THF) and allylmagnesium chloride (Scheme 44).[103]

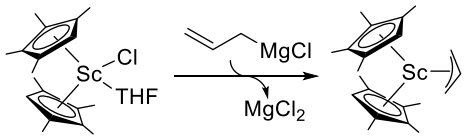

69$_{Sc}$

Scheme 44 Synthesis of monoallyl complex **69$_{Sc}$**

Previously in the chemistry of scandium, the *ansa*-cyclopentadienyl mono-allyl derivative {$Me_2Si[C_5H_2$-2,4-$(CHMe_2)_2]_2$}Sc(η^3-C_3H_5) had been prepared in a similar way.[104] This ionic metathesis strategy differs from the one developed ten years ago where $(C_5Me_5)_2Sc(C_3H_5)_3$ and [$Me_2Si(C_5H_3$-3-$CMe_3)_2$]Sc(η^3-C_3H_5) resulted from the insertion reaction of an allene with the corresponding metallocene hydrides.[105]

The complex **69$_{Sc}$** displayed fluxional behavior in solution and was characterized by X-ray diffraction as a non-solvated monomer (Fig. 46). This allyl scandocene was further used as precursor of the ion pair [$(C_5Me_4H)_2Sc$]-[(μ-Ph)BPh_3] upon protonation with $HNEt_3BPh_4$. The latter complex was subjected to KC_8 reduction in the presence of N_2, yielding the dinitrogen complex [$(C_5Me_4H)_2Sc]_2$(μ-η^2:η^2-N_2). This strategy, which involves the initial synthesis of an allyl derivative, is of high interest for the activation of small molecules with low reactivity such as molecular nitrogen.

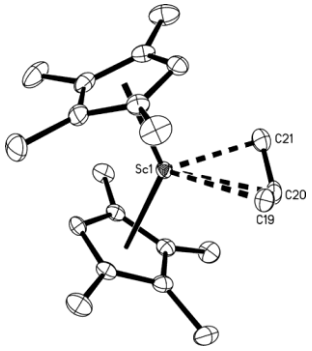

Fig. 46 ORTEP plot of **69$_{Sc}$** with thermal ellipsoids set at the 50% probability level. Hydrogen atoms are omitted for clarity. Reprinted with the authorization of the American Chemical Society.[103]

The mono(allyl) metallocene $(C_5Me_4H)_2Y(\eta^3$-$C_3H_5)$ [**69$_Y$**] was obtained as same as its scandium analog by treatment of the chlorometallocene precursor with one equiv. of allylmagnesium, followed by prolonged heating under vacuum (Scheme 45).[106]

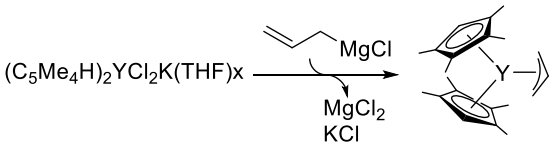

69$_Y$

Scheme 45 Synthesis of monoallyl complex **69$_Y$**

Monoallyl yttrium complex **69$_Y$** was extensively characterized, including by single crystal X-ray diffraction. In this complex, the longest Y-(C_3H_5) interaction is the central carbon of the allyl moiety, as is typical of other $(C_5Me_4R)_2Ln(\eta^3$-$C_3H_5)$ (R = H or Me) complexes.[107(**Lu, Cp***),108(**Nd, Sm, Tm, Cp***),9(**Sm, Cp***),109(**Lu, Y, Cp***)]

The reaction of **69$_Y$** with 1 equiv. $HNEt_3BPh_4$ yielded the non-solvated cation [$(C_5Me_4H)_2Y$][(μ-$Ph)_2BPh_2$] (Scheme 46).

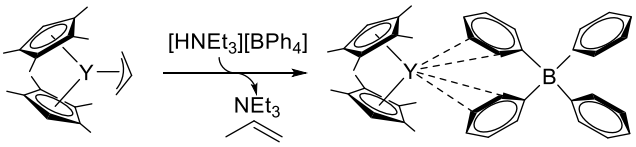

69$_Y$

Scheme 46 Protonation of allyl yttrocene **69$_Y$** to yield the corresponding cationic yttrium species

Upon hydrogenation with 1 atm of H_2, **69$_Y$** yielded the yttrium hydride complex, $[(C_5Me_4H)_2Y(\mu\text{-}H)]_x$ in 98% yield (Scheme 47). The allyl hydrogenation method clearly appears, again, as a valuable route for the preparation of hydride complexes.[106]

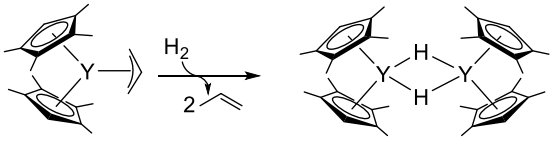

69$_Y$

Scheme 47 Hydrogenolysis of allyl yttrocene **69$_Y$** to yield the corresponding yttrium hydride

A well-known synthetic strategy in organolanthanide chemistry was developed by Evans, which was devoted to the synthesis of sterically hindered tris-cyclopentadienyl derivatives of the smallest lanthanides (from Tb to Lu and also including Y and Sc). This methodology uses the peculiar chemical reactivity of allyl complexes of lanthanides, as an alternative route to the classical ionic metathesis. It involves the intermediate preparation of an allyl complex $[(C_5H_4SiMe_3)_2Lu(\mu\text{-}C_3H_5)]_4$ [**70$_{Lu}$**] *via* the metathetic reaction of $[(C_5H_4SiMe_3)_2Lu(\mu\text{-}Cl)]_2$ with $(C_3H_5)MgCl$ according to Scheme 48.[110]

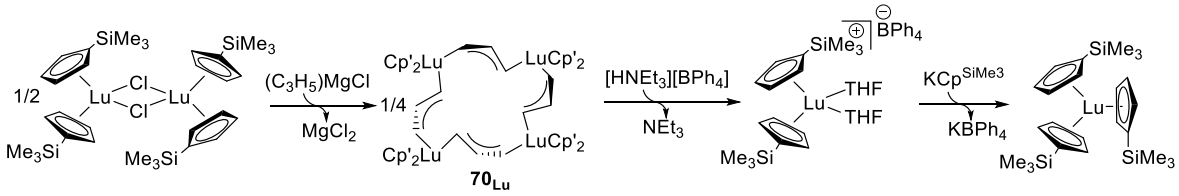

70$_{Lu}$

Scheme 48 Synthetic strategy for the preparation of sterically hindered triscyclopentadienyl complexes of the late lanthanides involving the intermediate allyl complex **70$_{Lu}$** (Cp' = $C_5H_4SiMe_3$)

The resulting allyl complex **70$_{Lu}$** crystallizes as a non-solvated tetramer as determined by X-ray diffraction studies (Fig. 47).

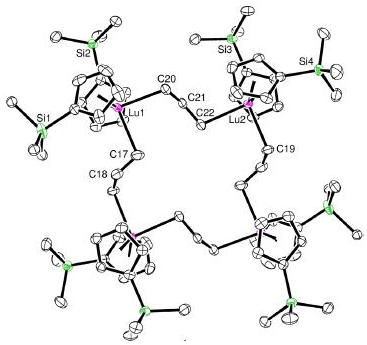

Fig. 47 ORTEP plot of **70$_{Lu}$** with thermal ellipsoids set at the 50% probability level and hydrogen atoms are omitted for clarity. Reprinted the permission of the American Chemical Society.[110]

In a second step, this monoallyl derivative subsequently reacts with $[HNEt_3][BPh_4]$ to generate the ionic pair $[(C_5H_4SiMe_3)_2Lu(THF)_2]^+[BPh_4]^-$, which affords upon addition of $KC_5H_4SiMe_3$ the triscyclopentadienyl $(C_5H_4SiMe_3)_3Lu$ in good yield.

More recently, the methylallyl yttrium derivative $(Cp^*)_2Y(\eta^3\text{-}CH_2CMeCH_2)$ ((Cp^* = C_5Me_5, **71$_Y$**) was classically synthesized from (methylallyl)magnesium chloride and $(Cp^*)_2YCl_2K(THF)$. This compound was prepared as a model to help at identifying by-products of photochemical activation. Its X-ray crystal structure was determined (Fig. 48).[111]

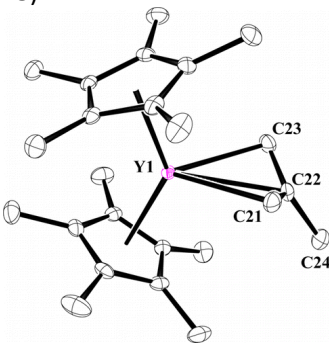

Fig. 48 ORTEP plot of **71$_Y$**. Ellipsoids are drawn at the 50% probability level. The second molecule and the hydrogen atoms are omitted for clarity. Reprinted with the authorization of the American Chemical Society.[111]

Photochemical activation of rare-earth-metal bis-(pentamethylcyclopentadienyl) allyl complexes $(Cp^*)_2Ln(\eta^3\text{-}C_3H_4R)$ (Ln = Y, Lu; **71$_{Ln}$**: R = Me; **72$_{Ln}$**: R = H) was used by Evans and co-workers to reduce dinitrogen, affording $[(Cp^*)_2Ln]_2(\mu\text{-}\eta^2\text{:}\eta^2\text{-}N_2)$ complexes. In the presence of isoprene, similar photolytic activation of complexes **72$_{Ln}$** (Ln = Y, Lu) provided polyisoprene, which was the result of radical rather than coordinative polymerization, according to the authors, while sulfur was reduced under the same conditions to generate $[(Cp^*)_2Ln]_2(\mu\text{-}S)$ complexes (Scheme 49).[111]

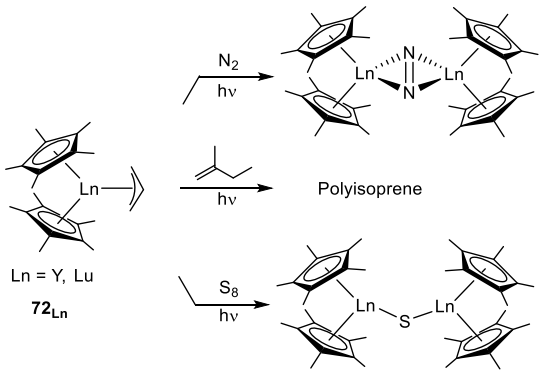

Scheme 49 Photochemical activation of **72$_{Ln}$** (Ln = Y, Lu) in the presence of various substrates

The mono(allyl) complexes in the bis(pentamethylcyclopentadienyl) series, $Cp^*_2Ln(C_3H_5)$ [**72$_{Ln}$**], were the subject of several reactivity studies during the last two decades, and they have in part been mentioned in the previous edition of COMC.[1] Among these studies, the most important contribution came from the group of Evans, who investigated, apart from above-mentioned activation reactions, the chemical potential of the Ln-(allyl) bond towards several insertion reactions and hydrogenolysis.

This group examined in 2008 the reaction of complexes **72$_{Ln}$** (Ln = Y, La, Sm) with (trimethylsilyl)diazomethane. Elements of different ionic radius (small yttrium, large lanthanum and intermediate samarium) were chosen in order to get an overview of the reactivity of these complexes. It was observed that in all three cases clean insertion takes place, instead of the more classical metalation encountered with $(Cp^*)_2Sm$ or $[(Cp^*)_2SmH]_2$,[112] affording the lanthanide hydrazonato complexes of formula $(Cp^*)_2Ln[\eta^2(N,N')\text{-}RNN{=}CHSiMe_3]$ (R = $CH_2{=}CHCH_2$, Scheme 50).[113] The complexes were crystallographically characterized where the double bond of the allyl substituent is oriented toward the metal center in the lanthanum complex, with no detection of a metal-carbon interaction, whereas in samarium and yttrium ones this bond points away from the metals.

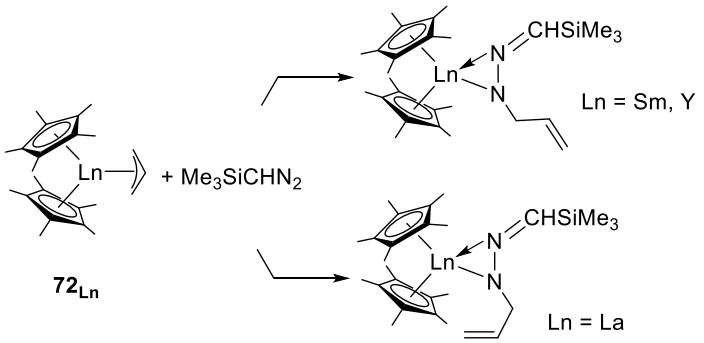

Scheme 50 Reaction of complexes **72$_{Ln}$** (Ln = Y, La, Sm) with (trimethylsilyl)diazomethane

Very soon after, the lanthanide metallocene allyl complexes $(Cp^*)_2Ln(C_3H_5)(THF)$ (**72'$_{Ln}$**, Ln = Ce, Sm, Y) were readily transformed into $(Cp^*)_2Ln(hpp)$ (hpp = 1,3,4,6,7,8-hexahydro-2H-pyrimido[1,2-α]pyrimidinate) by deprotonation in the presence of Hhpp,[114] which is another illustration of the acid-base reactivity of the Ln(allyl) moiety (Scheme 51). It must be emphasized however that both $(Cp^*)_2Sm$ and $[(Cp^*)_2SmH]_2$ led to the same $(Cp^*)_2Ln(hpp)$ when submitted to the reaction with Hhpp, which shows the duality of reactivity of the metal-allyl fragment depending on the reagent considered (see the reactivity observed towards (trimethylsilyl)diazomethane, as discussed immediately above).

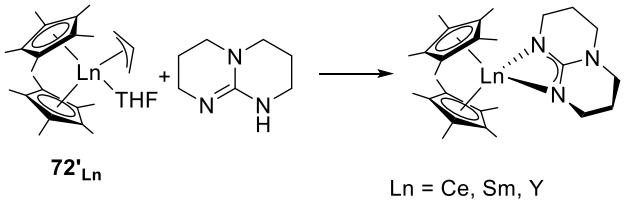

Scheme 51 Acid-base reaction of complexes **72'$_{Ln}$** (Ln = Ce, Sm, Y) with Hhpp (hpp = 1,3,4,6,7,8-hexahydro-2H-pyrimido[1,2-α]pyrimidinate)

In 2010, nitric oxide NO was found to cleanly react with $(Cp^*)_2Ln(C_3H_5)(THF)$ (**72'$_{Ln}$**, Ln = Y, La, Sm) to form $\{(Cp^*)_2Ln[\mu\text{-}ONN(CH_2CH{=}CH_2)O]\}_2$ complexes, which were structurally characterized. The formation of $ONN(CH_2CH{=}CH_2)O^-$ anion was proposed to arise from insertion of NO into the Ln-C(allyl) bond followed by coupling of the (allyl-NO) radical anion with a second molecule of NO (Scheme 52).[115]

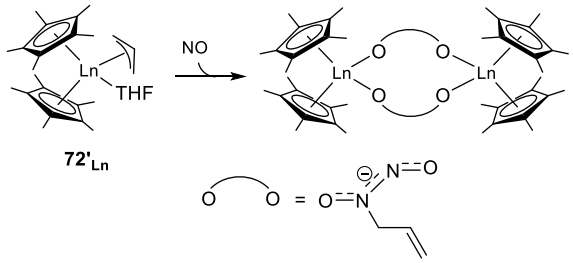

Scheme 52 Insertion of NO into Ln-allyl fragment in **72'$_{Ln}$** allyl complexes (Ln = Y, La, Sm)

The same group also showed at the same time that N_2O undergoes facile insertion into metal-carbon bonds of several allyl metallocene complexes to form $(C_3H_5N_2O)$ ligands: the products $[(Cp^*)_2Ln(\mu\text{-}\eta^1{:}\eta^2\text{-}O\text{-}N{=}N\text{-}C_3H_5)]_2$ (Ln = Y, Sm, La) were obtained in reactions of N_2O with the bis(Cp*) allyl complexes (as THF adducts **72'$_{Ln}$**, Ln = Y, Sm, La), instead of the expected metallocene oxides. Similar reactivity was observed in the tetramethylcyclopentadienyl series, with the formation of $[(C_5Me_4H)_2Ln(\mu\text{-}\eta^1{:}\eta^2\text{-}O\text{-}N{=}N\text{-}C_3H_5)]_2$ (M = Sc, Y) from the mono(allyl) lanthanidocenes **71$_{Ln}$** (Ln = Sc, Y).[116]

Later, the Evans' group studied insertion reactions with chalcogenides reagents. They reported that **71$_{Sc}$** reacts with PhEEPh (E = S, Se, Te) to form the products $[(C_5Me_4H)_2Sc(SPh)]_2$, $(C_5Me_4H)_2Sc(SePh)$

and $(C_5Me_4H)_2Sc(TePh)$, respectively, along with $(C_3H_5)EPh$ release (Scheme 53, up).[117] In presence of 2,2'- dipyridyl disulfide, pySSpy, the monometallic sulfur derivative $(C_5Me_4H)_2Sc(Spy\text{-}\kappa^2\text{-}S,N)$ is obtained (Scheme 53, down).

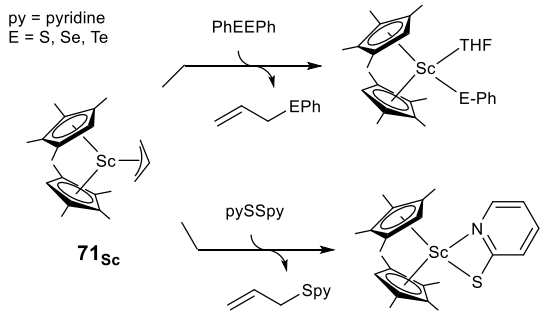

Scheme 53 Reactions of allyl scandocene **71$_{Sc}$** with chalcogenides

A σ-bond metathesis mechanism was proposed to account for such experimental results, as an example of Sc-C (*via* η^1-allyl) bond reactivity (Scheme 54).

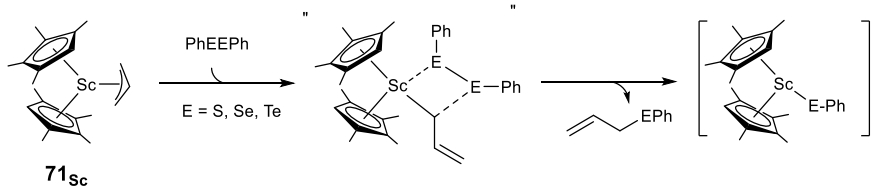

Scheme 54 Mechanistic pathway of the insertion of chalogenides in Sc-allyl moiety [117]

Beside these reactions, which are related to the insertion in a Ln-allyl bond of a metallocene derivative, a particular reactivity is to be reported. It concerns the reaction of **72$_Y$** with the borane 9-borabicyclo[3.3.1]nonane (9-BBN) that afforded a compound containing two yttrium metallocene borane complexes $(Cp^*)_2Y[\eta^3\text{-}C_3H_4(BC_8H_{14})]$ [**73$_Y$**] and $(Cp^*)_2Y(\mu\text{-}H)_2(BC_8H_{14})$, in a single crystal, as revealed by X-ray crystallographic analysis (Fig. 49)[118]

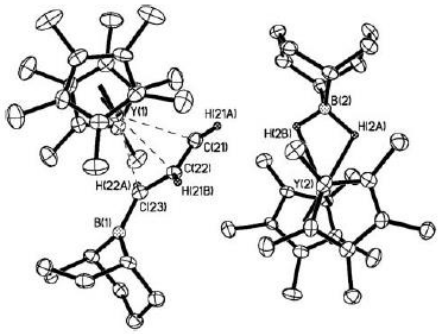

Fig. 49 ORTEP plot of $(Cp^*)_2Y[\eta^3\text{-}C_3H_4(BC_8H_{14})]$ [**73$_Y$**] and $(Cp^*)_2Y(\mu\text{-}H)_2(BC_8H_{14})$, in a single crystal, thermal ellipsoids are drawn at the 50% probability level. The second molecule and the hydrogen atoms are omitted for clarity. Reprinted with the authorization of the Royal Chemical Society.[118]

The two compounds are proposed to be formed after a several steps process, **73$_Y$** being the result of the uncommon addition of 9-BBN in the olefin – arising from the yttrium allyl starting compound **62$_Y$** – with the allyl group in an η^1-coordination mode, based on *in situ* ^1H and ^{11}B NMR spectroscopy studies (Scheme 55).

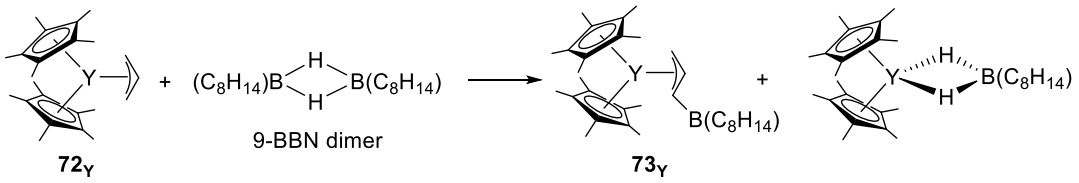

Scheme 55 Reactions of allyl yttrocene **72$_Y$** with 9-BBN

Later, in 2014, it was found that hydrogenolysis of a 1:1 mixture of $(Cp^*)_2Lu$-(η^3-C_3H_5) [**72$_{Lu}$**] and $(Cp^*)_2Y(\eta^3$-$C_3H_5)$ [**72$_Y$**] forms a mixture of hydride complexes, from which the heterobimetallic "tuckover" compound $(Cp^*)_2Lu(H)_2YCp^*_2$ could be isolated, in addition to the already known $[(Cp^*)_2LuH]_2$ and $[(Cp^*)_2YH]_2$ (Scheme 56). Also, 1:1 mixtures of bis(Cp*) allyl complexes with lanthanum and lutetium or yttrium yielded exclusively the heterobimetallic products under the same conditions.[119]

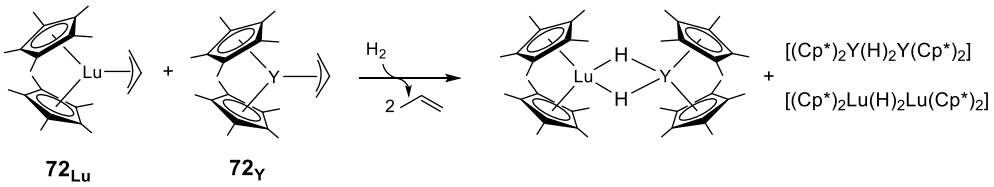

Scheme 56 Heterobimetallic hydride preparation from hydrogenolysis of mixtures of allyl lanthanidocenes

The previously mentioned review from Carpentier[2] cites quite extensively the two families of *ansa*-cyclopentadienyl-fluorenyl[120,121] (Cp-Flu) and *ansa*-indenyl- allyl complexes of the lanthanides published in the mid-2000s (Fig. 50).[122] In terms of reactivity, these complexes were initially found as efficient and stereoselective (*syndio*- for the former ones and *iso*- for the latter ones) single-component catalysts for styrene polymerization. We can however specify that in the Cp-Flu series (complexes (a) in Fig. 50), the combination of the chloro neodymium precursor with $Mg(allyl)_2$, which leads to the *in situ* formation of the corresponding allyl-Nd derivative, is much less active than the single-component catalyst, although almost as *syndio*-selective.[123] Among these catalysts, some were the subject of more in-depth studies of their reactivity in polymerization that were not reported in the above cited review.

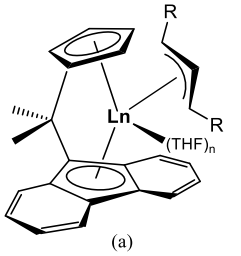

(a)

R = H, n = 1 — **74$_{Ln}$** (Ln = Y, La, Nd, Sm)

R = $SiMe_3$, n = 0 — **74'$_{Nd}$** (Ln = Nd)

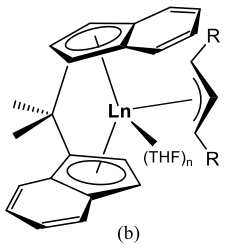

(b)

R = H, n = 1: **75$_{Ln}$** (Ln = Y, Nd)

R = $SiMe_3$, n = 0: **75'$_{Ln}$** (Ln = Y, Nd)

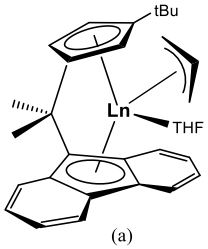

(a)

74''$_{Ln}$ (Ln = Y, Nd)

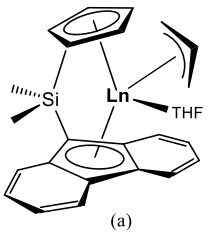

(a)

75'''$_{Ln}$ (Ln = Y, Nd)

Fig. 50 Examples of *ansa*-(Cp-Flu)(allyl) ((a) form) and *ansa*-(indenyl)(allyl) ((b) form) complexes of the lanthanides

The mechanism of initiation of the syndiospecific styrene polymerization catalyzed by single-component *ansa*-(Cp-Flu) neodymium allyl was investigated by experimental/computational joint studies.[124] It was found by ^{13}C NMR studies of oligomers prepared by chain-growth polymerization using {$C_5H_4CMe_2$(9-$C_{13}H_8$)}Nd[η^3-1,3-($SiMe_3$)$_2C_3H_3$]/excess Mg(*n*Bu)$_2$ that 2,1-insertion is preferential to 1,2-insertion pathway. Moreover, according to the authors, the DFT studies revealed that with both *ansa*-dimethylmethylene **74$_{Ln}$** and *ansa*-dimethylsilylene **74$_{Ln}$'''** the insertion of styrene monomer takes place in the η^3-coordinated allyl moiety without the need to switch to η^1 hapticity (calculations performed on the europium complex), in contrast to the mechanism proposed in the case of organoaluminum-mediated chain transfer polymerization of 1,3-dienes with Nd-based catalysts.[125] In the same paper from Carpentier and coworkers, when comparing the two CMe_2- and $SiMe_2$-bridged complexes, it was concluded that the activity in styrene polymerization could be predicted to be higher in the former series.[124] Finally, the nature of the initiating ligand was deduced to be of prime importance in these single-component *ansa*-(Cp-Flu) neodymium complexes, with a very clear preference for Nd-allyl *vs* Nd-alkyl according to DFT.

Seeking to determine the origin of syndiospecificity in styrene polymerization observed with the bulky *ansa*-lanthanidocene allyl in the Cp-Flu series, authors from the same research group performed other DFT investigations, which were published posteriorly in 2010. It was proposed that the origin of the *syndio* control was due to a chain-end control mechanism (CEM), resulting from the conjunction of the minimization of two repulsion effects: the classical phenyl (incoming monomer)-phenyl (last unit inserted) one during the growing of the polymer chain, and also of the repulsion between the fluorenyl ligand and the incoming styrene unit. [126] This family of *ansa*-(Cp-Flu) allyl complexes were finally shown to display high versatility, with the possibility of producing syndiotactic styrene-rich co-polymer materials including isoprene and/or ethylene.[127]

Later, in 2011, Carpentier and coworkers found that the combination of the bulky allyl *ansa*-lanthanidocene **74'$_{Nd}$** (Fig. 50) with di(*n*-butyl)magnesium in excess behaved efficiently as binary catalytic system for the stereo-controlled coordinative polymerization of styrene under reversible chain transfer regime (CCTP, coordinative chain transfer polymerization), yielding syndiotactic PS with high activity (TOF 2,500 h^{-1}). [128] A CCTP behavior was observed as well for *rac*-{$Me_2C(Ind)_2$}Y[η^3-1,3-($SiMe_3$)$_2C_3H_3$] (**75'$_Y$**, Ind = indenyl) under reversible transfer coordinative polymerization conditions, while this complex was previously shown to be active as single-component catalyst, but the dispersity was improved in the presence of an excess of Mg(^{n}Bu)$_2$. By adjusting the amount of Mg(^{n}Bu)$_2$, up to 200 polymer chains can be generated per lanthanide center.[129] In terms of selectivity, isotactic PS was produced with this yttrium catalyst combination with high activities (TOF up to 2,100 h^{-1}).[128] Thorough mechanistic investigations, also confirmed by the support of theoretical studies, demonstrated that the initiation of the polymerization resulted from the insertion of styrene into the Ln-allyl (single component) or Ln-alkyl (chain transfer) moiety, and that an enantiomorphic site control mechanism (ECM) was operative to account for the *iso*-selectivity observed.[130]

The *ansa*-indenyl allyl complex of yttrium *rac*-{$Me_2C(Ind)_2$}Y[η^3-1,3-($SiMe_3$)$_2C_3H_3$] [**75'$_Y$**] (Fig. 50) was also reported in 2007 as active as single-component catalyst towards isoprene homopolymerization, affording 1,4-*trans* rich PI with moderate activity (TOF 70 h^{-1}). The same authors subsequently showed that when di(ethyl)zinc was added in excess, reversible Y/Zn chain transfer was observed, with a comparable activity (TOF 76 h^{-1}), while maintaining the 1,4-*trans* selectivity (ca. 90%). In turn, in combination with Mg(^{n}Bu)$_2$ a good level of transfer was noticed, but at the expense of the 1,4-*trans* selectivity (up to 47% 3,4 units).[129]

To complete the polymerization studies with this complex, the copolymerization of isoprene and styrene mediated by *rac*-{$Me_2C(Ind)_2$}Y[η^3-1,3-($SiMe_3$)$_2C_3H_3$] [**75$_Y$**] in the absence of co-reagent afforded statistical copolymers with blocky distribution of the two monomers. Well-defined and

crystalline 1,4-*trans*-PI-*b*-iPS diblock copolymers were also prepared by sequential addition of the two monomers.[129]

3.3.6 (Allyl)LnXX' compounds

When the same synthetic procedure as for the synthesis of $Cp^{NMe2}Ln(\eta^3\text{-}C_3H_5)_2$ (Ln = Y, Ho, Lu) complexes was done in the case of the larger size neodymium element (Scheme 34, *vide infra*), it gave a mono(allyl) chloro derivative $[Cp^{NMe2}Nd(\eta^3\text{-}C_3H_5)(\mu\text{-}Cl)]_2$ [**76$_{Nd}$**], instead of the expected bis allyl half-sandwich (Scheme 57). This neodymium complex was found to be dimeric through (μ-Cl) bridges with one substantially longer Nd-Cl bond than the other one, anticipating a possible reactivity.[82]

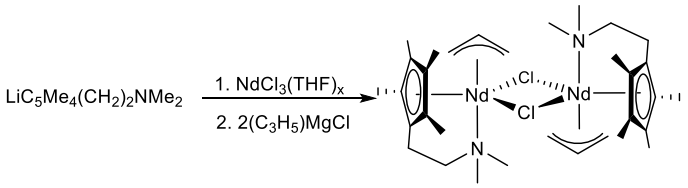

76$_{Nd}$

Scheme 57 Synthesis of mono(allyl)(chloro) complex **76$_{Nd}$**

This chloro-allyl half-sandwich neodymium complex was found to be fairly active (TOF 1,000-2,000 h^{-1}) towards the polymerization of isoprene when combined with a borate activator and excess (10 equiv.) of AlR_3 cocatalyst. Interestingly, the selectivity switched from 85% 1,4-*trans* PI ($AlMe_3$) to 85% 3,4-PI ($Al(^iBu)_3$) depending on the aluminum reagent used. In common with the other complexes bearing this Cp^{NMe2} ligand (*vide infra*), the use of Al^iBu_3 *vs.* $AlMe_3$ with **76$_{Nd}$** provided reversible transfer between the lanthanide metal and the aluminum during the polymer chain growing process. Finally, the neodymium complex **76$_{Nd}$** was found to be inactive on its own without activator/co-catalyst, as already observed for the bis(allyl)Cp^{NMe2} complexes.

Table 5 Structural and analytical data of bis-substituted mono(allyl) complexes (in brackets only the relevant complexes only, otherwise for all complexes)

Compound number	Molecular Formula	X-ray data Ln-C(allyl) distances (Å)	NMR data	References
61$_{Sc}$, **61$_{Y}$**, **61$_{La}$**, **61$_{Sm}$**, **61$_{Nd}$**	$Ln(BH_4)_2(\eta^3\text{-}C_3H_5)(THF)_n$ (Ln = Sc, n = 2 ; Ln = Y, La, Sm, Nd, n = 3)	Y-C = 2.629, 2.636, 2.619 Sc-C = 2.508, 2.467, 2.419 La-C = 2.717, 2.810, 2.813 Sm-C = 2.663(3), 2.696(3), 2.685(3) Nd−C = 2.719(7), 2.740(6), 2.699(6)	^1H ^{11}B (**61$_{Y}$**, **61$_{La}$**)	84,86
62$_{Y}$, **62$_{La}$**	$[(1,7\text{-}Me_2TACD)Ln(\eta^3\text{-}C_3H_5)]_2$ (Ln = Y , La)	La−C = 2.834(5), 2.843(5), 2.828(5)	^1H, ^{13}C (**62$_{La}$**)	88
62$_{Sc}$	$(1,7\text{-}Me_2TACD)Sc(\eta^3\text{-}C_3H_5)$	-	^1H, ^{13}C	90
63$_{Y}$, **63$_{La}$**	$[(1,7\text{-}Me_2TACD)Ln(\eta^3\text{-}C_3H_5)_2K(THF)]_n$ (Ln = Y, La)	-	^1H, ^{13}C	88
64$_{Nd}$, **64$_{Sm}$**	$[Ln(Me_3TACD)(\eta^3\text{-}C_3H_5)(\mu\text{-}H)]_2$ (Ln = Nd, Sm)	Sm-C = 2.749(4), 2.762(4), 2.825(3) Nd-C = 2.759(3), 2.799(3), 2.853(2)	^1H, ^{13}C (**64$_{Sm}$**)	91

65$_{Nd}$	{2-[$Ph_2P(O)$]$C_6H_4NC(^tBu)N$(2,6-$Me_2C_6H_3$)}$_2$Nd(C_3H_5)	Nd-C = 2.67(2) to 2.78(2)	-	93
66$_Y$, **66$_{La}$**	[Ln(tbbp)(η^3-C_3H_5)(THF)$_{1-2}$] (Ln = Y, La)	Y-C = 2.611(4), 2.646(4), 2.670(4	^{1}H, ^{13}C	98
67$_{La}$, **67$_{Ce}$**, **67$_{Nd}$**, **67$_{Sm}$**	[Ln(etbbp)(η^3-C_3H_5)(THF)$_{1-2}$] (Ln = La, Ce, Nd, Sm)	La = 2.744(2), 2.8009(17), 2.8087(18) Ce-C = 2.729(4), 2.765(3), 2.770(3)	^{1}H, ^{13}C	98
68$_{Sc}$	[($C_5Me_4SiMe_3$)Sc(η^3-C_3H_5)(η^6-$PhNMe_2$)][$B(C_6F_5)_4$];	Sc-C = 2.575(6), 2.584(9), 2.523(5)	^{1}H, ^{13}C (**68'$_{Sc}$**, **68''$_{Sc}$**), ^{19}F(**68'$_{Sc}$**), ^{11}B (**68'$_{Sc}$**)	75
68'$_{Sc}$	[($C_5Me_4SiMe_3$)Sc(η^3-C_3H_5)(η^6-PhMe)][$B(C_6F_5)_4$];	Sc-C = 2.454(3), 2.498(5), 2.417(3)		
68''$_{Sc}$	($C_5Me_4SiMe_3$)Sc(η^3-C_3H_5)(μ,η^6-Ph)BPh_3]	Sc-C = 2.409(2), 2.452(2), 2.515(2)		
68$_Y$, **68'$_Y$**, **68$_{La}$**, **68'$_{La}$**	[($C_5Me_4SiMe_3$)Ln(η^3-C_3H_5)$(THF)_2]^+$[$B(C_6X_5)_4]^-$ (Ln = Y, La; X = H, F)	**68''$_{La}$**: La-C = 2.844(5), 2.803(5), 2.684(5)	^{1}H, ^{13}C, ^{11}B, ^{19}F (**68$_Y$**, **68$_{La}$**)	6
69$_{Sc}$, **69$_Y$**	($C_5Me_4H)_2$Ln(η^3-C_3H_5) (Ln = Sc, Y)	Sc-C = 2.4702(11), 2.4774(11), 2.4618(11) Y-C = 2.590(3), 2.594(3), 2.603(3) ; 2.585(3), 2.592(3), 2.603(3)	^{1}H, ^{13}C, ^{45}Sc (**69$_{Sc}$**)	103, 106
70$_{Lu}$	[($C_5H_4SiMe_3)_2$Lu(μ-η^1:η^1-C_3H_5)]$_4$	Lu−C = 2.508(3), 2.482(3), 2.485(3)	^{1}H	110
71$_Y$	($C_5Me_5)_2$Y(η^3-CH_2CMeCH_2)	Y-C = 2.562(2), 2.7021(2), 2.570(2)	^{1}H, ^{13}C	111
73$_Y$	(Cp*)$_2$Y[η^3-$C_3H_4(BC_8H_{14})$]	Y-C = 2.681(5), 2.661(5), 2.632(5)	^{1}H, ^{11}B	118
74$_Y$, **74$_{La}$**, **74$_{Nd}$**, **74$_{Sm}$** ; **74'$_{Nd}$** ; **74''$_Y$**, **74''$_{Nd}$** ; **74'''$_Y$**, **74'''$_{Nd}$**	{C_5H_3R-EMe_2(9-$C_{13}H_8$)}Ln[η^3-1,3-(R')$_2C_3H_3(THF)_n$]: E = C, Si; R = H, ^{t}Bu ; R' = H, $SiMe_3$; n = 0, 1	**71$_{Nd}$**: Nd-C = 2.656(12) , 2.700(11), 2.725(9) ; **71"$_{Nd}$**: Nd-C = 2.639(5), 2.756(5), 2.818(5) ; **71'''$_Y$**: Y-C = 2.583(2), 2.571(10) ; 2.649(2)	^{1}H (**71$_Y$**, **71$_{La}$**, **71''$_Y$**, **71'''$_Y$**), ^{13}C (**71$_Y$**, **71''$_Y$**, **71'''$_Y$**)	121
75$_Y$, **75$_{Nd}$** ; **75'$_Y$**, **75'$_{Nd}$**	*rac*-{$Me_2C(Ind)_2$}Ln[η^3-1,3-$R_2C_3H_3(THF)_n$]: R = H, $SiMe_3$; n = 0,1	**72'$_Y$**: Y-C in CCDC-648472	^{1}H (**72'$_Y$**), ^{13}C (**72'$_Y$**)	122
76$_{Nd}$	[Cp^{NMe2}Nd(η^3-C_3H_5)(μ-Cl)]$_2$	Nd-C = 2.666(5), 2.702(4), 2.685(5)	-	82

3.4. Aza-allyl Lanthanide complexes

Zhang *et al*. reported in 2010 a new method to prepare lanthanide hetero-allyl complexes by insertion of a ketenimines into the Ln-C σ-Bond of a lanthanide precursor:[131] the reaction of [Cp_2Ln(μ-Me)]$_2$ and Cp_2LnPh with PhRC=C=N^{t}Bu gives 1-aza-allyl organometallic complexes Cp_2Ln[^{t}BuNC(R')CRPh] (Ln = Y, Er, Yb; **77$_{Ln}$**: R = Ph, R' = Me; **78$_{Ln}$**: R = Ph, R' = Ph; **79$_{Ln}$**: R = H, R' = Me; **80$_{Ln}$**: R = H, R' = Ph) (Scheme 58).

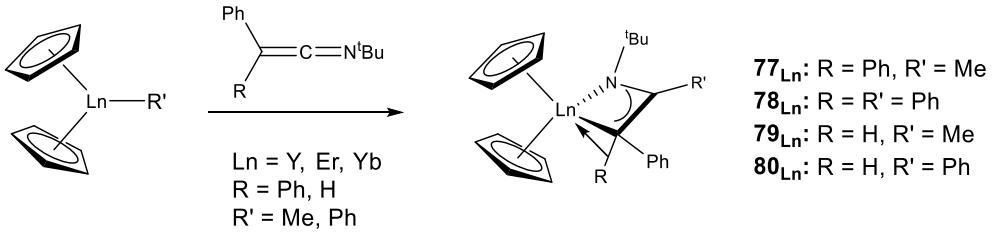

Scheme 58 Synthesis of aza(allyl) complexes **77$_{Ln}$, 78$_{Ln}$, 79$_{Ln}$, 80$_{Ln}$**

The erbium congener **77$_{Er}$** was isolated as X-ray quality crystals (Fig. 51). The structural data revealed that the resulting aza(allyl) ligand in that complex has a strong η^3-interaction with the Er^{3+} ion. Thus, the coordination sphere of the metal atom is partly saturated by one agostic interaction to one hydrogen atom from the ligand. A similar structure was observed for ytterbium (**77$_{Yb}$**) and yttrium (**77$_{Y}$**) congeners.

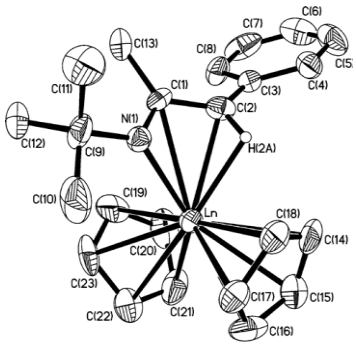

Fig. 51 ORTEP plot of $Cp_2Er[^tBuNC(Me)CHPh]$ (**77$_{Er}$**) with the probability ellipsoids drawn at the 30% level. Hydrogen atoms are omitted for clarity. Reprinted with the permission of the American Chemical Society.[131]

Recently, it was observed that the treatment of rare-earth metal dialkyl complexes supported by a pyrrolyl-functionalized β-diketiminato ligand with the formula $[MeC(NDipp)CHC(Me)NCH_2CH_2NC_4H_2$-2,5-$Me_2]Ln(CH_2SiMe_3)_2(THF)$ (Ln = Y, Er; Dipp = 2,6-$^iPr_2C_6H_3$) with 2,4,6-trimethylpyridine leads to the mononuclear azaallyl $[MeC(NDipp)CHC(Me)NCH_2CH_2NC_4H_2$-2,5-$Me_2]Ln(\eta^3$-$CH_2$-2-$NC_5H_2$-4,6-$Me_2)_2$ (**81$_{Ln}$**, Ln = Y, Er) *via* sp^3 C-H activation (Scheme 59, shown for the erbium congener). The complexes were isolated as suitable X-ray crystals, where the η^3-aza-allyl arrangement was evidenced by Ln-C and Ln-N bond lengths of *ca.* 2.4-2.8 Å, *i.e.* in the typical range for this coordination mode.[57]

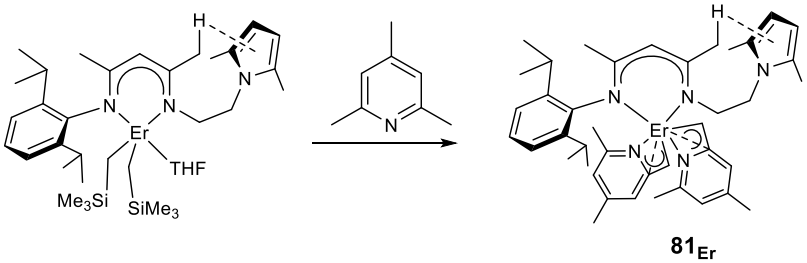

81$_{Er}$

Scheme 59 Synthesis of **81$_{Er}$** via C-H activation of 2,4,6-trimethylpyridine by the (pyrrolyl-functionalized β-diketiminato)dialkyl erbium precursor

Table 6 Structural and analytical data of aza-allyl complexes (in brackets only the relevant complexes only, otherwise for all complexes)

Compound number	Molecular Formula	X-ray data Ln-C(allyl) distances (Å)	NMR data	References

77$_{Y}$, **77**$_{Er}$, **77**$_{Yb}$; **78**$_{Y}$, **78**$_{Er}$, **78**$_{Yb}$; **79**$_{Y}$, **79**$_{Er}$, **79**$_{Yb}$; **80**$_{Y}$, **80**$_{Er}$, **80**$_{Yb}$	$Cp_2Ln[^tBuNC(R')CRPh]$ (R = Ph, R' = Me; R = Ph, R' = Ph; R = H, R' = Me; R = H, R' = Ph)	**77**$_{Ln}$: Y-C =2.917(6), 2.902(5), 2.754(5) Er-C = 2.892(5), 2.903(5), 2.725(5) Yb-C = 2.892(7), 2.940(7), 2.740(6) **78**$_{Ln}$: Y-C =2.874(10), 2.907(8), 2.795(8) Yb-C = 2.856(7), 2.899(7), 2.743(7) Yb-C = 2.880(7) ; 2.943(7) ; 2.761(7)	^{1}H (**77**$_{Y}$, **78**$_{Y}$, **79**$_{Y}$, **80**$_{Y}$), ^{13}C (**77**$_{Y}$, **78**$_{Y}$, **79**$_{Y}$, **80**$_{Y}$)	131
81$_{Y}$, **81**$_{Er}$	[MeC(NDipp)CHC(Me)$NCH_2CH_2NC_4H_2$-2,5-Me_2]Ln(η^3-CH_2-2-NC_5H_2-4,6-Me_2)$_2$ (Ln = Y, Er; Dipp = 2,6-$^iPr_2C_6H_3$)	Y-C = 2.465(5), 2.727(5) Er-C= 2.450(5), 2.709(5)	^{1}H, ^{13}C (**81**$_{Y}$)	57

3.5 Lanthanide complexes with unusual allyl coordination mode

The equimolar reaction between $Y(CH_2SiMe_3)_3(THF)_2$ precursor and $HL^2(^iPr)$ pro-ligand [$HL^2(^iPr)$ = $Cp^{Me}PN$-type ligand $C_5Me_4H{-}PPh_2{=}N{-}2,6\text{-}^iPr_2\text{-}C_6H_3$] in the presence of LiCl afforded two distinct bis(alkyl) complexes based on ^{1}H NMR spectroscopic analysis (Scheme 60).[132]

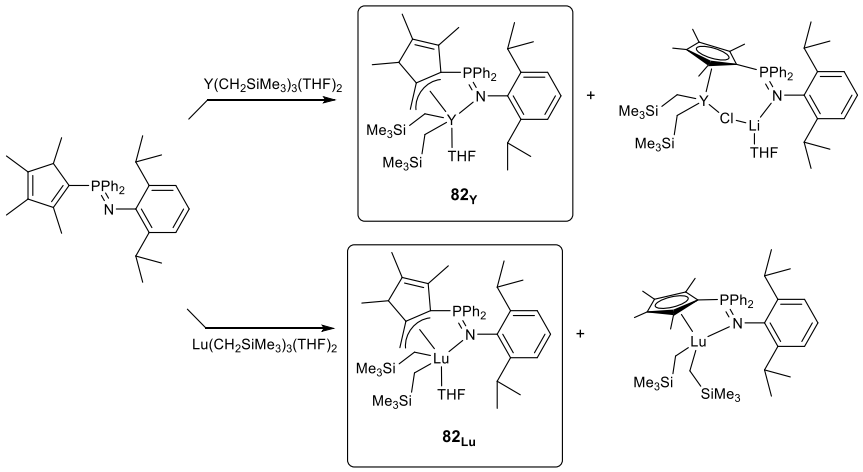

Scheme 60 Synthesis of complexes **82**$_{Ln}$

Recrystallization of the crude material from these reaction mixtures furnished the complexes $[C_5HMe_3(\eta^3\text{-}CH_2){-}PPh_2{=}N{-}2,6\text{-}^iPr_2\text{-}C_6H_3]Y(CH_2SiMe_3)_2(THF)$ [**82**$_{Y}$] and $(C_5Me_4{-}PPh_2{=}N{-}2,6\text{-}^iPr_2\text{-}C_6H_3)Y(CH_2SiMe_3)_2(LiCl)(THF)$ in a ≈ 9/1 ratio, respectively. The X-ray diffraction studies of the former complex revealed an uncommon η^3-allyl/κ-N coordination mode of the ligand with Y^{3+} (Fig. 52). The Y-C(allyl) distances [2.749(3), 2.669(3), and 2.724(3) Å] are similar, suggesting a symmetrical allylic moiety bounded to yttrium atom. Such a coordination mode has been already observed in (η^5-$C_5Me_4{-}C_5H_4N)[C_5HMe_3(\eta^3\text{-}CH_2){-}C_5H_4N\text{-}\kappa]Y(CH_2SiMe_3)$[133] and $(C_5Me_5)Y(\eta^5\text{-}C_5Me_4CH_2{-}C_5Me_4CH_2\text{-}\eta^3)$,[134] although the allyl was found to be dissymmetric in both cases. When the central metal was changed to lutetium, a mixture of two bis(alkyl) complexes was further isolated, one of which, $[C_5HMe_3(\eta^3\text{-}CH_2){-}PPh_2{=}N{-}C_6H_3{}^iPr_2]Lu(CH_2SiMe_3)_2(THF)$) [**82**$_{Lu}$], exhibited a η^3-allyl/κ-N coordination mode similar to that found for the yttrium derivative from ^{1}H NMR studies.

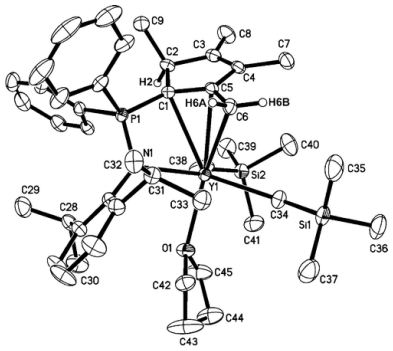

Fig. 52 Molecular structure of **82$_Y$**. Thermal ellipsoids are set at the 40% probability level. Reprinted with the permission of the American Chemical Society.[132]

In the reaction of $[(C_5Me_5)_2YH]_2$ with cyclooctatetraene C_8H_8, $(C_5Me_5)Y[(\eta^5\text{-}C_5Me_4CH_2\text{-}C_5Me_4CH_2\text{-}\eta^3)]$ [**83$_Y$**] formed unexpectedly among other by-products solely in benzene (Scheme 61).[134]

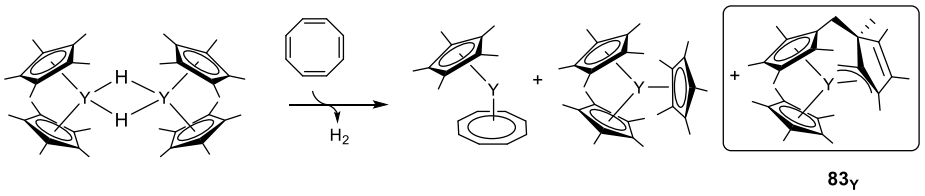

83$_Y$

Scheme 61 Formation of complex **83$_Y$** from ligands redistribution after reaction with cyclooctatetraene

The X-ray diffraction analysis of **83$_Y$** (Fig. 53) indicated that the Y^{3+} metal center is coordinated to one $(C_5Me_5)^-$ ligand in η^5- coordination mode and two $(C_5Me_5)^-$ rings that are linked by a CH_2 group to form a new type of *ansa-allyl*-cyclopentadienyl dianion ligand of the type $(C_5Me_4CH_2\text{-}C_5Me_4CH_2)^{2-}$. The coordination of the dianion to Y^{3+} reveals an unusual pentahapto-trihapto chelation ($\eta^5\text{-}C_5Me_4CH_2\text{-}C_5Me_4CH_2\text{-}\eta^3)^{2-}$ where the Y-C(η^3-allyl) bonds are not symmetrical [Y-C(allyl) in the range of 2.450 – 2.990 Å].

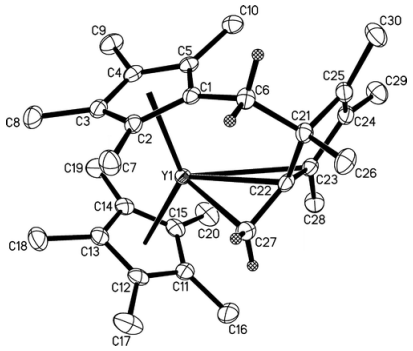

Fig. 53 ORTEP plot drawn at the 50% probability level of **83$_Y$**. Hydrogen atoms are omitted for clarity. Reprinted with the authorization of the American Chemical Society.[134]

An allylic Ln,C,P π-type interaction was proposed in phosphoniomethylidene complexes of scandium and lutetium, [{MeC(NDipp)CHC(NDipp)Me}Ln(CHPPh$_3$)X] (**84$_{Sc}$**: R = Me; **84$_{Lu}$**: R = CH_2SiMe_3; **84'$_{Sc}$**: X = I; **84''$_{Sc}$**: X = OTf), on the basis of X-ray diffraction studies corroborated with DFT calculations (Scheme 62, Fig. 54. a,b,c).[135]

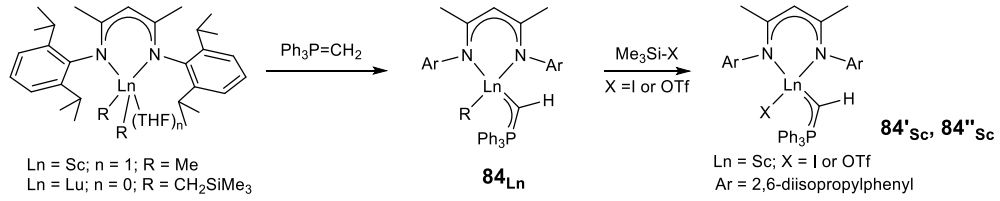

Scheme 62 Synthesis of complexes **84**$_{Ln}$, **84'**$_{Sc}$, **84''**$_{Sc}$

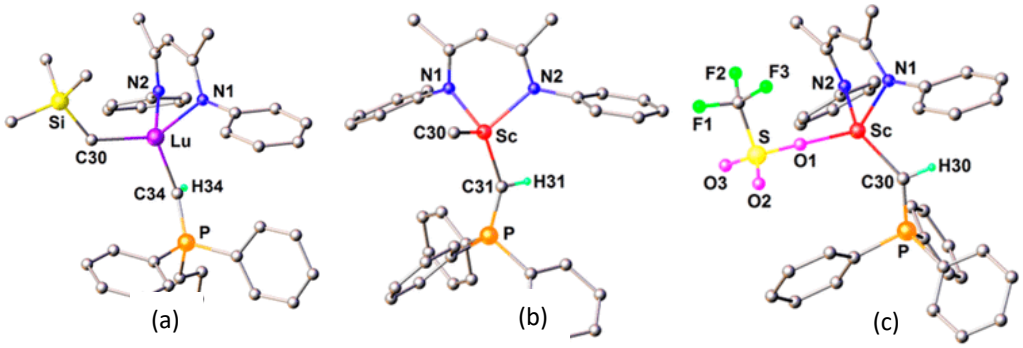

Fig. 54 Molecular structure of **84**$_{Lu}$ (a), **84**$_{Sc}$ (b) and **84''**$_{Sc}$ (c), represented with ball and stick. Isopropyl groups and hydrogen atoms are omitted for clarity. Reprinted with the permission of the American Chemical Society. [135]

An η^3-benzyl-type coordination mode is observed in the dihydrido-1,2-diphenylethane-1,2-diyl complex [(NCN)LuH(THF)]$_2$-(PhCHCHPh) (**85**$_{Lu}$), which results from the reaction of the dihydride [(NCN)LuH$_2$]$_2$(THF)$_3$ with diphenylacetylene in THF after 24 h (NCN = PhC(NC$_6$H$_3$^{i}Pr$_2$-2,6)$_2$) (Scheme 63). [136] This interaction is replaced by a π-interaction of the phenyl group in benzene.

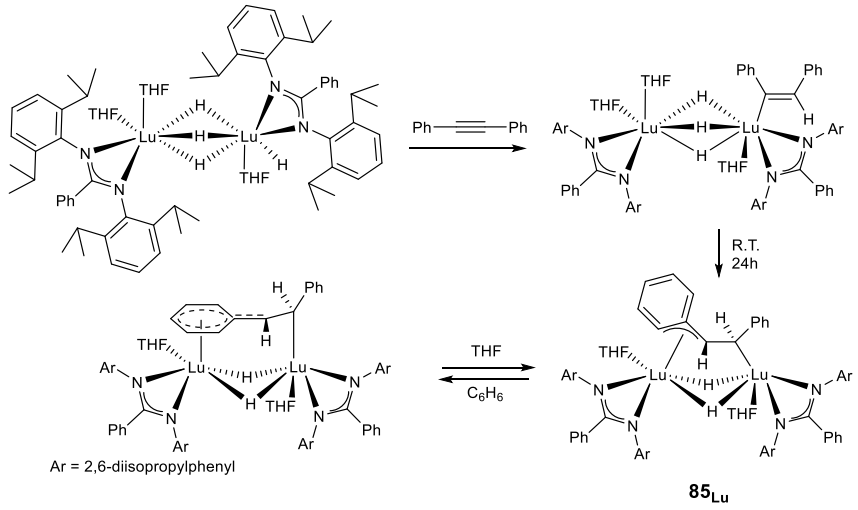

Scheme 63 Formation of complex **85**$_{Lu}$

The ''PhCHCHPh'' moiety in complex **85**$_{Lu}$ is linked to one lutetium metal atom in an η^2-fashion with the ethane-1,2-diyl carbon atoms and to the other lutetium metal atom in an η^3-coordination mode with one benzyl carbon, one *ipso*-phenyl carbon and one *ortho*-phenyl carbon atoms (Fig. 55).

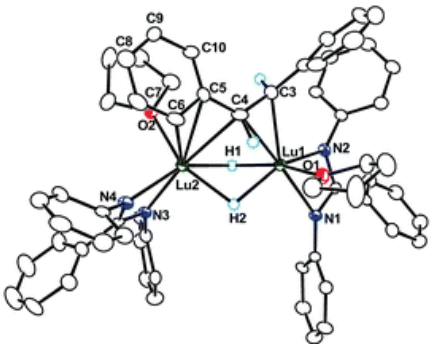

Fig. 55 ORTEP plot of the dihydrido-1,2-diphenylethane-1,2-diyl complex [(NCN)LuH(THF)]$_2$-(PhCHCHPh) (**85$_{Lu}$**) with thermal ellipsoids drawn at the 30% probability level. The isopropyl group and hydrogen atoms (except the bridging hydride) are omitted for clarity. Reprinted with the authorization of the Royal Chemical Society.[136]

Addition of 2 equiv. of the pyridyl-functionalized cyclopentadienyl ligand C_5Me_4H-C_5H_4N to $Y(CH_2SiMe_3)_3(THF)_2$ generated the expected bis-Cp derivative $(C_5Me_4H$-$C_5H_4N)_2YCH_2SiMe_3$ together with the well-defined yttrium mono(alkyl) complex $(C_5Me_4H$-$C_5H_4N)[C_5HMe_3(\eta^3$-$CH_2)$-C_5H_4N-$\kappa]YCH_2SiMe_3$ (**86$_Y$**) (Scheme 64).[133]

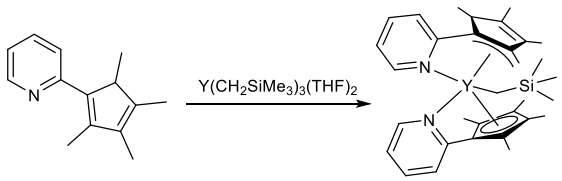

86$_Y$

Scheme 64 Formation of complex **86$_Y$**

The X-ray diffraction analysis of complex [**86$_Y$**] exhibited a rare κ/η^3-allylic coordination mode, resulting from the unexpectedly C-H bond activation of one methyl group of the Cp ligand. The C-C bond distances of the $C_5HMe_3(\eta^3$-$CH_2)$ unit clearly showed that the electrons are delocalized over the three C atoms of the allyl group rather than in the Cp ring, with the Y-C(η^3-allyl) bonds being not symmetrical [Y-C(allyl) in the range of 2.50 – 2.96 Å] (Fig. 56).

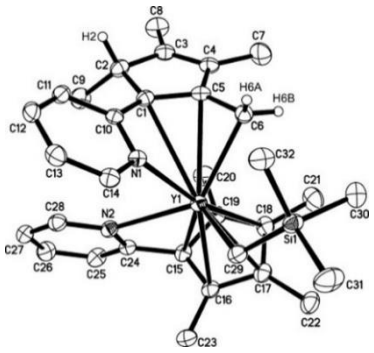

Fig. 56 ORTEP plot with thermal ellipsoids set at 40% probability level of **86$_Y$**. Hydrogen atoms are omitted for clarity. Reprinted with the authorization of WILEY-VCH Verlag GmbH. [133]

Deprotonation of the bulky pyridyl-Flu ligand ($C_{13}H_9$-C_5H_4N) in presence of Ln-$(CH_2SiMe_3)_3(THF)_2$ led to the rare earth-metal–dialkyl complexes of the type (η^3-$C_{13}H_8$-$C_5H_4N)Ln(CH_2SiMe_3)_2(THF)$ (**87$_{Ln}$**, Ln = Y, Sc, Lu) (Scheme 65).[78]

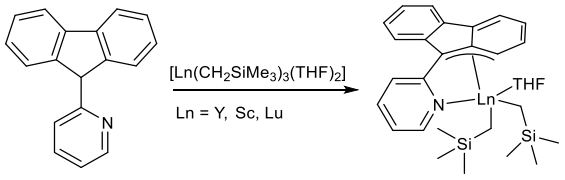

87$_{Ln}$

Scheme 65 Formation of complexes **87$_{Ln}$**

The crystal structure of the three complexes **87$_{Ln}$** has been successfully resolved and displays in each case an unusual asymmetric η^3-allyl bonding mode of the Flu moiety to the metal (Fig. 57, yttrium complex **87$_{Y}$**). Computational studies of the scandium counterpart **87$_{Sc}$** also suggested that the ligand is coordinated to the metal in η^3-allyl/κ^1 fashion. On the other hand, it was found by calculation that upon alkyl abstraction, the ligand is preferably coordinated to the metal in η^5-cyclopentadienyl/κ^1 mode within the resulting cationic Sc complex.[137]

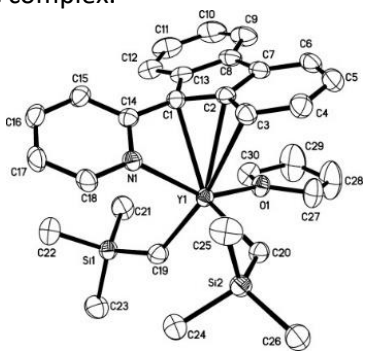

Fig. 57 Molecular structure of (η^3-$C_{13}H_8$-C_5H_4N)Y(CH_2SiMe_3)$_2$(THF) (**87$_{Sc}$**). Displacement ellipsoids are drawn at the 40% probability level. Hydrogen atoms are omitted for clarity. Reprinted with the permission of WILEY-VCH Verlag GmbH.[78]

In addition, reaction of tris(aminobenzyl) yttrium with 1 equiv. of the same bulky pyridyl-Flu ligand produced the aminobenzyl unsolvated yttrium analogue (η^3-$C_{13}H_8$-C_5H_4N)Y($CH_2C_6H_4$-*o*-NMe_2)$_2$ (**87'$_{Y}$**) (Scheme 66), which exhibits similar coordination mode of the Flu moiety to the metal in an asymmetric η^3-allyl fashion (Fig. 58). Upon activation with [Ph_3C][$B(C_6F_5)_4$]/Al^iBu_3, this complex displayed poor activities toward the polymerization of styrene with moderate selectivity.

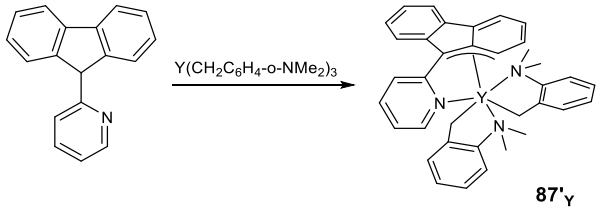

87'$_{Y}$

Scheme 66 Formation of complex **87'$_{Y}$** starting from tris(aminobenzyl) yttrium precursor.

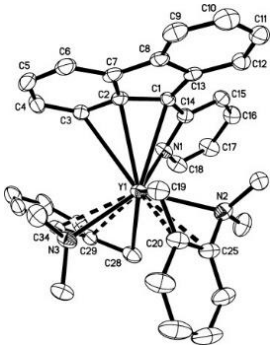

Fig. 58 Molecular structure of (η^3-$C_{13}H_8$-C_5H_4N)Y($CH_2C_6H_4$-*o*-NMe_2)$_2$ (**87'$_Y$**). Displacement ellipsoids are drawn at the 40% probability level. Hydrogen atoms are omitted for clarity. Reprinted with the permission of WILEY-VCH Verlag GmbH.[78]

With the aim to improve the activity and selectivity in the polymerization of olefins, Guo and coworkers reported the synthesis of a family of complexes (η^3:η^1-FluSiMe$_2$N^{t}Bu)Ln(CH_2SiMe_3)(THF)$_2$ (**88$_{Ln}$**, Ln = Sc, Lu, Y) complexes by reacting the pro-ligand FluSiMe$_2$NH^{t}Bu with 1 equiv. of Ln(CH_2SiMe_3)$_3$(THF)$_n$ (Scheme 67).

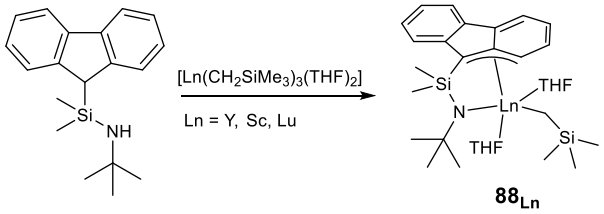

88$_{Ln}$

Scheme 67 Synthesis of complexes **88$_{Ln}$**

X-ray diffraction studies of single crystals of the three complexes revealed a related asymmetric η^3-allyl mode of coordination of the Flu moiety to the metal (Figure 59).[138]

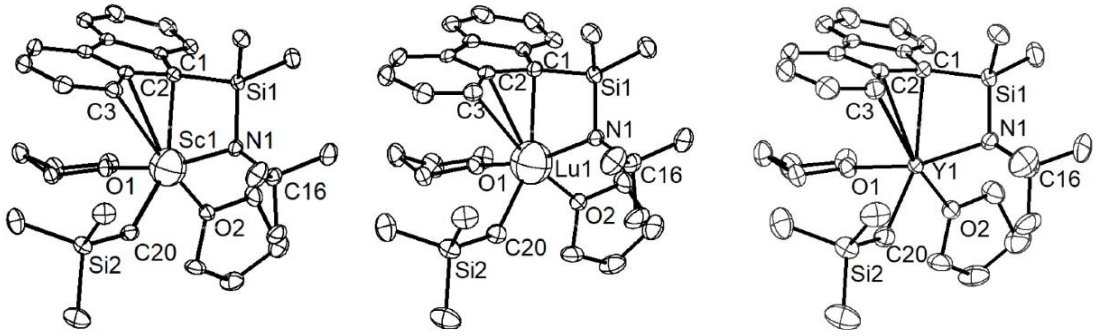

Fig. 59 ORTEP plots of complexes (η^3:η^1-FluSiMe$_2$N^{t}Bu)Ln(CH_2SiMe_3)(THF)$_2$ (**88$_{Ln}$**, Ln = Sc, Lu, Y) with thermal ellipsoids set at the 30% probability level. Hydrogen atoms are omitted for clarity. Reprinted with the permission of MDPI.[138]

When compared to (η^3-$C_{13}H_8$-C_5H_4N)Y($CH_2C_6H_4$-*o*-NMe_2)$_2$ precatalyst, complexes **88$_{Ln}$** present enhanced catalytic activities and high regio-/seoselectivities in the 1,4-*cis* polymerization of isoprene and myrcene or in the syndiotactic polymerization of styrene, in presence of boron-based activator combined with aluminum alkyl.

Table 7 Structural and analytical data of lanthanide complexes with unusual coordination mode (in brackets only the relevant complexes only, otherwise for all complexes)

Compound number	Molecular Formula	X-ray data Ln-C distances (Å)	NMR data	References
82$_{Y}$, 82$_{Lu}$	[C_5HMe_3(η^3-CH_2)−PPh_2=N−2,6-$^{i}Pr_2$-C_6H_3]Ln(CH_2SiMe_3)$_2$(THF) (Ln = Y, Lu)	Y-C = 2.749(3), 2.669(3), 2.724(3)	^{1}H, ^{13}C, ^{31}P	132
83$_{Y}$	(C_5Me_5)Y[(η^5-$C_5Me_4CH_2$-$C_5Me_4CH_2$-η^3)]	Y-C = 2.6985(15), 2.9897(16), 2.4502(16)	-	134
84$_{Sc}$, 84$_{Lu}$, 84'$_{Sc}$, 84''$_{Sc}$	[{MeC(NDipp)CHC(NDipp)Me}Ln($CHPPh_3$)X] (**84$_{Sc}$**: R = Me; **84$_{Lu}$**: R = CH_2SiMe_3; **84'$_{Sc}$**: X = I; **84''$_{Sc}$**: X = OTf)	**84$_{Sc}$**: Sc-C = 2.105(2) **84'$_{Sc}$**: Sc-C = 2.044(5) **84''$_{Sc}$**: Sc-C = 2.060(3) **84$_{Lu}$**: Lu-C = 2.192(11)	^{1}H, ^{13}C, ^{31}P, ^{31}F (**84''$_{Sc}$**)	135
85$_{Lu}$	[(NCN)LuH(THF)]$_2$(PhCHCHPh)	Lu-C = 2.604(7), 2.785(6), 2.775(7)	^{1}H, ^{13}C	136
86$_{Y}$	(η^5-C_5Me_4−C_5H_4N)[C_5HMe_3(η^3-CH_2)−C_5H_4N-κ]Y(CH_2SiMe_3)	Y–C = 2.961(3), 2.792(3), 2.501(3)	^{1}H, ^{13}C	133
87$_{Ln}$	(η^3-$C_{13}H_8$-C_5H_4N)Ln(CH_2SiMe_3)$_2$(THF) (Ln = Y, Sc, Lu)	Y-C = 2.689(2), 2.755(2), 2.916(2)	^{1}H, ^{13}C	78, 137, 138
87'$_{Y}$	(η^3-$C_{13}H_8$-C_5H_4N)Y($CH_2C_6H_4$-*o*-NMe_2)$_2$	Y-C = 2.689(2); 2.755(2); 2.916(2	^{1}H, ^{13}C	78
88$_{Sc}$, 88$_{Lu}$, 88$_{Y}$	(η^3:η^1-FluSiMe_2N^{t}Bu)Ln(CH_2SiMe_3)(THF)$_2$ (Ln = Sc, Lu, Y)	**88$_{Sc}$**: Sc-C = 2.065(3), 2.395(3), 2.730(3) **88$_{Lu}$**: Lu-C = 2.180(3), 2.504(4), 2.746(4) **88$_{Y}$**: Y-C = 2.213(3), 2.566(3), 2.769(3)	^{1}H, ^{13}C	138

3.6. Allyl complexes of the lanthanides as intermediates

Allyl lanthanide species have been postulated to be formed during some specific olefinic chemical processes that take place in the presence of lanthanides, like the lanthanum-mediated dehydrogenation of butenes[139] and C-H bond activation of propene,[140] based on spectroscopic analyses and theoretical calculations.

4 Conclusion

Allyl complexes of the lanthanides, as well as alkene(alkenyl) and alkyne(alkynyl) derivatives of these elements, have seen a considerable surge of interest in the last fifteen years. A significant amount of new complexes with a wide variety of structures have been prepared, and among them new families of mono and bis-allyl complexes in particular have emerged, such as novel cationic complexes, which prefigure reactive species involved in some catalytic processes, or mixed allyl complexes sometimes including another type of reactive ligand. Otherwise, substituted allyl ligands or ligands incorporating a heteroatom have been the subject of several studies, allowing the synthesis of novel compounds.

Synthesis strategies are diversifying, using, for allyl derivatives and depending on the precursor used, traditional ionic metathesis or acid-base reactions with a pro-ligand, as an opportunity offered by the allyl ligand in a “soft” synthetic manner to subtly add a new ligand to the coordination sphere of a lanthanide. With regard to alkene(alkenyl) and alkyne(alkynyl) complexes, which generally result from C-H activation or non-common reduction processes, the variety of compounds reported is

another illustration of the structural diversity observed with organometallic chemistry of the lanthanide elements. Quite often the families of complexes, from lanthanum to scandium, go hand in hand with the size of the lanthanides: we find typical structures with the largest, others with the smallest, where the choice of the lanthanide precursors and the reagents is of particular importance in that context.

As far as allyl complexes are concerned, the allyl ligand is rather versatile, often terminal, sometimes bridged, it can have a somewhat static or fluxional character, it is usually trihapto but can eventually slip into monohapto. This feature is apparent in crystalline structures, whereas in solution, NMR spectroscopy, even for paramagnetic compounds, is a very useful tool for studying the molecular arrangement of the allyl ligand on a metal.

In terms of reactivity, the chemistry of insertion into the lanthanide-allyl bond has continued to develop, or to generate hydrides or cationic species. Applications in catalysis have also largely been demonstrated, notably in hydrosilylation. Moreover, the use of allylic complexes has been particularly extended to polymerization reactions, following the initial work on the polymerization of dienes, and towards styrene and polar monomers as well. New allylic catalysts, including single-component systems – where the absence of cocatalyst may eventually be an advantage – with a strong stereoregulating and controlled character, have been specially designed and developed.

There is no doubt that this very special branch of the exciting organometallic lanthanide chemistry will continue to develop in the future.

References

1. Marks, T.J.; Ernst, R.D. *In Comprehensive Organometallic Chemistry*; Wilkinson, G.; Stone, F.G. A., Abel, E.W. *Eds.; Pergamon: Oxford, UK* **1982**, pp 196-197, 205-206. Edelmann, F.T. In *Comprehensive Organometallic Chemistry II*; Abel, E.W.; Stone, F.G.A., Wilkinson, G. *Eds.; Elsevier: Oxford, UK* **1995**, pp 26–28; Edelmann, F. T. In *Comprehensive Organometallic Chemistry III*; Mingos, D.M.P.; Crabtree, R.H., *Eds.; Elsevier: Oxford, UK* **2007**, pp 17–21.
2. Carpentier, J-F.; Guillaume, S.M.; Kirillov, E.; Sarazin, Y. *C. R. Chim.* **2010**, *13*, 608–625.
3. Taube, R.; Windisch, H.; Maiwald, S.; Hemling, H.; Schumann, H. *J. Organomet. Chem*. **1996**, *513*, 49–61.
4. Taube, R.; Maiwald, S.; Sieler, J. *J. Organomet. Chem*. **2001**, *621*, 327–336.
5. Sanchez-Barba, L.F.; Hughes, D.L.; Humphrey, S.M.; Bochmann, M. *Organometallics* **2005**, *24*, 3792–3799
6. Robert, D.; Abinet, E.; Spaniol, T.P.; Okuda, J. *Chem. Eur. J.* **2009**, *15*, 11937–11947
7. Abrams, M.B.; Yoder, J.C.; Loeber, C.; Day, M.W.; Bercaw, J.E. *Organometallics* **1999**, *18*, 1389–1401
8. Porri, L.; Giarrusso, A. Conjugated diene polymerization. In *Comprehensive Polymer Science*; Eastmond, G., Ledwith, A., Russo, S., Sigwalt P., Eds.; Pergamon: Oxford, UK, 1989; Volume 4, pp. 53–108
9. Evans, W.J.; Ulibarri, T.A.; Ziller, J.W. *J. Am. Chem. Soc.* **1990**, *112*, 2314–2324.
10. Taube, R.; Windisch, H.; Maiwald, S. *Macromol. Symp.* **1995**, *89*, 393–409.
11. Kuran, W. Coordination Polymerisation of conjugated dienes. In *Principles of Coordination Polymerisation*; J. Wiley and Sons, Chichester, 2001; Chapter 5, pp. 275–329.
12. Fischbach, A.; Anwander, R. *Adv. Polym. Sci.* **2006**, *204*, 155–281
13. Friebe, L.; Nuyken, O.; Obrecht, W. *Adv. Polym. Sci.* **2006**, *204*, 1-154
14. Jothieswaran, J.; Fadlallah, S.; Bonnet, F.; Visseaux, M. *Catalysts* **2017**, *7*, 378
15. Kirillov, E.; Saillard, J.-Y.; Carpentier, J-F. *Coord. Chem. Rev.* **2005**, *249*, 1221–1248
16. Gromada, J.; Carpentier J-F.; Mortreux, A. *Coord. Chem. Rev.* **2004**, *248*, 397-410.
17. Hou, Z.; Luo, Y.; Li, X. *J. Organomet. Chem.* **2006**, *691*, 3114-3121.

18. Porri, L. Ricci, G. Giarusso, A, Shubin, N. Lu, Z. *Recent developments in lanthanide catalysts for 1,3-diene polymerization*. in: *Olefin Polymerization: Emerging Frontiers*, ACS Symposium Series, P. Arjunan, J.E. McGrath, T.L. Hanlon (Eds.), 1999, vol. 749, pp. 15-30.
19. Zhang, Z.; Cui, D.; Wang, B.; Liu, B.; Yang, Y. *Struct Bond* **2010**, *137*, 49-108
20. Coperet, C. *Hydrogenation with early transition metal, lanthanide and actinide complexes. In: Handbook of Homogeneous Hydrogenation*, Edited by De Vries, J. G. Elsevier, C. J. **2007***, Vol.1*, p.11.
21. Taube, R.; Windisch, H.; Görlitz, F.H.; Schumann, H. *J. Organomet. Chem.* **1993**, *445*, 85–91
22. Hong, S.; Marks, T.J. *Acc. Chem. Res.* **2004**, *37*, 673-686.
23. Douglass, M.R.; Marks, T.J.; *J. Am. Chem. Soc.* **2000**, *122*, 1824-1825.
24. Anwander, R. *Rare earth metals in homogeneous catalysis*. *In: Applied Homogeneous Catalysis with Organometallic Compounds*, Edited by Cornils, Boy; Herrmann, Wolfgang A **1996**, *Vol.2*, p.866
25. Nolan, S.P.; Marks, T.J. *J. Am. Chem. Soc.* **1989**, *111*, 8538-8542.
26. Casey, C.P.; Hallenback, S.L.; Pollock, D.W.; Landis, C.L. *J. Am. Chem. Soc.* **1995**, *117*, 9770-9771.
27. Casey, C.P.; Hallenback, S.L.; Wright, J.M.; Landis, C.L. *J. Am. Chem. Soc.* **1997**, *119*, 9680-9690.
28. Casey, C.P.; Fagan, M. A.; Hallenback, S. L. *Organometallics* **1998**, *17*, 287-289.
29. Casey, C.P.; Fisher, J.J. *Inorg. Chim. Acta* **1998**, *270*, 5-7.
30. Casey, C.P.; Fisher Klein, J.; Fagan, M.A. *J. Am. Chem. Soc*. **2000**, *122*, 4320-4330.
31. Casey, C.P.; Lee, T.Y.; Tunge, J.A.; Carpenetti II D.W. *J. Am. Chem. Soc.* **2001**, *123*, 10762-10763.
32. Casey, C.P.; Tunge, J.A.; Lee, T.Y.; Carpenetti II D.W. *Organometallics* **2002**, *21*, 389-396.
33. Casey, C.P.; Tunge, J.A.; Fagan, M. A. *J. Organomet. Chem.* **2002**, *663*, 91-97.
34. Casey, C.P.; Tunge, J.A.; Lee, T.Y.; Fagan, M.A. *J. Am. Chem. Soc.* **2003**, *125*, 641-2651.
35. Burns, C. J.; Andersen, R.A. *J. Am. Chem. Soc.* **1987**, *109*, 915-917.
36. Eaborn, C.; Hitchcock, P. B.; Izod, K.; Lu, Z.R.; Smith, J. D. *Organometallics* **1996**, *15*, 4783-4790.
37. Evans, W.J.; Perotti, J.M.; Brady, J.C.; Ziller, J.W. *J. Am. Chem. Soc.* **2003**, *125*, 5204-5212.
38. Schumann, H.; Schutte, S.; Kroth, H.J.; Lentz, D. *Angew. Chem. Int. Ed. Engl.* **2004**, *43*, 6208-6211.
39. Schumann, H.; Heim, A.; Schutte, S.; Lentz, D. *Z. Anorg. Allg. Chem.* **2006**, *632*, 1939-1942.
40. Berg, D. J.; Tosha, B.; Xuening, F. *J. Organomet. Chem.* **2010**, *695*, 2703-2712.
41. Selikhov, A.N.; Mahrova, T.V.; Cherkasov, A.V.; Fukin, G.K.; Larionova, J.; Long, J.; Trifonov, A.A. *Organometallics* **2015**, *34*, 1991−1999.
42. Zhang, G.; Deng, B.; Wang, S.; Wei, Y.; Zhou, S.; Zhu, X.; Huang, Z.; Mu, X. *Dalton Trans.* **2016**, *45*, 15445–15456.
43. Zhang, G.; Wei, Y.; Guo, L.; Zhu, X.; Wang, S.; Zhou, S.; Mu, X. *Chem. Eur. J.* **2015**, *21*, 2519–2526.
44. Selikhov, A.N.; Plankin, G.S.; Cherkasov, A.V.; Shavyrin, A.S.; Louyriac, E.; Maron, L.; Trifonov, A.A. *Inorg. Chem.* **2019**, *58*, 5325−5334.
45. Selikhov, A.N.; Shavyrin, A.S.; Cherkasov, A.V.; Fukin, G.K.; Trifonov, A.A. *Organometallics* **2019**, *38*, 4615−4624.
46. Selikhov, A.N.; Boronin, E.N.; Cherkasov, A.V.; Fukin, G.K.; Shavyrin, A.S.; Trifonov, A.A. *Adv. Synth. Catal.* **2020**, *362*, 5432-5443.
47. Khristolyubov, D. O.; Lyubov, D. M.; Shavyrin, A. S.; Cherkasov, A. V.; Fukin, G. K.; Trifonov, A. A. *Inorg. Chem. Front.* **2020**, *7*, 2459–2477.
48. Long, J.; Tolpygin, A. O.; Cherkasov, A. V.; Lyssenko, K. A.; Guari, Y.; Larionova, J.; Trifonov, A.A. *Organometallics* **2019**, *38* (4), 748–752.
49. Evans, W. J.; Giarikos, D.G.; Robledo, C.B.; Leong, V.S., T.A.; Ziller, J.W. *Organometallics* **2001**, *20*, 5648-5652.
50. Roitershtein, D.M.; Ziller, J.W.; Evans, W.J. *J. Am. Chem. Soc.* **1998**, *120*, 11342-11346.
51. Campazzi, E.; Solari, E.; Scopelliti, R.; Floriani, C. *Chem. Commun.* **1999**, 1617.
52. M.P. Coles, P.B. Hitchcock, M.F. Lappert, A.V. Protchenko, *Organometallics* **2012**, *31*, 2682−2690
53. P.J. Shapiro, W.D. Cotter, W.P. Schaefer, J.A. Labinger, J.E. Bercaw, J. Am. Chem. Soc. 1994, 116, 4623
54. Huang, W.; Abukhalil, P.M.; Khan, S.I.; Diaconescu, P.L. *Chem. Commun.* **2014**, *50*, 5221-5223.

55. Selikhov, A.N.; Mahrova, T.V.; Cherkasov, A.V.; Fukin, G.K.; Kirillov, E.; Lamsfus, C.A.; Maron, L.; Trifonov, A.A. *Organometallics* **2016**, *35*, 2401−2409.
56. Guo, L.; Zhu, X.; Zhang, G.; Wei, Y.; Ning, L.; Zhou, S.; Feng, Z.; Wanf, S.; Mu, X.; Chen, J.; Jiang, Y. *Inorg. Chem.* **2015***, 54*, 5725-5731.
57. Zhu, X.; Li, Y.; Guo, D.; Wang, S.; Wei, Y.; Zhou, S. *Dalton Trans*., **2018**, 47, 3947-3957.
58. Feng, Z.; Huang, Z.; Wang, S.; Wei, Y.; Zhou, S.; Zhu, X. *Dalton Trans.* **2019**, *48 (29)*, 11094–11102.
59. Zhang, F.; Zhang, J.; Zhang, Y.; Hong, J.; Zhou, X. *Organometallics* **2014**, *33 (21)*, 6186–6192.
60. White, R.E.; Carlson, C.N.; Veauthier, J.M.; Simpson, C.K.; Thompson, J.D.; Scott, B.L.; Hanusa, T.P.; John, K.D., *Inorg. Chem.* **2006**, *45*, 7004-7009
61. Simpson, C.K.; White, R.E.; Carlson, C.N.; Wrobleski, D.A.; Kuehl, C.J.; Croce, T.A.; Steele, I.M.; Scott, B.L.; Hanusa, T.P.; Sattelberger, A.P.; John, K.D. *Organometallics* **2005**, *24*, 3685- 3691
62. L.F. Sanchez-Barba, D.L. Hughes, S.M. Humphrey, M. Bochmann, *Organometallics* **2005**, *24*, 5329-5334
63. Standfuss, S.; Abinet, E.; Spaniol, T.P.; Okuda J. *Chem. Commun*. **2011**, *47*, 11441–11443.
64. Pu, M.P.; Li, Q.-S.; Xie, Y.; King, R.B.; Schaefer, H.F. *J. Phys. Chem. A* **2011**, *115*, 4491–4504
65. Shannon, R.D. *Acta Crystallogr*., *Sect. A* **1976**, 32, 751-767
66. White, R.E.; Hanusa, T.P.; Kucera, B.E. *J. Am. Chem. Soc*. **2006**, *128*, 9622-9623
67. White, R.E.; Hanusa, T.P.; Kucera, B.E. *J. Organomet. Chem.* **2007**, *692*, 3479–3485
68. White, R.E.; Hanusa, T.P. *Organometallics* **2006**, *25*, 5621
69. Kuehl, C.J.; Simpson, C.K.; John, K.D.; Sattelberger, A.P.; Carlson, C.N.; Hanusa, T.P. *J. Organomet. Chem.* **2003**, *683*, 149
70. Rightmire, N.R.; Hanusa, T.P.; Rheingold, A.L. *Organometallics* **2014**, *33*, 5952−5955
71. Taube, R. Catalytic Reaction Mechanisms and Structure-Reactivity Relationships in the Stereospecific Butadiene Polymerization. In *Metalorganic Catalysts for Synthesis and polymerization*; Kaminsky, W., Ed.; Springer: Berlin, Germany, 1999, pp. 531–546
72. Porri, L.; Ricci, G.; Giarrusso, A.; Shubin, N.; Lu, Z. *ACS Symp. Ser.* **2000**, *749*, 15-30
73. Ajellal, N.; Furlan, L.; Thomas, C.M.; Casagrande Jr, O.L.; Carpentier, J.-F. *Macromol. Rapid Commun*. **2006**, *27*, 338–343
74. Abinet, E.; Martin, D; Standfuss, S.; Kulinna, H.; Spaniol, T.P.; Okuda, J. *Chem. Eur. J.* **2011**, 17, 15014–15026.
75. Yu, N; Nishiura, M.; Li, X.; Xi, Z.; Hou, Z. *Chem. Asian J.* **2008**, *3*, 1406 – 1414
76. Cui, D; Jian, Z; Liu, X. (Changchun Applied Chemistry), CN101704848A (**2010**)
77. Jian, Z; Cui, D.; Hou, Z.; Li, X. *Chem. Commun.* **2010**, *46*, 3022-3024
78. Jian, Z.; Cui, D.; Hou, Z. *Chem. Eur. J.* **2012**, *18*, 2674–2684
79. Jian, Z.; Tang, S; Cui, D. *Chem. Eur. J.* **2010**, *16*, 14007-14015
80. Bonnet, F.; Violante C.; Roussel, P.; Mortreux, A.; Visseaux, M. *Chem. Commun.* **2009**, *23*, 3380–3382
81. Jian, Z; Tang, S.; Cui, D. *Macromolecules* **2011**, 44, 7675–7681
82. Jende, L.N.; Hollfelder, C.O.; Maichle-Mössmer, C.; Anwander, R. *Organometallics* **2015**, *34*, 32-41
83. Luo, Y.; Chi, S.; Chen, J. *New J. Chem*. **2013**, 37, 2675–2682
84. Fadlallah, S.; Terrier, M.; Jones, C.; Roussel, P.; Bonnet, F.; Visseaux, M. *Organometallics* **2016**, *35*, 456–461
85. Maiwald, S.; Taube, R.; Hemling, H.; Schumann, H. *J. Organomet. Chem*. **1998**, *552*, 195−204
86. Fadlallah, S.; Jothieswaran, J.; Capet, F.; Bonnet, F.; Visseaux, M. *Chem. Eur. J*. **2017**, *23*, 15644–15654
87. Fadlallah, S.; Jothieswaran, J.; Del Rosal, I.; Maron, L.; Bonnet, F.; Visseaux, M. *Catalysts* **2020**, *10*, 820
88. Cui, P.; Spaniol, T.P.; Okuda, J. *Organometallics* **2013**, *32*, 1176−1182
89. Taube, R.; Windisch, H.; Weissenborn, H.; Hemling, H.; Schumann, H.J. *J. Organomet. Chem*. **1997**, *548*, 229−236
90. Cui, P.; Spaniol, T.P.; Maron, L.; Okuda, J. *Chem. Commun*., **2014**, *50*, 424-426

91. Martin, D.; Kleemann, J.; Abinet, E.; Spaniol, T.P.; Maron, L.; Okuda J. *Eur. J. Inorg. Chem*. **2013**, 3987–3992
92. Cui, D.; Nishiura, M.; Tardif, O.; Hou, Z. *Organometallics* **2008**, *27*, 2428–2435
93 . Tlpygin, A.O.; Linnikova, O.A.; Kovylina, T.A.; Cherkasov; A.V.; Fukin, G.K.; Trifonov, A.A. *Russ. Chem. Bull., Int. Ed.* **2020**, *69(6)*, 1114-1121
94. Barbier-Baudry, D.; Bonnet, F.; Dormond, A.; Finot, E.; Visseaux, M. *Macromol. Chem. Phys*. **2002**, *203*, 1194–1200
95. Woodman, T.J.; Schormann, M.; Hughes, D.L.; Bochmann, M. *Organometallics* **2003**, *22*, 3028–3030
96. Woodman, T.J.; Schormann, M.; Hughes, D.L.; Bochmann, M. *Organometallics* **2004**, *23*, 2972–2979
97. Sánchez-Barba, L.F.; Hughes, D.L.; Humphrey, S.M.; Bochmann, M. *Organometallics* **2006**, *25*, 1012–1020
98. Abinet, E.; Spaniol, T.P.; Okuda, J. *Chem. Asian J.* **2011**, *6*, 389–391
99. Wu, C.; Liu, B.; Lin, F.; Wang, M.; Cui, D. *Angew. Chem. Int. Ed*. **2017**, *56*, 6975–6979
100. Chen, R.; Yao, Cy; Wang, M.; Xie, H.; Wu, C.; Cui, D. *Organometallics*, **2015**, *34*, 455-461
101. Chen, J.; Gao, Y.; Xiong, S.; Delferro, M.; Lohr, T.L.; Marks T.J. *ACS Catal*. **2017**, *7*, 5214−5219
102. Tsutsui, M.; Ely, N. *J. Am. Chem. Soc.* **1975**, *97*, 3551-3553
103. Demir, S.; Lorenz, S.E.; Fang, M.; Furche, F.; Meyer, G.; Ziller, J.W.; Evans, W.J. *J. Am. Chem. Soc*. **2010**, *132*, 11151–11158
104. Yoder, J.C.; Day, M.W.; Bercaw, J.E. *Organometallics* **1998**, *17*, 4946–4958
105. Abrams, M.B.; Yoder, J.C.; Loeber, C.; Day, M.W.; Bercaw, J.E. *Organometallics* **1999**, *18*, 1389–1401
106. Lorenz, S.E.; Schmiege, B.M.; Lee, D.S.; Ziller, J.W.; Evans, W.J. *Inorg. Chem.* **2010**, *49*, 6655–6663
107. Evans, W.J.; Lee, D.S.; Johnston, M.A.; Ziller, J.W. *Organometallics* **2005**, *24*, 6393-6397
108. Evans, W.J.; Seibel, C.A.; Ziller, J.W. *J. Am. Chem. Soc.* **1998**, *120*, 6745-6752
109. Evans, W.J.; Kozimor, S.A.; Brady, J.C.; Davis, B.L.; Nyce, G.W.; Seibel, C.A.; Ziller, J.W.; Doedens, R.J. *Organometallics* **2005**, *24*, 2269-2278
110. Peterson, J.K.; MacDonald, M.R.; Ziller, J.W.; Evans, W.J. *Organometallics* **2013**, *32*, 2625−2631
111. Fieser, M.E.; Johnson, C.W.; Bates, J.E.; Ziller, J.W.; Furche, F.; Evans, W.J. *Organometallics* **2015**, *34*, 4387−4393
112. Evans, W.J.; Montalvo, E.; Champagne, T.M.; Ziller, J.W.; DiPasquale, A.G.; Rheingold, A.L. *J. Am. Chem. Soc*. **2008**, *130*, 16–17
113. Evans, W.J.; Montalvo, E.; Champagne, T.M.; Ziller, J.W.; DiPasquale, A.G.; Rheingold, A.L. *Organometallics* **2008**, *27*, 3582–3586
114. Evans, W.J.; Montalvo, E.; Dixon, D.J.; Ziller, J.W.; DiPasquale, A.G.; Rheingold, A.L. *Inorg. Chem*. **2008**, *47*, 11376-11381
115. Casely, I.J.; Suh, Y.S.; Ziller, J.W.; Evans, W.J. *Organometallics* **2010**, *29*, 5209–5214
116. Demir, S.; Montalvo, E.; Ziller, J. W.; Meyer, G.; Evans W. J. *Organometallics* **2010**, *29*, 6608–6611
117. Demir, S.; Mueller, T.J.; Ziller, J.W.; Evans W.J. *Organometallics* **2011**, 30, 3083–3089
118. Evans, W.J.; Lorenz, S.E., Ziller, J.W. *Chem. Commun*., **2007**, 4662–4664
119. Fieser, M.E.; Mueller, T.J.; Bates, J.E.; Ziller, J.W.; Furche, F.; Evans W.J. *Organometallics* **2014**, *33*, 3882−3890
120. Kirillov, E.; Lehmann, C.W.; Razavi, A.; Carpentier, J.-F. *J. Am. Chem. Soc.* **2004**, *126*,12240-12241
121. Rodrigues, A.-S.; Kirillov, E.; Lehmann, C.W.; Roisnel, T.; Vuillemin, B.; Razavi, A.; Carpentier, J.-F. *Chem. Eur. J.* **2007**, *13*, 5548–5565
122. Rodrigues, A.; Kirillov, E.; Roisnel, T.; Razavi, A.; Vuillemin, B.; Carpentier, J.F. *Angew. Chem. Int. Ed*. **2007**, *46*, 7240–7243
123. Rodrigues, A.S. ; Kirillov, E. ; Vuillemin, B. ; Razavi, A.; Carpentier, J.-F. *J. Mol. Catal. A: Chem*. **2007**, *273*, 87–91
124. Perrin, L.; Sarazin, Y.; Kirillov, E.; Carpentier, J.-F., Maron, L. *Chem. Eur. J.* **2009**, *15*, 3773 – 3783

125. Fischbach, A.; Perdih, F.; Herdtweck, E.; Anwander, R. *Organometallics* **2006**, *25*, 1626-1642
126. Perrin, L.; Kirillov, E.; Carpentier, J.F.; Maron, L. *Macromolecules* **2010**, *43*, 6330–6336
127. Rodrigues, A.S.; Kirillov, E.; Vuillemin, B.; Razavi, A.; Carpentier, J.-F. *Polymer* **2008**, *49*, 2039–2045
128. Sarazin, Y.; de Frémont, P.; Annunziata,L.; Duc, M.; Carpentier, J.F. *Adv. Synth. Catal*. **2011**, *353*, 1367–1374
129. Annunziata, L.; Duc, M.; Carpentier J.F. *Macromolecules* **2011**, *44*, 7158–7166
130. Annunziata, L.; Rodrigues, A.S.; Kirillov, E.; Sarazin, Y.; Okuda, J.; Perrin, L.; Maron, L.; Carpentier, J.F. *Macromolecules* **2011**, *44*, 3312–3322
131. Zhang, Z.; Bu, X.; Zhang, J.; Liu, R.; Zhou, X.; Weng L. *Organometallics* **2010**, *29*, 2111–2117
132. Jian, Z.; Petrov, A.R.; Hangaly, N.K.; Li, S.; Rong, W.; Mou, Z.; Rufanov, K.A.; Harms, K.; Sundermeyer, J.; Cui, D. *Organometallics* **2012**, *31*, 4267−4282
133. Jian, Z.; Cui, D. *Chem. Eur. J*. **2011**, *17*, 14578-14585
134. Evans, W.J.; Schmiege, B.M.; Lorenz, S.E.; Miller, K.A.; Champagne, T.M.; Ziller, J.W.; DiPasquale, A.G.; Rheingold, A.L. *J. Am. Chem. Soc.* **2008**, *130*, 8555-8563
135. Mao, W.; Xiang, L.; Maron, L.; Leng, X.; Chen, Y. *J. Am. Chem. Soc.* **2017**, *139*, 17759−17762
136. Cheng J.; Wang H.; Nishiura M.; Hou Z. *Chem. Sci.,* **2012**, *3*, 2230–2233
137. Wang, X.; Zhou, G.; Liu, B.; Luo, Y. *Organometallics* **2018**, *37*, 882−890
138. Guo, G.; Wu, X.; Yan, X.; Yan, L.; Li, X.; Zhang, S.; Qiu, N. *Polymers*, **2019**, *11*, 836
139. Cao, W.; Hewage, D.; Yang, D.-S. *J. Chem. Phys.* **2018**, *148*, 044312
140. Kumari, S.; Cao, W.; Hewage, D.; Silva, R.; Yang, D.-S. *J. Chem. Phys.* **2017**, *146*, 074305